

UNIVERSITÉ DE MONTRÉAL

TAILORING THE SURFACE CHARGE OF CELLULOSE NANOCRYSTALS (CNC)
USING A POLYCATION

BAHAREH ZAKERI

DÉPARTEMENT DE GÉNIE CHIMIQUE
ÉCOLE POLYTECHNIQUE DE MONTRÉAL

MÉMOIRE PRÉSENTÉ EN VUE DE L'OBTENTION
DU DIPLÔME DE MAÎTRISE ÈS SCIENCES APPLIQUÉES
(GÉNIE CHIMIQUE)

JUILLET 2017

UNIVERSITÉ DE MONTRÉAL

ÉCOLE POLYTECHNIQUE DE MONTRÉAL

Ce mémoire intitulé :

TAILORING THE SURFACE CHARGE OF CELLULOSE NANOCRYSTALS (CNC)
USING A POLYCATION

présenté par : ZAKERI Bahareh

en vue de l'obtention du diplôme de : Maîtrise ès Sciences Appliquées

a été accepté par le jury d'examen constitué de:

M. FRADETTE Louis, Ph. D. président

Mme HEUZEY Marie-Claude, Ph. D. membre et directrice de recherche

M. TAVARES Jason-Robert., Ph. D. membre et codirecteur de recherche

M. CARREAU Pierre, Ph. D. membre

DEDICATION

Dedicated To:

Alireza

My parents

My grandmother

ACKNOWLEDGEMENTS

Thanks to my supervisors Prof. Heuzey and Prof. Tavares for their direction and financial support. I would particularly like to thank to Prof. Bernard. Riedl and Prof. Theo van de Ven for their great discussions and comments.

I would like thanks to *Natural Sciences and Engineering Research Council of Canada* (NSERC), *FPIInnovations* and the *Centre de Recherche sur les Systèmes Polymères et Composites à Haute Performance* (CREPEC) for technical and financial support of this project.

I would like to thank all the staff and members of the laboratories of Polytechnique and university of Montreal specially Matthieu, Wendell and Vincent.

Thanks to all my friends and colleagues in Polytechnique specially; Faezeh, Helia, Changsheng, Ahmed, Donya and Bahareh.

Finally, I would also like to thank my parents, my brother and specially my husband for their love, patience, and encouragement.

RÉSUMÉ

Dans ce travail, la surface de nanocristaux de cellulose (CNC) a été modifiée en utilisant un polymère cationique, le polyéthylèneimine (PEI), pour améliorer leur compatibilité avec des milieux non polaires. La modification de surface, réalisée par un procédé simple et sans utiliser de solvants organiques, a été confirmée par différentes techniques analytiques : spectroscopie XPS, spectroscopie FT-IR et mesures de potentiel zêta. Une analyse thermogravimétrique (TGA) a été réalisée pour étudier la stabilité thermique des CNC séchés-modifiés (mCNC). La spectroscopie UV-Vis a également été réalisée pour étudier le taux de sédimentation des mCNC dans l'eau, ainsi que la stabilité du modificateur. Les charges de surface des mCNC ont été modifiées par les polycations, et les mCNC ont précipité dans l'eau ; ils pouvaient cependant être dispersés dans le toluène. On a également montré que les mCNC étaient stables sur une plage de températures adéquate (jusqu'à 200 °C), compatible avec la dispersion en polymère fondu. Être en contact avec un milieu neutre (l'eau et huile minérale) n'a pas affecté l'efficacité du modificateur de surface. De plus, une augmentation significative des propriétés viscoélastiques et du comportement gel est observée pour les suspensions aqueuses de mCNC, attribuée à l'effet électrovisqueux et à la formation d'une structure d'agglomérats du PEI/CNC en suspension aqueuse. Ces résultats indiquent que PEI a un grand potentiel pour être utilisé commercialement comme modificateur de surface des CNC grâce à un processus efficace, à faible coût et respectueux de l'environnement.

Au-delà du traitement par PEI, la modification de surface de CNC a été préliminairement examinée utilisant deux grades de chitosanes. Les résultats obtenus ont démontré que le chitosane peut adsorber sur la CNC chargée négativement par interaction électrostatique et modifier ses propriétés de surface. Les CNC séchées-modifiées avec le chitosane (CHI-CNC) précipitent dans l'eau, mais se dispersent dans toluène. Les propriétés viscoélastiques de la suspension aqueuse CNC à une concentration de CNC de 1% massique augmentent de manière significative en ajoutant une faible quantité de chitosane (1% massique par rapport à la charge en CNC). Ceci est attribué à la structure du chitosane et une affinité élevée entre le chitosane et la CNC. En raison des propriétés bénéfiques du mélange CNC-chitosane, une étude plus approfondie de ce biopolymère en tant que modificateur de surface est proposée.

ABSTRACT

In this work, the surface of cellulose nanocrystals (CNC) was modified using a cationic polymer, polyethyleneimine (PEI), to improve their compatibility with non-polar media through a simple process without using any organic solvents. The successful surface modification was confirmed through different analytical techniques: XPS, FT-IR spectroscopy and zeta potential measurements. Thermogravimetric analysis (TGA) was carried out to investigate the thermal stability of dried-modified CNC (mCNC). UV-Vis spectroscopy was also performed to study the precipitation rate of mCNC in water, as well as the stability of the modifier. The surface charge of mCNC was changed through this modification and mCNC precipitated in fresh water; they could however be dispersed in toluene. The mCNC were also shown to be stable in an adequate temperature range (up to 200 °C) for polymer melt processing. Being in contact with a neutral media (water and mineral oil) did not affect the efficiency of the surface modifier. In addition, a significant increase in viscoelastic properties and gel-like behavior were observed for PEI/CNC aqueous suspensions, ascribed to the electroviscous effect and to the formation of an agglomerates structure resulting from the hydrophobic nature of PEI/CNC aqueous suspension. These results indicate that PEI has a great potential to be used commercially as a CNC surface modifier through an efficient, low cost and eco-friendly process.

In addition, the surface modification of CNC using two grades of chitosan was preliminary investigated. The obtained results showed that chitosan adsorbs on negatively charged CNC through electrostatic interaction and changes the surface properties of CNC. Dried-modified CNC with both chitosan grades (CHI-CNC) sedimented in water, however CHI-CNC dispersed in toluene. The viscoelastic properties of CNC aqueous suspension at CNC concentration of 1 wt.% significantly increased when adding a low amount of chitosan (1% wt.% respect to CNC) due to chitosan structure and high affinity between chitosan and CNC. Thanks to the beneficial properties of CNC and chitosan, the use of this biopolymer as a surface modifier of CNC is proposed for further investigation.

TABLE OF CONTENTS

DEDICATION	III
ACKNOWLEDGEMENTS	IV
RÉSUMÉ.....	V
ABSTRACT	VI
TABLE OF CONTENTS	VII
LIST OF TABLES	X
LIST OF FIGURES.....	XI
LIST OF APPENDICES	XIII
LIST OF ABBREVIATIONS	XIV
CHAPTER 1 INTRODUCTION.....	1
CHAPTER 2 LITERATURE REVIEW	4
2.1. Cellulose nanocrystals (CNC).....	4
2.2. The structure and properties of cellulose nanocrystals	7
2.2.1. The chemical structure of CNC.....	7
2.2.2. The morphology and surface properties of CNC	8
2.2.3. Mechanical properties of CNC.....	9
2.2.4. Thermal properties of CNC.....	10
2.3. The market and applications for CNC.....	11
2.4. Colloidal stability of particles	14
2.4.1. Theories of colloidal stability.....	14
2.4.2. Effect of polymer adsorption on the colloidal stability.....	17
2.5. Surface modification of CNC.....	19

2.6. Conclusion of the literature review and organization of the thesis	26
CHAPTER 3 CNC SURFACE MODIFICATON WITH PEI	28
3.1. Materials.....	28
3.2. Preparation of samples	28
3.3. Characterization of modified CNC	30
3.3.1.X-Ray Photoelectron Spectroscopy (XPS)	30
3.3.2. Fourier Transform Infrared spectroscopy (FTIR)	33
3.3.3. Particle size measurements through dynamic light scattering	35
3.3.4. Zeta potential measurements	37
3.3.6. Contact angle measurements	41
3.3.7. The dispersion of mCNC in fresh DI water and organic solvents	43
3.3.8. Precipitation rate and the stability of modifier using UV-Vis spectroscopy.....	44
3.3.9. Thermogravimetric Analysis (TGA).....	48
3.4. Discussion	50
CHAPTER 4 CNC SURFACE MODIFICATION WITH CHITOSAN.....	54
4.1. Chitosan.....	54
4.2. Structure characterization of CHI-CNC	56
4.3. Zeta potential measurements	57
4.4. Thermogravimetric analysis of CHI-CNC	58
4.5. Dispersion of CHI-CNC in fresh DI water.....	59
4.6. Conclusion.....	60

CHAPTER 5 CONCLUSION AND RECOMMENDATIONS..... 62

BIBLIOGRAPHY 65

APPENDICES.....78

LIST OF TABLES

Table 2-1. The crystallinity and dimensions of CNC provided from different sources	6
Table 2-2. Modulus and tensile strength of CNC compare to other stiff materials.....	10
Table 2-3. The production capacity of cellulose nanocrystals in 2015 ("TAPPI Nanotechnology," December 2015).....	11
Table 3-1. XPS analysis of CNC before and after surface modification with PEI.....	33
Table 3-2. Z-average hydrodynamic size and PDI of pristine CNC and mCNC at (T= 25 °C).....	37
Table 3-3. ζ - potential of pristine CNC and mCNC at different pH (T=25 °C).....	37
Table 3-4. Characteristic thermal degradation temperatures.....	50
Table 4-1. The properties of the two grades of chitosan used in this study	55
Table 4-2. The zeta potential value of CHI-CNC and neat chitosan.....	57
Table 4-3. Characteristic thermal degradation temperatures of CHI-CNC and neat chitosan	59

LIST OF FIGURES

Figure 2.1. The chemical structural of the cellulose components from tree to the anhydroglucose molecule (Madhu Kaushik1, 2015).....	4
Figure 2.2. The molecular structure of cellulose (adapted from (Moon R 2011)).	5
Figure 2.3. The isolation of cellulose nanocrystals through sulfuric acid hydrolysis (adapted from (Yujie Meng & Siqun Wang, 2016)).	5
Figure 2.4. The number of publications on cellulose nanocrystals in recent years (Web of Science).	7
Figure 2.5. Morphology of CNC: (a) Scanning electron microscopy (SEM); (b) transmission electron microscopy (TEM); (c) Atomic Force Microscopy (AFM) (Anuj Kumar1, 2014).	9
Figure 2.6. The variation of CNC specific surface area as a function of diameter (Mariano et al., 2014).....	9
Figure 2.7. Global nanocellulose market ,2015-2021 (adapted from (market, 2016)).	12
Figure 2.8. Forecasting of CNC demand in 2017 in different application fields (adapted from ("La nanocellulose, le nouvel or vert," 2017)).	13
Figure 2.9 a) Potential energy of the interaction; b) the schematic of electric double layer between two particles (adapted from (H. L. F. von Helmholtz, 1880)).	15
Figure 2.10. Stabilization of a colloidal system by a polymer (adapted from (Xiangjun Gong a, 2014)). .	17
Figure 2.11. The different methods of CNC surface modification.....	20
Figure 2.12. Esterification of CNC surfaces (adapted from (S. Lin, 2013)).	21
Figure 2.13. The etherification reaction of surface hydroxyl groups of CNC (Philippe Tingaut, 2010). ...	21
Figure 2.14. The surface oxidation of CNC to carboxylate groups by TEMPO oxidation in water (Akira Isogai *, 2011).	22
Figure 2.15. Schematic of polymer grafting on CNC surface (adapted from (Roy et al., 2009)).	23
Figure 2.16. Grafted PCL on CNC surface using stannous octoate (Dufresne, 2010).	24
Figure 3.1. Schematic illustration of CNC surface modification with PEI	30
Figure 3.2. XPS survey spectra and decomposition of C1s signal into its constituent contributions for (a,b) pristine CNC and (c,d) mCNC with PEI/CNC 2%	31
Figure 3.3. FT-IR spectra of pristine CNC and mCNC with PEI/CNC ratio 1 and 2 %	34
Figure 3.4. The CNC particle size distribution in CNC water suspension at concentrations of 0.1 and 1 wt.%	36

Figure 3.5. a) Steady shear viscosity η (open symbols), complex viscosity η^* (solid symbols) as a function of shear rate $\dot{\gamma}$ and angular frequency ω , respectively b) Storage modulus G' (solid symbols) and loss modulus G'' (open symbols) as a function of angular frequency ω	40
Figure 3.6.Prepared samples for contact angle measurements.....	42
Figure 3.7 . Contact angles of: (a) pristine CNC and (b) mCNC (PEI/CNC 2%).....	42
Figure 3.8.Dispersion state of (a) pristine CNC (b) mCNC (PEI/CNC 2%) in (1) DI water (2) ethanol (3) isopropanol (4) toluene (5) cyclohexane.	43
Figure 3.9.The dispersion of mCNC in DI water a) before ultrasonication b) 5 min c)15 min after applying ultra sonication energy.....	44
Figure 3.10. UV-Vis transmittance (at 656.732 nm) for pristine CNC and mCNC (PEI/CNC 2wt.%) water suspensions as a function of time and mineral oil cycling.	46
Figure 3.11. Percentage of the intensities of UV transmittance measured at maximum wavelength (656.732 nm) for water suspension of pristine and modified CNC (at concentration 1 wt.%) as a function of time at different PEI ratio.....	47
Figure 3.12 Weight loss as a function of a) temperature b) time at 220°C for pristine CNC, mCNC and neat PEI.....	49
Figure 3.13.Schematic drawing of CNC surface modification with polyethyleneimine.....	52
Figure 4.1.The structure of chitosan and its characteristic properties (adapted from (Chinmayee Saikia, 2015)).....	54
Figure 4.2. FTIR spectra of a) pristine CNC and b) CHI1000-CNC c) CHI87-CNC.	56
Figure 4.3. Weight as a function of temperature for pristine CNC, CHI-CNC, and neat CHI.....	58
Figure 4.4.The dispersion state of 1) pristine CNC and 2) modified CNC with Chitosan in DI water (a) CHI1000-CNC (b) CHI87-CNC.....	60

LIST OF APPENDICES

APPENDIX A: Survey N1s and O1s of pristine CNC and mCNC at different PEI ratios.....	78
APPENDIX B: Rheological behavior of PEI/CNC aqueous suspensions.....	82
APPENDIX C: TGA analysis of mCNC in nitrogen.....	87
APPENDIX D: The dispersion state of mCNC in mineral oil.....	88
APPENDIX E: Rheological behavior of chitosan/CNC aqueous suspensions.....	89
APPENDIX F: The results of for modified CNC with PEI ratio 5%.....	91

LIST OF ABBREVIATIONS

ASA	Alkenyl succinic anhydride
CHI	Chitosan
CNC	Cellulose nanocrystals
CNT	Carbon nanotube
CHI-CNC	Dried-modified CNC with chitosan
DADMAC	Polydiallyldimethylammonium-chlorides
DDA	Degree of deacetylation
DI	Deionized
DLS	Dynamic light scattering
DLVO	Deryagin, Landau, Vewey and Overbeek
DMF	Dimethyl formamide
FTIR	Fourier Transform Infrared spectroscopy
HDTMA	Hexa-decyl-trimethylammonium bromide
kDa	Kilodalton
mCNC	Dried-modified cellulose nanocrystal with PEI
PCL	Polycaprolactone
PDI	Polydispersity index
PE	Polyethylene

PEI	Polyethyleneimine
PICVD	Photo-initiated chemical vapor deposition
PLA	Poly(lactic acid)
PLLA	Poly (L-lactic acid)
ROP	Ring Opening Polymerization
PP	Polypropylene
PRI	Relative Polarity Index
TEM	Transmission electron microscopy
TEMPO	(2,2,6,6-tetramethylpiperidin-1-yl)oxidanyl
TGA	Thermogravymetric analysis
THF	Tetrahydrofuran
XPS	X-Ray Photoelectron Spectroscopy

CHAPTER 1 INTRODUCTION

Cellulose nanocrystals (CNC) are renewable and biodegradable materials that have unique properties such as low density, high aspect ratio, high mechanical properties as well as low cost [1-3]. This nanomaterial has a great potential to use in different industries (automobile, packaging etc.) [4] and received a great deal of attention in recent years.

CNC are produced through acid hydrolysis (with H_3PO_4 , HCl , or H_2SO_4 [5]) or periodic oxidation [6, 7] of cellulosic material such as wood pulp, cotton, alga, tunicate [2, 5]. Commercial CNC are generally produced as stable aqueous suspensions mostly through sulfuric acid hydrolysis of wood pulp [8, 9]. The CNC surface is hydrophilic and negatively charged due to the presence of sulfate half-ester groups [2, 10]; This hydrophilic nature has restricted the use of CNC as nanofillers to hydrophilic [11] or water soluble polymers [12-14].

The major obstacle for using CNC in conventional polymer matrix and developing their application as an industrial nanofiller is their hydrophilicity nature and tendency to form agglomerates, which causes significant problems especially when dispersing into non-polar media such as polyolefins [15, 16]. Therefore, surface modification is necessary to improve the compatibility between the CNC surface and non-polar suspending media [17, 18].

In the other hand, CNC have highly reactive surfaces that can be readily functionalized. Hence, the surface of CNC can be tuned by surface chemical modification. Several covalent and non-covalent modification approaches have been developed to functionalize CNC surface and to improve their surface properties [19] including, acetylation [20], esterification [21], etherification [22], periodic oxidation [23], coupling agent treatment [24], polymer (copolymer) grafting [25] and gas phase treatments [26, 27]. Except for gas phase methods, most of these methods are tedious and involve the use of organic solvents, which can cause environmental issues and increase production expenses [27]. It is noteworthy that chemical modification may change the structure of cellulose to some extent and consequently decrease its mechanical and thermal properties [28].

The surface of CNC can also be modified using non-covalent approaches [29-35]. Cationic surface modification [30-32] is a traditional non-covalent method to modify the CNC surface due to the presence of half-ester groups (OSO_3^-) on most commercial CNC.

In terms of modification process, the adsorption of surfactants on CNC through a simple mixing with a surface modifier is easier and more economic compared to chemical surface modification. However, this method has some drawbacks: most studies reported that non-covalent surface modification of CNC is inefficient, namely due to incomplete surface modification and low thermal stability of non-covalent bonds [36]. This can negatively affect the thermal and mechanical properties of the final products. In addition, previous studies reported the desorption and low efficiency of surface modifiers with increasing the temperature (above 70 °C) [37, 38].

The main challenge in industrial surface modification of CNC is to design an efficient, simple, thermally stable and low cost modification protocol without any negative effect on CNC or matrix properties [39].

Polyethyleneimine (PEI)¹ is a cationic polymer composed of repeating units of amines groups and two aliphatic carbons [40]. This polymer exists in both linear and branched molecular structures; a branched PEI contains all types of primary, secondary and tertiary amine groups while a linear PEI composed of only secondary and primary amine groups [41]. This cationic polymer exhibits one of the highest charge densities among polyelectrolytes when protonated in aqueous media [42]. Compared to common commercial surface modifiers, PEI has a higher density of amine groups [43] and a unique branched structure [44] that can interact with the negative groups on CNC at lower concentration, without the drawbacks associated with thermal stability of low molecular surfactant and incomplete surface coverage. Recent studies have demonstrated that PEI is an appropriate candidate to functionalize carbon fillers [45-48] to improve interfacial properties and their compatibility with polymer matrix.

¹ $\text{H}(\text{NHCH}_2\text{CH}_2)_n\text{NH}_2$

Objective

The main objective of this work is to modify CNC with PEI through a low-cost, efficient, and eco-friendly process, thereby increasing the hydrophobicity and compatibility with non-polar media. As a point of comparison, surface modification of CNC is also undertaken and studied with chitosan (CHI). CHI is produced through the partial de-acetylation of the second most abundant biopolymer (chitin) in nature after cellulose. CHI also possesses many interesting characteristics such as, biocompatibility and biodegradability as well as non-toxicity. The positive charges on CHI resulting from the presence of several amino groups can also allow the binding of anionic compounds, such as CNC surface treated by sulfuric acid.

Outline:

Chapter 1: *Introduction;* In this chapter, the challenges were described and the main objective of this work was presented.

Chapter 2 *Literature review;* This chapter presents a background of the research, leading to research objectives.

Chapter 3. *CNC surface modification with PEI;* In this chapter, CNC modification using polyethyleneimine (PEI) is described and the properties of modified CNC are characterized.

Chapter 4. *CNC surface modification with chitosan;* to complete the studied the modification of CNC surface using two grades of chitosan as another cationic polymer are briefly discussed. This chapter serves as a starting point for further investigation of CNC surface modification with chitosan.

Chapter 5. *Conclusion and perspectives.* The thesis closes with concluding remarks and recommendation for further studies.

CHAPTER 2 LITERATURE REVIEW

2.1. Cellulose nanocrystals (CNC)

Cellulose is one of the renewable biopolymer which is provided by nature and thanks to the production rate of cellulose (100 billion metric tons/year), this biopolymer can be used as a permanent and low cost source for more decades [49]. Nowadays, cellulose is used as a raw material in various applications such as paper industries, food, and pharmaceutical industries. Because of its and low cost, availability as well as its interesting chemical and physical properties [3].

The chains of this high molecular weight biopolymers are self-assembled into microfibrils and composed of amorphous and crystalline domains (Fig 2.1).

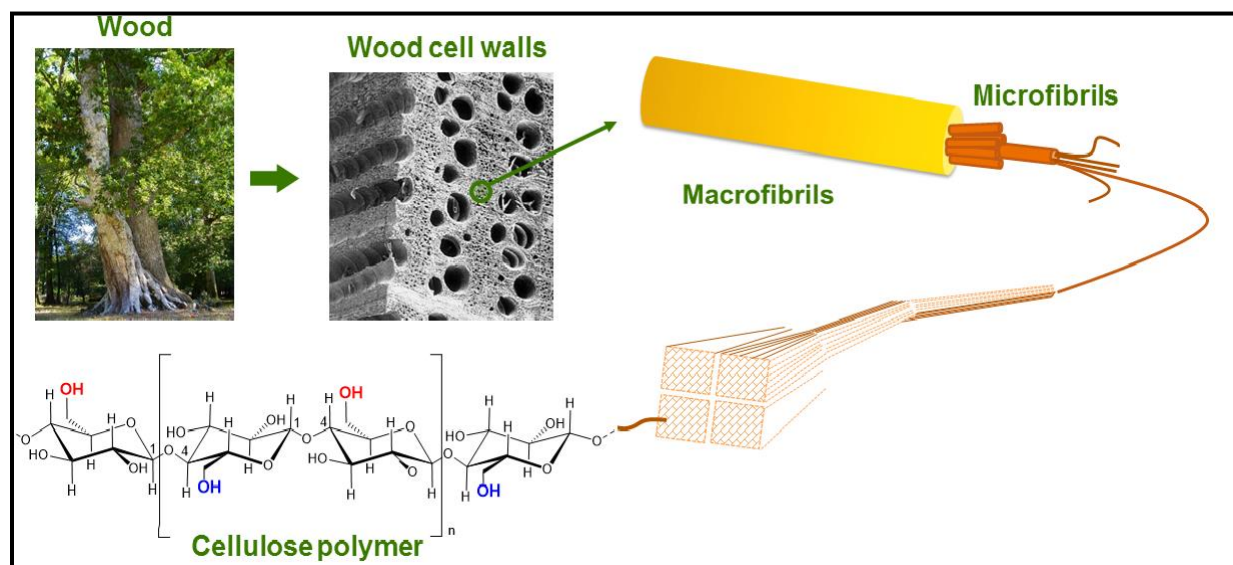


Figure 2.1. The chemical structural of the cellulose components from tree to the anhydroglucose molecule [50].

From a chemical point of view, cellulose is composed of 1,4-anhydro-D-glucopyranose units (Fig 2.2).

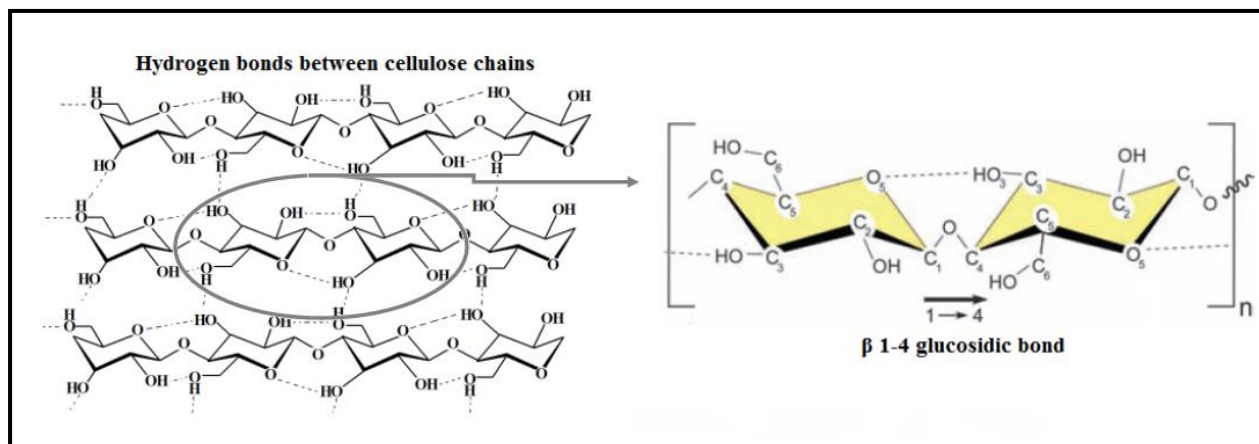


Figure 2.2. The molecular structure of cellulose (adapted from [51]).

Commercial CNC are produced mostly through sulfuric acid hydrolysis of wood pulp. In this process, the disordered amorphous domains are released to the crystalline domains (Fig .2.3) [9, 52].

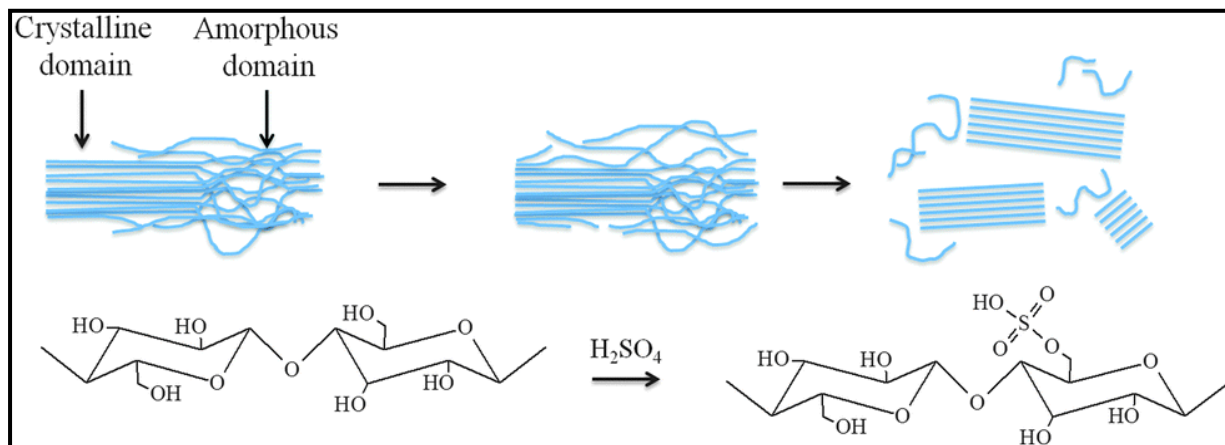


Figure 2.3. The isolation of cellulose nanocrystals through sulfuric acid hydrolysis (adapted from [52]).

The source of cellulose materials affects the dimensions and the degree of crystallinity of produced CNC (Table 2.1) [1, 53, 54].

Table 2-1. The crystallinity and dimensions of CNC provided from different sources

Source	Length (nm)	Width(nm)	Crystallinity (%)	Ref.
Cotton	100-300	5-10	70-90	[2]
Alga	≥ 1000	20	-	[2]
Bacterial	100-1000	10-50	72-74	[2]
Tunicate	100-3000	10-30	83-90	[16]
Wood pulp	100-300	3-15	70-85	[2, 8]
Hard wood	140-150	4-5	40-65	[8]

CNC has attracted significant interest of researchers during recent years, largely attributed to the potential of cellulose nanocrystals to be used as a renewable and rigid nanomaterial. The number of publications on cellulose nanocrystals considering all mentioned terms in recent years are presented in Fig 2.4. Several names and abbreviations have been used for this nanomaterial in literature; “rod-like cellulose microcrystals”, “nanocrystalline cellulose”, “cellulose nano whiskers” and “cellulose nanocrystals”. *TAPPI’s International Nanotechnology Division* recommended **cellulose nanocrystals** as standard term for this nanomaterial in 2011.

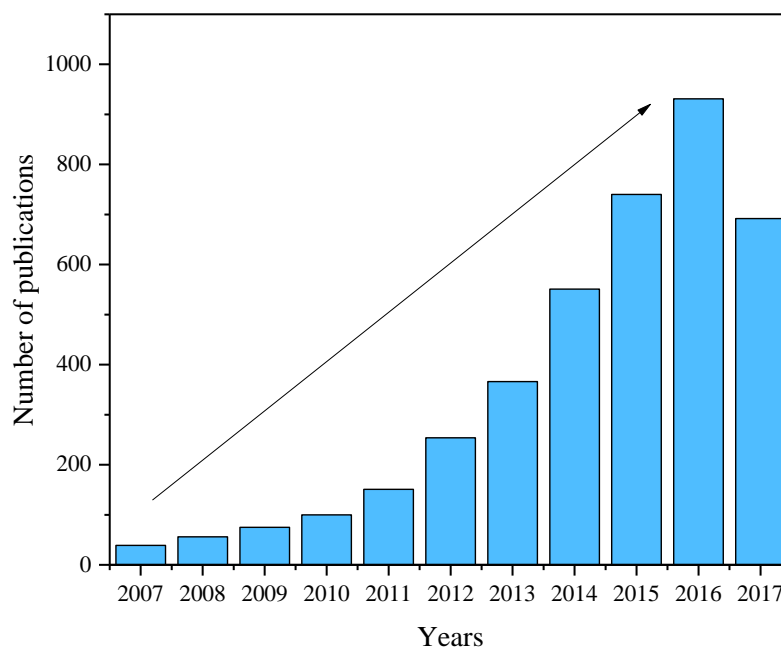


Figure 2.4. The number of publications on cellulose nanocrystals in recent years (*Web of Science*²).

2.2. The structure and properties of cellulose nanocrystals

2.2.1. The chemical structure of CNC

One of the most specific characteristics of CNC is the presence of three hydroxyl groups in each unit of CNC resulting a reactive surface with multiple active hydroxyl groups (Fig 2.2). These hydroxyl groups depending on their position act as a primary or secondary alcohol [55, 56]. Intermolecular and intramolecular hydrogen bonding occur between OH groups of CNC; Intramolecular hydrogen bonds occur between the oxygen of glucose unit (O) and OH group of the C₃ carbon [56]. The intermolecular hydrogen bonds occur between the oxygen of glucose units and other OH groups[57] (Fig 2.2).

² May 15,2017

As mentioned in Chap. 1, the sulfate half-ester groups are introduced on the CNC surface during sulfuric acid hydrolysis via an esterification reaction (sulfation) between surface hydroxyl groups and H₂SO₄ molecules. Therefore, the surface of CNC is highly negatively charged, which leads to well-dispersed aqueous colloidal suspensions due to the presence of OSO₃⁻. The surface charge of CNC can be controlled through the duration time and temperature of acid hydrolysis [58, 59]. Phosphate [60] and carboxyl [61] groups can also be introduced on CNC surface during acid hydrolysis. However, commercial CNC are produced through sulfuric acid hydrolysis [58, 59]. The sulfate half-ester groups on the surface make CNC hydrophilic and, therefore, incompatible with hydrophobic matrix. This results in low mechanical properties and inefficient reinforcement because of poor dispersion induced by inferior interfacial interactions between CNC and non-polar polymer matrix [62].

2.2.2. The morphology and surface properties of CNC

CNC have a rod-like or needle-like morphology (Fig.2.5). The morphology and geometrical dimensions of CNC are varied depending on its cellulosic source (Table 2.1) [2, 53, 63]. In addition, the dimensions of CNC also depend on the hydrolysis conditions [2, 64, 65]. The dimensions of commercial cellulose nanocrystals³ are 7 ± 3 nm diameter and 120 ± 8 nm long, giving a high geometric average aspect ratio in the range of 11 to 32. The dimensions and ion strength of CNC affect the CNC surface properties and play an important role in the behavior of CNC in different media [8, 66-69].

³ -Produced by *FPIInnovation (Canada)*

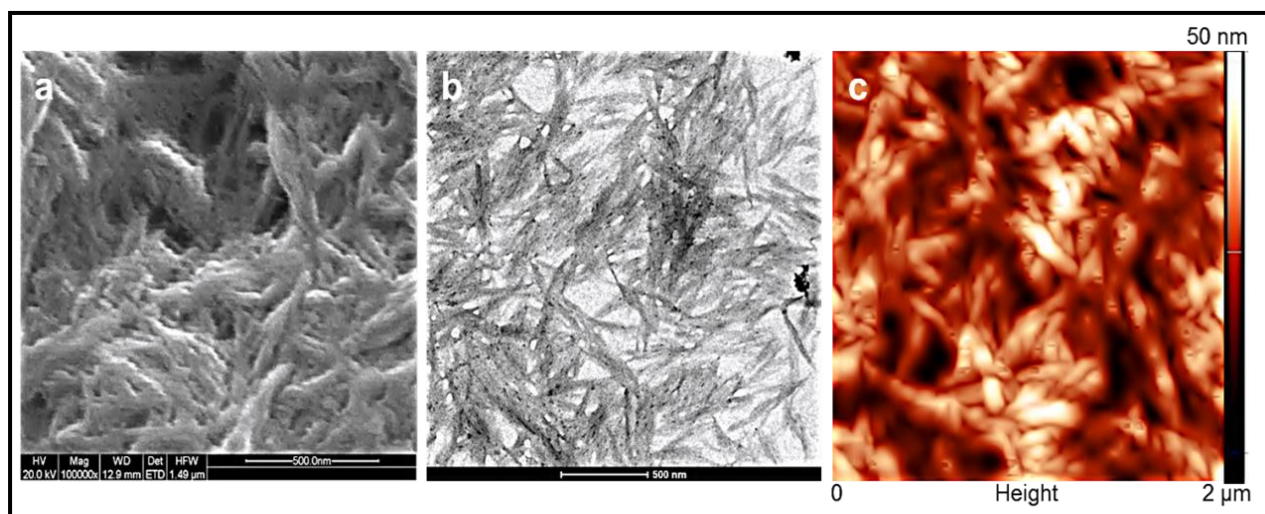


Figure 2.5. Morphology of CNC: (a) Scanning electron microscopy (SEM); (b) transmission electron microscopy (TEM); (c) Atomic Force Microscopy (AFM) [70].

The specific surface area of CNC ($50\text{-}150\text{ g/m}^2$) is depend on its particle size. *Dufresne et al.* reported the variation of CNC specific surface area as a function of diameter (Fig 2.6) [71].

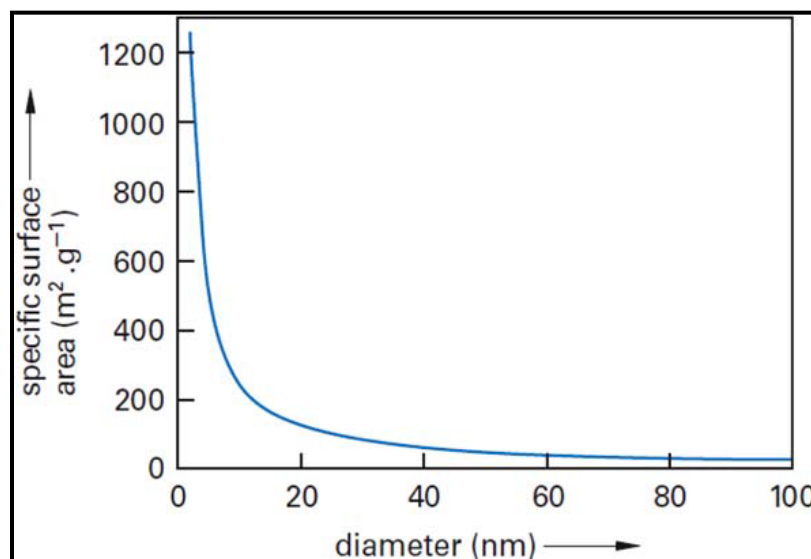


Figure 2.6. The variation of CNC specific surface area as a function of diameter[71]. (Density of 1.5 g cm^{-3})

2.2.3. Mechanical properties of CNC

Cellulose nanocrystals possess attractive mechanical properties that can vary based on their source, morphology, geometrical dimensions, crystal structure, degree of crystallinity as well as

the synthesis process [2, 64, 72-74]. The mechanical properties of CNC are also varied in two directions attributed to rod-like shape of this nanomaterial; the tensile strength of CNC is in the range of 7.5–7.7 GPa while the axial modulus ranges from 110-220 GPa [2, 75-77]. These remarkable mechanical properties are within the range of other nanofillers, such as clay nanoplatelets or carbon nanotubes [2]. The modulus and tensile strength of CNC compared to other stiff materials are in the range that would qualify them for use as nanofillers in polymer matrix (Table 2.2). However, the low density, its high potential for surface modification, and its renewable and biodegradable nature distinguishes it from the other nanofillers [9].

Table 2-2. Modulus and tensile strength of CNC compare to other stiff materials

Materials	Density g/cm ³	Tensile strength (GPa)	Modulus (longitudinal) (GPa)	Modulus (transverse) (GPa)	Reference
Kevlar	1.4	3.5	124-130	2.5	[2]
Carbon fiber	1.8	1.5-5.5	150-500	-	[2]
Steel wire	7.8	41	210-369	-	[2]
Carbon nanotube (CNT)	1.5-2	10-60	300-1000	-	[78]
Nanoclay	1.8-2.2	-	120-180	-	[79]
CNC	1.6	7.5-7.7	130-250	10-50	[2]

2.2.4. Thermal properties of CNC

Many parameters influence the thermal stability of CNC, such as type, temperature and time of acid hydrolysis as well as the concentration of acid during the process [36, 80]. These parameters

also affect the degree of crystallinity of CNC [36, 80-83]. The onset temperature for CNC degradation was reported in literature in the range of 230–280°C [36, 80-83]. Moreover, the presence of acid sulfate groups decrease the thermal stability through the dehydration reaction [84]. Usually, the higher number of sulfate groups on the surface of CNC, the lower the degradation temperature [84]. If hydrochloric acid is used instead of sulfuric acid to hydrolyze the cellulose, the thermal stability of the prepared CNC improves, but the nanocrystals tend to aggregate due to a deficiency of electrostatic repulsion [85].

2.3. The market and applications for CNC

CNC have unique properties such as excellent mechanical properties, high aspect ratio, renewability, biodegradability, as well as lower cost versus common nanomaterials (carbon nanotubes, nanoclay, etc.), leading to an increase in the its applications in recent years. The production of CNC in industrial scale and the use of this nanomaterial in industrial application are the main subjects in this field.

Alberta Innovates-Technology Futures has constructed the first pilot plant to produce cellulose nanocrystals in the world. The joint venture of *Domtar Corp.* and *FPIInnovations (CelluForce)* built a large commercial-scale plant to produce cellulose nanocrystals in North America. The world production capacity of cellulose nanocrystals in 2015 are presented in Table 2.3.

Table 2-3. The production capacity of cellulose nanocrystals in 2015 [86]

Company	Capacity (kg/day)
CelluForce, Canada	1000
American Process, U.S	500
Holmen, Sweden	100
Alberta Innovates, Canada	20
US Forest Products	10
Blue Goose Bio-refineries, Canada	10
India Council for AG Research	10
FPIInnovations, Canada	3

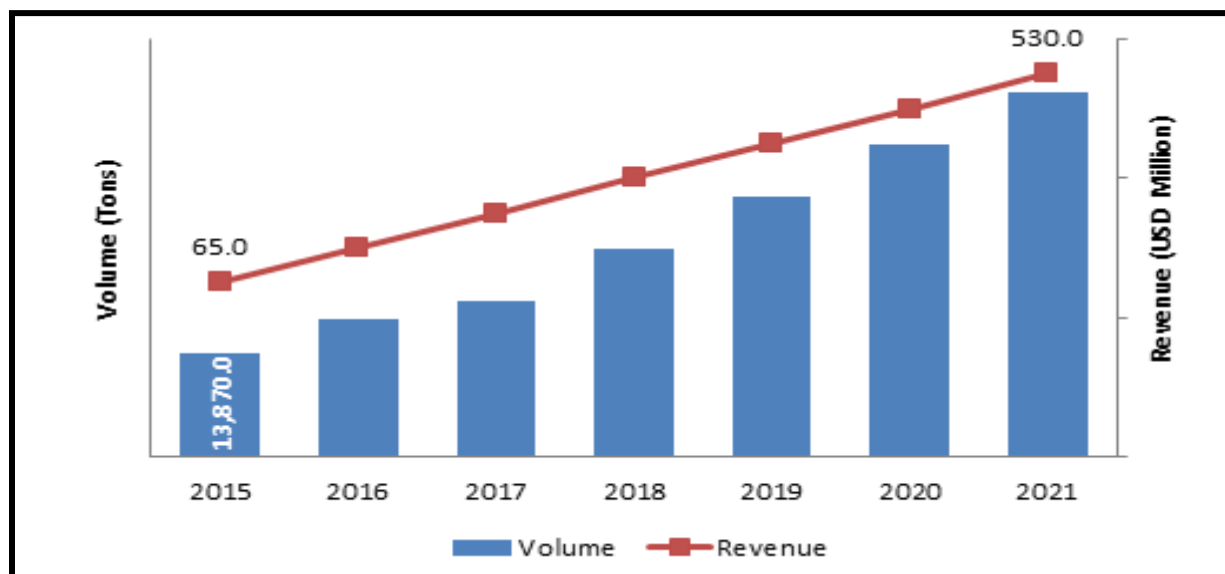


Figure 2.7. Global nanocellulose market 2015-2021(adapted from [87]).

North America will have the high demand for CNC and its end-user industries by 2020 [86]. The market size of CNC in terms of capacity and value will have large annual growth in the future years[87](Fig 2.7). On the other hand, it is predicted that more than 30% of CNC would be consumed in polymer composite to prepare polymer nanocomposites [88] due to their unique properties as well as its low cost⁴ compared to other nanomaterial such as carbon nanotube (Fig 2.8).

⁴ Price of analytical grade: 4.5-5.0 \$/g (www.celluloselab.com)

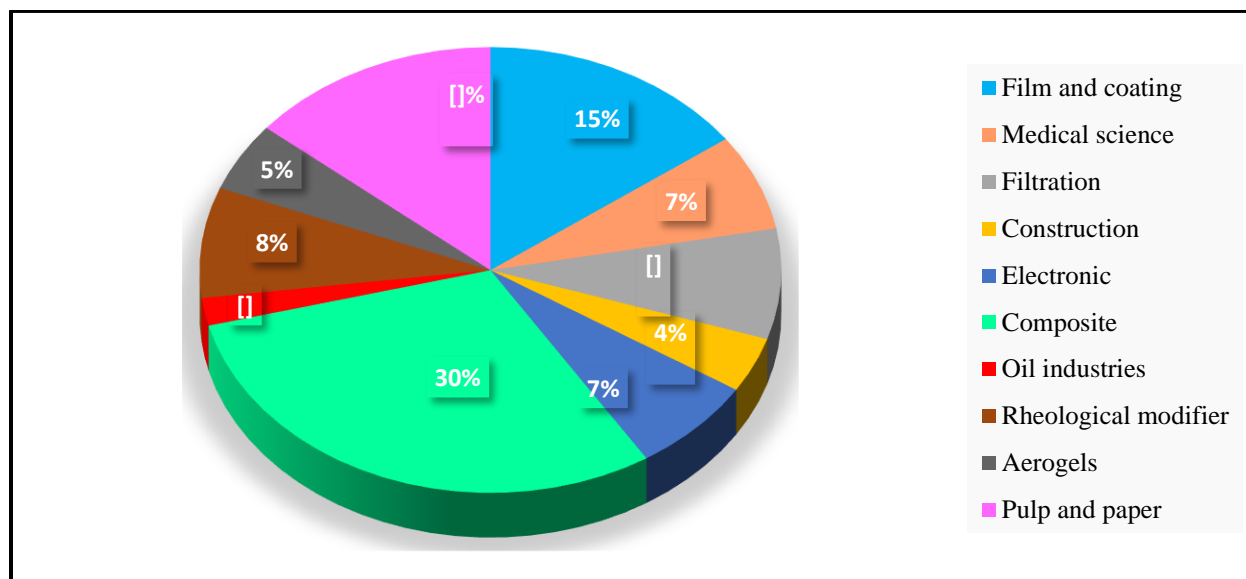


Figure 2.8.Forecasting of CNC demand in 2017 in different application fields (adapted from [88]).

The properties of CNC surface affect the fabrication process as well as the properties of produced composite (nanocomposite)[2, 89]. The fabrication of nanocomposite using commercial polymers as matrix and CNC has been mostly unsuccessful due the hydrophilic properties and poor compatibility of this nanofiller with hydrophobic polymer, restricting it use in hydrophilic or water-soluble polymers [12-14, 90]. In other words, the one of the major blockade in industrial production of CNC/polymer nanocomposites and developing applications for CNC is to achieve a good dispersion of CNC in common polymers such as polyolefins. Therefore, modification is necessary to improve the compatibility between the CNC and host polymer [91].

The dispersibility of CNC in polypropylene (PP) and polylactic acid (PLA) was studied by *Khoshkava et al.*, [62]. They reported that, the interfacial surface properties of CNC and host matrices strongly affect the dispersibility of CNC in polymer. They showed the effect of CNC surface modification on the dispersion level of CNC and resulting mechanical properties of polymer nanocomposite. In the other work, the dispersion level of modified CNC using polyethylene oxide in low density polyethylene (LDPE) was studied and the dispersibility improvement and reduced thermal stability of the CNC were demonstrated [82].

The effect of polypropylene molecular weight on dispersion and mechanical properties of CNC-PP composite in the presence of a compatibilizer using different processing methods was investigated by *Sojoudiasli et al.* [89]. They demonstrated that the low molecular weight PP

composite produced via twin-screw extrusion had higher mechanical properties than the composite produced through internal batch mixer due to the better dispersion of CNC in the PP matrix. In another study, the dispersion level of CNC in a solution of polylactide was investigated by *Bagheriasl et al.* [92] using rheological methods.

The core of most of studies in fabrication of CNC/polymer nanocomposite is mechanical properties of nanocomposites. Nevertheless, the barrier properties of CNC composite are also interesting [93, 94]. The crystallinity nature of CNC as well as its compacted network can decrease permeability of CNC/polymer composites [93, 94].

Cellulose nanocrystals can also be used in medical applications:

- CNC was proposed as an agent for protein/enzyme immobilization due to its nonporous structure as well as its large surface area [95].
- CNC also was proposed for drug delivery due to biocompatibility and its unique properties [96].
- Due to high surface area and possibility of CNC functionalization, CNC was proposed to produce bio-sensors and bio-imaging systems [97].

2.4. Colloidal stability of particles

Colloidal stability is achieved through a balance between the attraction and repulsion forces between adjacent particles.

2.4.1. Theories of colloidal stability

The stabilization of particles against aggregation can occur through two main mechanisms, (depending to the type of repulsion force):

- Electrostatic stabilization
- Steric stabilization

A combination of the two mechanisms is also possible which called “electrosteric” stabilization.

- **Electrostatic stabilization**

Balancing between attractive van der Waals forces and repulsive Coulomb forces of charged particles lead to electrostatic stabilization of colloids. Charged colloidal particles, for example, sulfated CNC, are stabilized by the electrostatic repulsive force between the particles. When two particles become close, the electric double layer (EDL) around the particles prevents their aggregation and keeping them apart [2, 10]. On the other hand, the charge of particles play an important role in the electrostatic stabilization of colloids. The schematic of electric double layer and the potential energy of the interaction between two particles are presented in Fig 2.9.

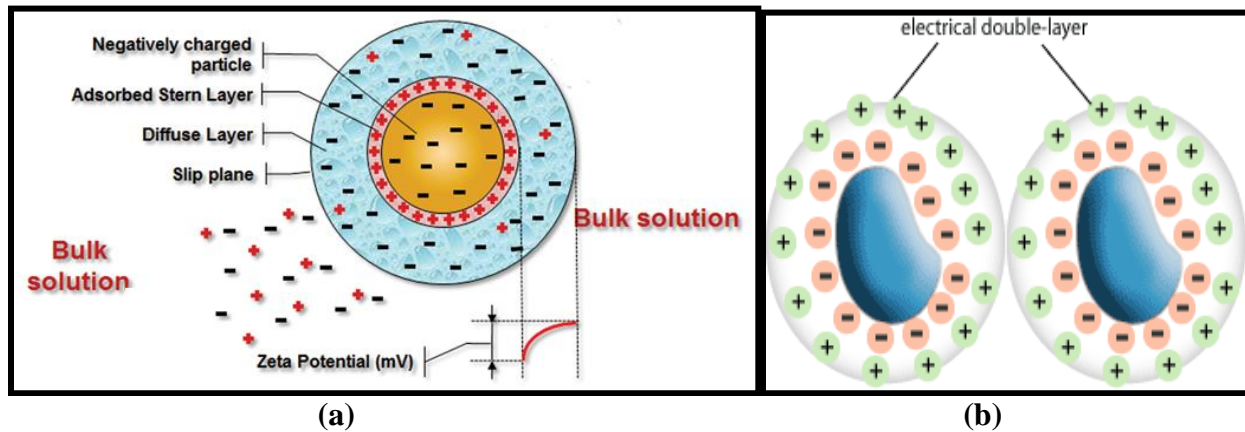


Figure 2.9 a) Potential energy of the interaction; b) the schematic of electric double layer between two particles (adapted from [98]).

The maximum value of the electrical potential is on the particle surface. With increasing distance from the surface, this potential drops and reaches 0 at the boundary of EDL (Fig 2.9a) [98]. The electric potential at the slipping plane is called *Zeta potential*. This value has an important role in interaction and stabilization of colloidal particles.

A linear model between the electrical potential ψ on the surface of particle and the distance from the surface has been developed by *Helmholtz's* as classical electrical double-layer model [98] (Eq.2.1.):

$$\psi = \frac{4\pi\delta\sigma}{\epsilon} \quad \text{Eq. 2.1}$$

where;

δ : the thickness of the fixed layer;
 σ : the density of surface charge;
 ε : the dielectric constant of the solution.

Another theory about the stability of colloidal system was developed by Deryagin, Landau, Vewey and Overbeek (DLVO) in 1940. In the DLVO theory, some assumptions are considered:

- Very low concentration of the dispersed phase;
- Only van der Waals forces and electrostatic forces have role on the dispersed particles;
- The distribution of charges is uniform on the surface of particles;
- Brownian motion, electrostatic forces and entropic dispersion determine the distribution of ions.

According to the DLVO theory, potential energy of particles (V_T) including attractive interaction due to van der Waals force (V_A) and the potential energy of the repulsive electrostatic interaction (V_R) determine the stability of colloidal system (Eq.2.2)[98] .

$$V_T = V_A + V_R \quad \text{Eq. 2.2}$$

Considering spherical particles:

$$V_A = - A/r/(12x) \quad \text{Eq. 2.3}$$

where:

A: Hamaker constant
r: radius of the particles
x: distance between the surface of particles

$$V_R = 2\pi\varepsilon\varepsilon_0r\zeta^2e^{-kx} \quad \text{Eq. 2.4}$$

where:

ζ : zeta potential
 k^{-1} : the characteristic length of the electric double layer
 ε : dielectric constant of the solvent
 ε_0 : permittivity in vacuum

As shown in Eq.2.4, V_R is proportional to square of the zeta potential and as a result V_T is strongly affected by the value of the zeta potential. On the other hand, the zeta potential is one of the main parameters known to affect the colloidal stability.

- **Steric stabilization**

Polymers can be adsorbed on particle surfaces and affect colloidal stability through the prevention of aggregation by repulsion in colloidal systems [99]. There are two types of polymeric stabilization [100, 101] (Fig 2.10);

- Steric stabilization of colloids: polymer attached to the particle surface and covering the particle, which produce a repulsive force and separates the particle from the neighbour particles.
- Depletion stabilization of colloids; free polymer (non-adsorbed molecules) separate the particles through repulsive forces between the particles.

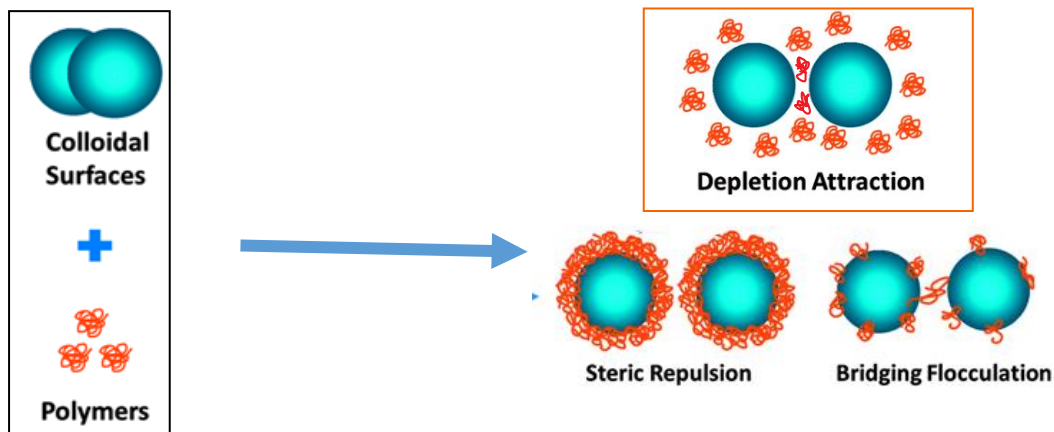


Figure 2.10. Stabilization of a colloidal system by a polymer (adapted from [101]).

2.4.2. Effect of polymer adsorption on the colloidal stability

The adsorption of polymer molecules from solution is one of the common method for surface modification of particles such as CNC. The polymers molecules can be adsorbed through non-covalent (physically) or covalent (chemically) interaction onto the surface of particles [102].

- **Polyelectrolytes**

Polyelectrolytes are water soluble polymers, which are charged (positively or negatively) in aqueous media. Polyelectrolytes have a wide range of charge density and molecular weight. Depending on their charge, these polymers adsorb onto charged surfaces through electrostatic attraction [103]. Depending on their molecular weight and structure, these polymeric molecules can have several dimensions (a few to several hundred nm) and can make a thin layer around the particles, which affect their state of dispersion. Polyelectrolytes play different roles in the stability of colloidal particles depending on the thickness of the layer, molecular weight, degree of surface coverage and chemical structure [104]. Polyelectrolytes determine the behavior of colloidal system (such as CNC colloidal system) by two main mechanisms:

a) Charge neutralization

CNC produced through the acid sulfuric hydrolysis, is dispersed in aqueous suspensions due to repulsion between their negatively charged surfaces. According to the charge neutralisation mechanism, the adsorbed cationic polyelectrolyte neutralises the negative charges on the particle surface (zero charges). By increasing the amount of polyelectrolyte beyond what is required to reach zero charge, the particle charge can be reversed and the suspension stabilized (again) [38] as also described by the DLVO theory [104].

b) Bridging of particles by polymer chains

In this mechanism, the adsorbed polymer can make bridges between the particles. Flocculation through bridging is more likely at 50% (or less) particle surface coverage [45, 46]. With increasing surface coverage, the possibility of steric stabilization increases. In addition, to induce bridging, the polymer chains should also extend beyond the EDL [47, 48].

Some parameters can affect the extension level of polymer chains such as molecular weight, polymer structure, kinetic effects, amount of surface coverage and polymer conformation (from equilibrium conformation to a flatter geometry) over time as well as ionic strength [105]. In addition, from bridging between the particles to occur, the adsorption density should not be too

high [106]. In other words, bridging can occur if there is a sufficient unoccupied surface on the particles to allow attachment of adsorbed polymer chains from other particles. The bridging mechanism is more likely to occur with linear and high molecular weight polymers with low or medium charges [107].

It should be mentioned that dispersion or stabilisation require a higher surface coverage of adsorbed polymer than what is needed for flocculation [99].

2.5. Surface modification of CNC

As mentioned in section 2.3, the main challenge of developing the CNC as nanofillers is its tendency to form agglomerates due to the strong interparticle hydrogen bonding [15, 16], particularly in non-polar media. The dispersion state or self-agglomerations states of CNC in their surrounding media will determine the properties of systems and predict the applications [108, 109]. In order to improve the dispersion of cellulose nanocrystals in organic solvents, several surface treatments or modifications can be performed [19]. CNC have a highly reactive surface that can be easily functionalized and, hence, tuned by chemical modification [19, 108, 109]. CNC surface modification can be divided into two main categories: covalent and non-covalent approaches (Fig .2.11).

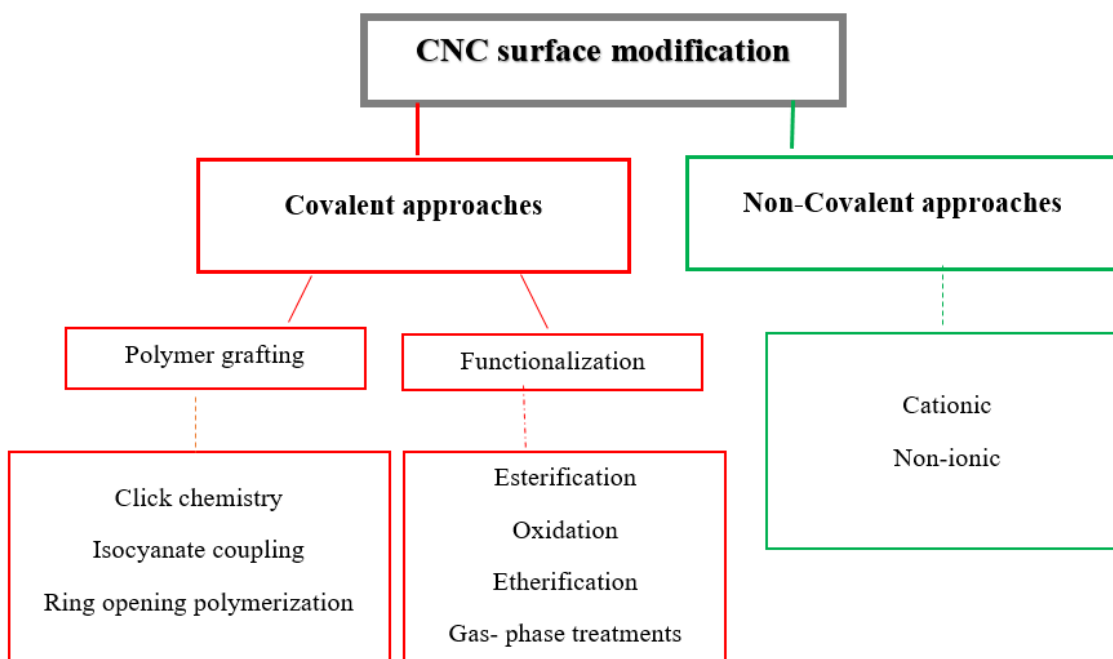


Figure 2.11. The different methods of CNC surface modification.

2.5.1. CNC surface modification using covalent methods

Various covalent approaches have been developed to functionalize CNC surface and to improve its hydrophobic properties [19] such as; oxidation [23], esterification [21], etherification [22], silane treatment [110], acetylation [20, 111], polymer grafting [25] and gas phase treatments [26, 27].

- **Esterification**

Surface esterification is the most common method for the chemical modification of CNC surface [58, 112]. In this method through the condensation reaction, carboxylic acid group (COOH) and an alcohol groups are introduced on the surface of CNC. Acetylation is the one of the simple method of esterification [113] which in that acetyl groups are introduced on the surface of CNC (Fig 2.12).

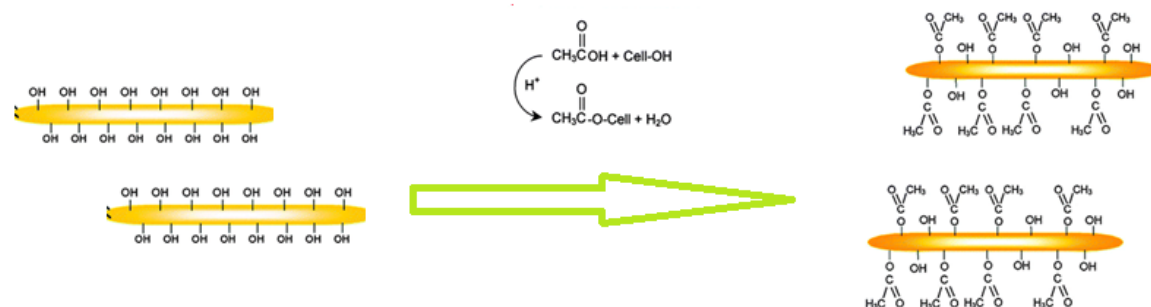


Figure 2.12. Esterification of CNC surfaces (adapted from [113]).

- **Etherification**

Nowadays, etherification is used as a chemical pre-treatment step for defibrillation of the cellulose fibers. This process is performed by the activation of fibers using alkali hydroxide (mostly sodium hydroxide) in aqueous media and converting of hydroxyl groups (Fig 2.13) using mono chloro acetic acid or sodium salt to carboxymethyl units (Fig 2.13) [114]. Nevertheless, this process has many drawbacks due to the use of toxic halocarbon reagents. In addition, the hydrophilicity level of the produced CNC increased compared to the original one, which can increase the problems of CNC dispersion in non-polar media and limit CNC applications.

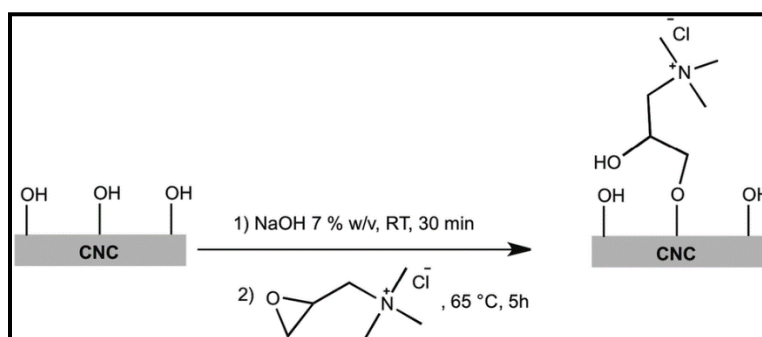


Figure 2.13. The etherification reaction of surface hydroxyl groups of CNC [114].

- **Oxidation**

In this method through the oxidation reaction with the help of 2,2,6,6-tetramethylpiperidine 1-oxyl (TEMPO) and a secondary oxidant -sodium hypochlorite or sodium chlorite- (to recycle the TEMPO) carboxyl and aldehyde groups are introduced on the surface of CNC (Fig.2.14). The

efficiency of this reaction is strongly dependent on several parameters such as reaction conditions and the purity of raw materials [115]. In addition, the reaction is very sensitive to pH changes for example, at pH below 8.0 the reaction rate is very slowly and also selectivity between primary and secondary alcohols[115, 116].

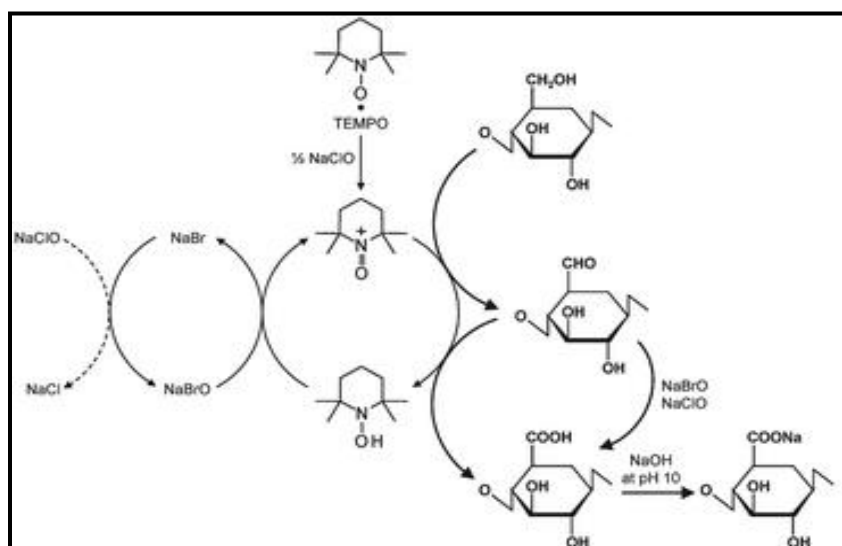


Figure 2.14. The surface oxidation of CNC to carboxylate groups by TEMPO oxidation in water[116].

- **Isocyanate coupling**

In this method of CNC surface modification, a chemical reaction occurs between the isocyanate groups and hydroxyl groups of CNC. This method of CNC functionalization is not common as much as the previous methods due to the high price and high toxicity level of raw materials, which restrict its application. However, it has some advantages compared to other chemical modification method namely; chemical stability of urethane unit, high reaction rate as well as the absence of by products during modification process [117] .

- **Polymer grafting**

Polymer (or copolymer) grafting is an another approach to chemical surface modification of CNC[118]. This method is preformed by the grafting (or in situ polymerization) of polymer chains

onto the surface of CNC (Fig 2.15) [119]. The methods of polymer grafting onto the surface of cellulosic materials can be divided on three main groups; (1) free radical polymerization, (2) ring-opening polymerization and (3) living radical polymerization [118, 120].

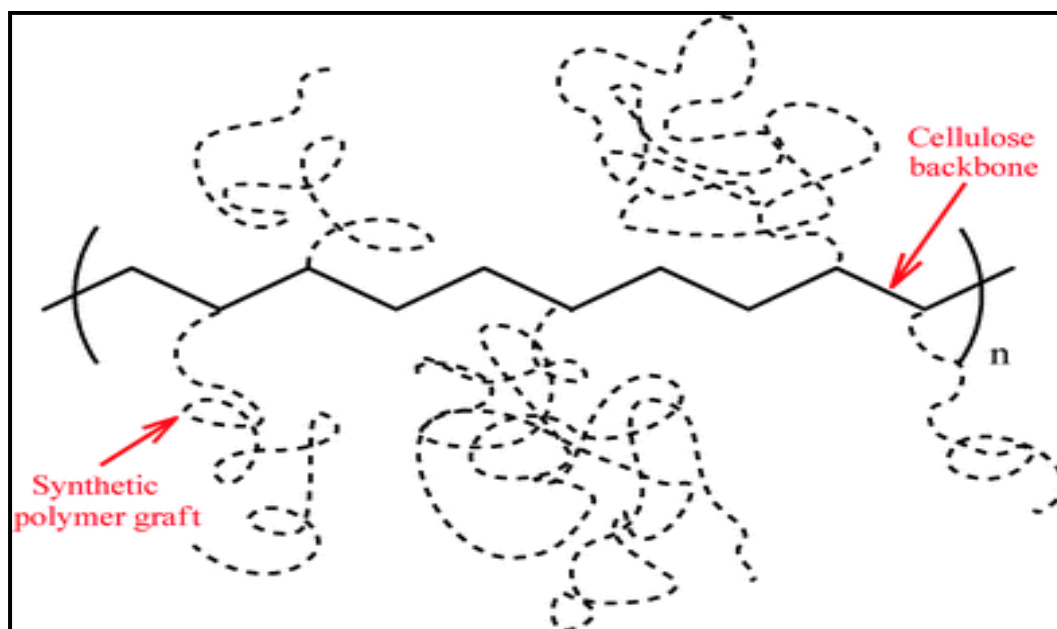


Figure 2.15. Schematic of polymer grafting on CNC surface (adapted from [118]).

As mentioned, ring opening polymerization (ROP) is used to graft and surface functionalize CNC [121]. *Goffin et al.* reported the grafting of poly L-lactic acid (PLLA) chains using ROP on the CNC surface without any impact on the crystallinity degree and morphology [122]. However, the thermal stability and mechanical properties of the functionalized CNC decreased due to the crystallization behavior and the presence of polymer short chains.

The grafting of polycaprolactone (PCL) on CNC (Fig 2.16) using stannous octoate ($\text{Sn}(\text{Oct})_2$) as a catalyst was also reported [123]. In this work, the grafted PCL chains were long enough and they did not show negative effect on the properties of CNC. They reported the compatibility of PCL-g-CNC with PCL matrix. However, the compatibility of grafted CNC with another matrix has not been reported.

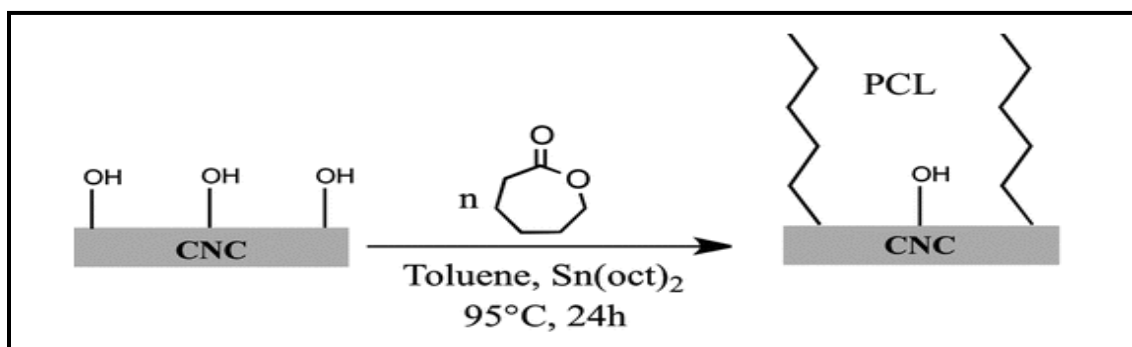


Figure 2.16. Grafted PCL on CNC surface using stannous octoate [123].

- **Gas phase treatments**

Gas phase treatments (solvent free approaches) are a new stream for surface functionalization. Heat, light and plasma can be used to functionalize substrates [27]. However, very little work has been conducted in the gas phase for CNC. *Javanbakht et al.* [26] modified the surface of CNC using gas-phase photo-initiated chemical vapor deposition (PICVD). In this study, the surface modification of the CNC was performed using a PICVD micro-reactor. In the process of surface modification, CNC was first mechanically dispersed in toluene and deposited onto polished copper, then, it was placed inside the tubular reactor. Afterwards, a gas mixture of H₂ and CO was injected and irradiated by two UV lamps. They demonstrated that this technique improves the compatibility of CNC surface with semi-polar and non-polar solvents. These methods are efficient and eco-friendly, However, in terms of process cost, this method requires specific equipment which may increase the production cost and hence, remain limited to higher value-added products.

Work conducted on cellulose in the gas phase may also be an interesting source of complementary information in this field. *Couturaud et al.* reported an increase in the compatibility of cellulose and poly(L-lactide) film as hydrophobic surface through plasma-induced grafting of L-lactide[124].

- **Click chemistry**

The clicking approach is also a new approach to surface engineering [125]. Recently, *Feese et al.* used the Cu(I)-catalyzed *Huisgen–Meldal–Sharpless* 1,3-dipolar cycloaddition reaction to surface immobilize cationic porphyrin[126]. Some functionalization of CNC was also

performed using click chemistry [127]. However, due to overall cost of click chemistry methods, they will be limited to specific cases.

As highlighted in the various descriptions, covalent modification methods are often time-consuming and involve the use of organic solvents, which can cause major environmental issues and increase the production expenses [27]. It is noteworthy that the chemical modification can change the structure of cellulose to some extent and consequently decrease the mechanical and thermal properties [28, 128].

2.5.2. CNC surface modification using non-covalent methods

Non-covalent surface modification through the physical adsorption of a surface modifier (surfactant) is another approach for CNC surface modification [30, 32]. Theoretically, coating the surface of CNC using a surfactant through simple mixing is the easiest method to increase the compatibility of CNC with non-polar media. Indeed, the adsorption of a surfactant (or polymer) on CNC should be easier to control than chemical reaction for modification [129]. Non-covalent surface modification of CNC can be done through cationic or non-ionic methods [28, 55].

Owing to the presence of negatively charged groups on commercial CNC surfaces, cationic surface modification is a more common non-covalent method to modify CNC surface [30-32]. However, non-ionic CNC surface modification has also been reported [130, 131].

The improvement of the CNC dispersion in organic solvents using a non-ionic surfactant (sorbitan monostearate) was reported by *Kim et al.* [132]. Based the results of turbidity analysis, they reported that the concentration of surfactant can determine the stability of the modified CNC in surrounding media. Recently, *Zhou et al.*[131] reported a new approach for non-ionic CNC surface modification based on the adsorption of saccharide-based amphiphilic block copolymers. They showed that the adsorption of xyloglucan oligosaccharide-poly (ethylene glycol)-polystyrene triblock copolymer onto the surface of CNC increases the dispersibility of CNC in non-polar solvents.

- **Cationic surface modification**

As mentioned in section 2.1, commercial CNC contain sulfate half-ester groups (OSO_3^-) on the surface. These groups form an electrostatic layer around the particles leading to a stable CNC aqueous suspension. In the other hand, these negative charges promote the electrostatic adsorption of cationic groups on the surface of CNC.

Heux et al. [29] used a phosphoric ester of polyoxyethylene 9-nonylphenylether (Beycostat NA) as a cationic surface modifier to prepare stable suspensions of CNC in non-polar solvents. They mentioned that a low weight ratio of surfactant to CNC (< 4 wt. %) in suspensions was not sufficient to obtain a good dispersion in organic solvents. The adsorbed amount of surfactant to achieve full coverage of CNC by the surfactant was determined to be 44-61%, corresponding to 0.79-1.56 g of surfactant per g of CNC. The method used by *Heux et al.* was a simple and effective technique to improve the dispersion level of CNC in non-polar media. However, to achieve efficient surface coverage a high amount of modifier was used, which affected the properties of final product. In a subsequent study, these modified CNC were nevertheless used to reinforce a polypropylene (PP) matrix [18] with improved dispersion. The enhancement of CNC dispersion in a low polarity solvent (tetrahydrofuran (THF)), through cationic surface modification with hexa-decyl-trimethylammonium bromide (HDTMA) as a cationic surfactant was also reported [33]. *Ansari et al.* [133] modified CNC using a cationic surfactant (dedecyltrimethylammonium chloride) through interactions between the positively charged ammonium groups and the negatively charge half-ester sulphate group. They found that the modified CNC showed superior mechanical properties in poly vinyl acetate due to the improvement of interfacial interaction as well as the improved dispersion level in the polymer matrix.

2.6. Conclusion of the literature review and organization of the thesis

There are several obstacles to modify the interactions of CNC with host matrix and develop the applications for this nanomaterial to enter the market of commercial nanofillers.

Various studies have been performed to change the surface properties and increase the compatibility of CNC with non-polar matrix. As mentioned, each covalent and non-covalent approaches have some limitations and restrictions. In the most developed methods of CNC surface

modification through the non-covalent approaches, large amounts of surface modifier are required to cover the CNC surfaces, which can affect the properties of the prepared composite and increase the cost of the final products. Until now, no industrial CNC modification method to improve their use in polymer composites has been reported. Therefore, to develop the CNC market and CNC applications, it is necessary to find a novel and effective surface modification method, which can be easily applied in industrial scale with minimum cost.

In this work, a cationic polymer, polyethyleneimine (PEI), is used to modify the surface of CNC. PEI has a high density of amine groups and a unique branched structure capable of binding with negative groups of the CNC surface at low concentrations. Recent studies have already demonstrated that PEI is an appropriate candidate to functionalize carbon fillers and improve the mechanical interfacial properties of composites [134].

The main objective of this work is to modify CNC surface through a low cost, efficient and eco-friendly process using PEI, to change the surface properties and increase the compatibility of CNC with non-polar media. The results of CNC modification with PEI are discussed in *Chapter 3*. In addition, the modification of CNC surface properties using two grades of a bio cationic polymer (chitosan) were also preliminary investigated and their results are presented in *Chapter 4*.

CHAPTER 3 CNC SURFACE MODIFICATION WITH PEI

3.1. Materials

➤ Cellulose nanocrystals (CNC)

Spray-dried cellulose nanocrystals (CNC) obtained through sulphuric acid hydrolysis of commercial dissolved softwood pulp were supplied by *CelluForce (Canada)*. The CNC was used in samples modification without any treatment.

➤ Polyethyleneimine (PEI)

PEI exists in both linear and branched molecular structures; a branched PEI contains all types of primary, secondary and tertiary amine groups while a linear PEI contains only secondary and primary amine groups[41]. This cationic polymer exhibits one of the highest charge densities among polyelectrolytes when protonated in aqueous solution [42]. The study of intrinsic viscosity and small-angle neutron scattering of aqueous solutions of branched PEI showed that the conformation of this polymer does not change significantly over the pH range of 2 to 11, due to its highly branched structure [105, 135]. In this study, branched PEI purchased from *Sigma Aldrich Canada* was used (99% purity, M_w 25,000 g mol⁻¹, polydispersity 2.5, density 1.030 g mL⁻¹).

3.2. Preparation of samples

In a typical batch of CNC modification, spray-dried CNC were added in deionized (DI) water at pH 6.8. An ultrasonic homogenizer (Cole-Parmer model CP505 500 W) was used to disperse CNC in DI water at a total energy dose of 2000 J/g_{CNC}. Ultrasonication was carried out in an ice bath to avoid local temperature increases and de-esterification of CNC surface groups [8]. To increase efficiency, ultrasonication was applied in three steps at progressively lower concentrations **1)** 500 J/g_{CNC} at CNC concentration of 2 wt. %; **2)** diluting the suspension to 1.5 wt. % of CNC and applying 500 J/g_{CNC} and **3)** decreasing the concentration to 1 wt. % and applying an additional 1000 J/g_{CNC}.

PEI was separately dissolved in DI water (at a concentration of 0.001 g.mL⁻¹) at pH 6.8. To promote dissolution, it was heated at 50 °C and mechanically stirred using a magnetic stirrer for 30 min at

a speed of 300 rpm. Then, the PEI solution was diluted to concentrations of 0.0001, 0.0002 and 0.0005 g mL⁻¹. They were subsequently added dropwise to the CNC suspensions and mechanically stirred at 50 °C at a speed of 500 rpm for 4 h. Modified CNC suspensions with 1 wt. % CNC concentration and different PEI/CNC ratios were prepared. No pH adjustment was done. The PEI/CNC suspensions were quickly frozen at -20 °C for 48 h and then were put into a freeze-dryer (FreeZone 2.5 plus, Labconco, Kansas City, MO) for 72 h under vacuum (temperature of internal chamber -87 °C), yielding a white flaky dried modified CNC (mCNC). Modified CNC were used for characterization in further sections.

		PEI (g)	CNC (g)
Modified CNC samples	• PEI/CNC 1%	0.01	1.00
	• PEI/CNC 2 %	0.02	1.00
	• PEI/CNC 5%	0.05	1.00

The schematics of CNC surface modification with PEI are presented in Fig. 3.1.

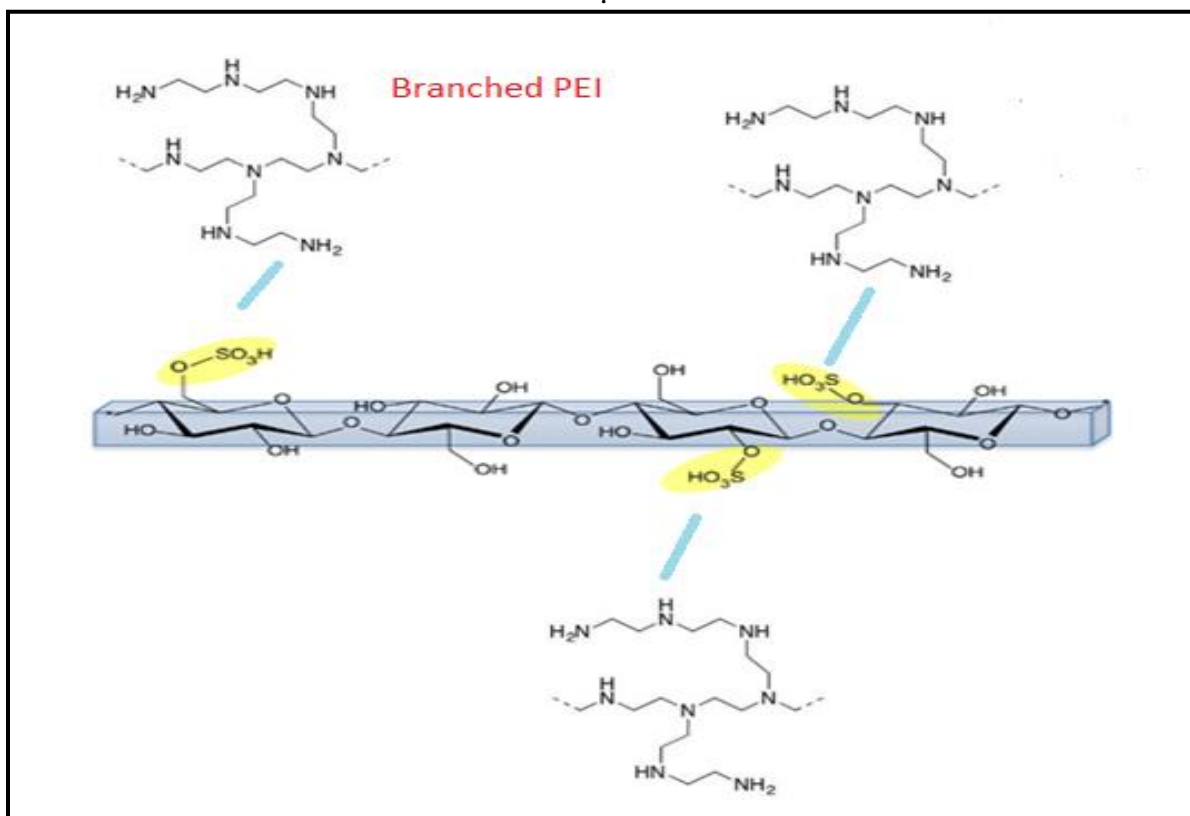


Figure 3.1. Schematic illustration of CNC surface modification with PEI

3.3. Characterization of modified CNC

3.3.1. X-Ray Photoelectron Spectroscopy (XPS)

XPS was used to characterize the surface of mCNC. C1s, O1s and N1s high-resolution spectra of the pristine CNC and mCNC were obtained by XPS model VG ESCALAB 3 MKII. A fine powder of pristine CNC and mCNC was used in XPS characterization. During the analysis, the pressure of chamber was kept at 5×10^{-9} Torr. The take-off angle was fixed at 90° with respect to the sample surface. All spectra were obtained with a source of Mg K α at 300W and the analyzed depth was less than 10 nm. In high resolution scans, the energy pass and energy step size were 20eV and 0.05eV respectively. The Shirley method was used to correct the background contribution [136].

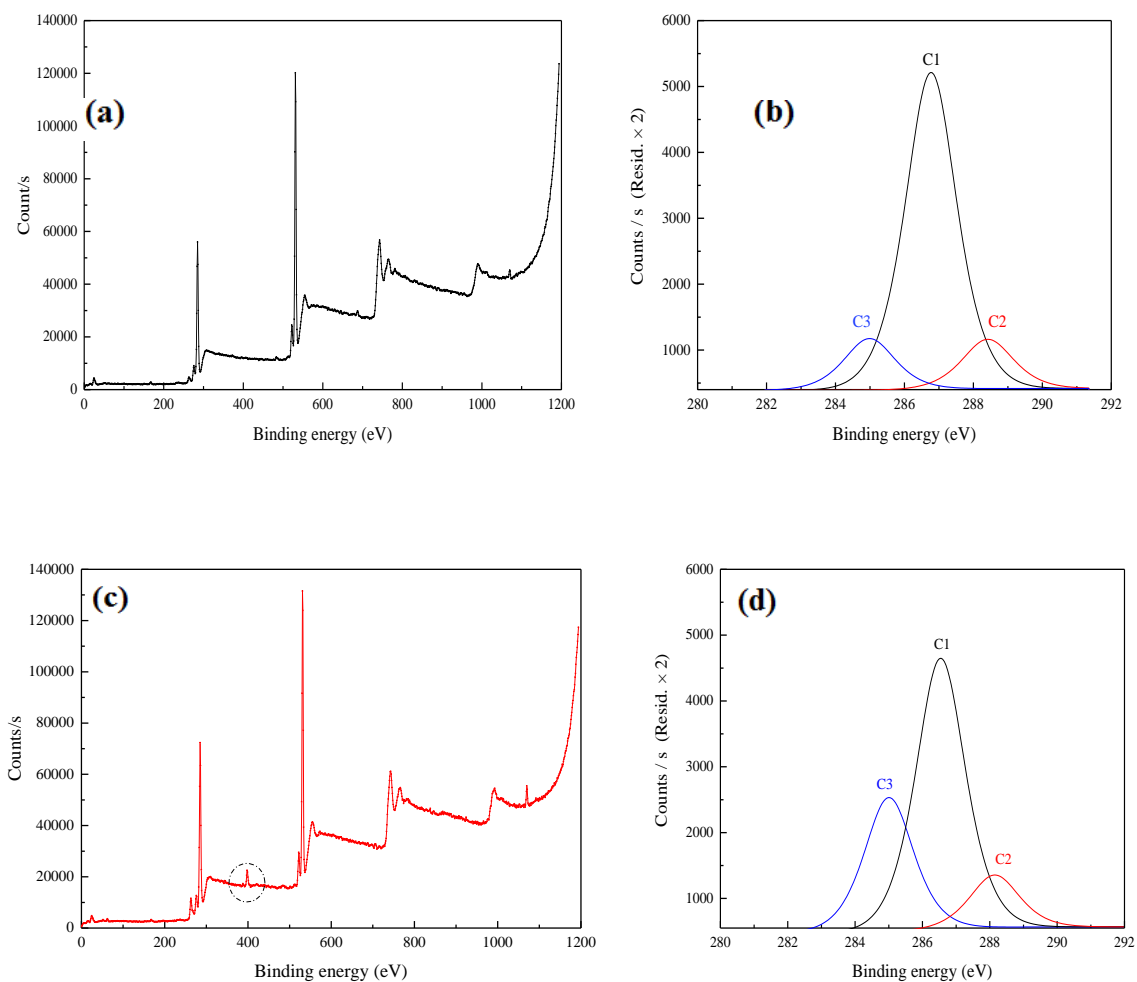


Figure 3.2. XPS survey spectra and decomposition of C1s signal into its constituent contributions for (a,b) pristine CNC and (c,d) mCNC with PEI/CNC 2%

No nitrogen signal was detected for the pristine CNC within the investigated range in the survey scan (Fig. 3.2a). After surface modification, a nitrogen peak appeared around 400 eV (Fig. 3.2c), indicative of PEI presence on the CNC surface. This result confirmed the successful modification and the presence of amine groups onto the CNC surface, the similar results was also reported in the case of CNC stabilized with the cationic surfactant 2,3-epoxypropyl trimethylammonium chloride (EPTMAC) [35]. The high-resolution C1s peaks for pristine and mCNC were resolved into three Gaussian component peaks, giving further information about the structure of bonded carbons before and after surface modification (Fig. 3.2b and 3.2d): C-C or C-H at 285.0 eV (C3),

C-O at 286.6 eV (C1) and O-C-O at 288.1 eV (C3) [137]. The ratio between the area under the peaks representing C-O (C1) and O-C-O (C2) bonds within cellulose chains, remained approximately constant before (1.04) and after (0.97) surface modification. This indicates that the modification did not change the nature of underlying cellulose. However, a substantial increase in the percentage of C-C or C-H (C3) was observed due to the presence of alkane chains from PEI, further in agreement with *Li et al.* [35]. The nitrogen level gives an indication of the PEI affinity for surface adsorption. The successful surface modification was also confirmed through the increase of both C and N, as well as the decrease in the O/C ratio in the case of mCNC (Table 3.1).

Table 3-1. XPS analysis of CNC before and after surface modification with PEI

Name	Binding Energy (eV)	Identification	Relative atomic %		
			Pristine CNC	mCNC	
				PEI/CNC 1 %	PEI/CNC 2 %
C1s	285.0	C-C or C-H (C3)	6.4	17.3	17.2
	286.6	C-O in cellulose (C1)	40.2	35.0	36.7
	288.1	O-C-O in cellulose (C2)	6.3	6.8	7.2
	TOTAL			53.0	59.1
N1s	399.2	Amine	-	2.4	2.1
	400.1	Amide	-	1.1	0.9
	401.7	Protonated N	-	0.3	0.3
	TOTAL			0	3.8
O1s	531.4	O=C-N	-	3.5	2.1
	532.6	C-OH in cellulose	28.2	20.2	20.6
	533.2	C-O-C	18.8	13.5	13.1
	TOTAL			47.0	37.2

BE: Binding energy of corresponding atomic orbital

Survey O1s and N1s for pristine CNC and mCNC are presented in appendix A.

3.3.2. Fourier Transform Infrared spectroscopy (FTIR)

FTIR was used to chemically characterize the CNC before and after surface modification. A fine powder of dried pristine CNC and modified CNC (mCNC) was used in FTIR characterization. A Perkin Elmer Spectrum 65 FTIR spectrometer equipped with a Zn/Sr crystal, in the range of 650–4000 cm^{-1} was used. For each sample 32 scans were recorded at a resolution of 4 cm^{-1} .

Fig. 3.3 presents the FTIR spectra of pristine CNC and mCNC for different PEI/CNC ratios. All characteristic peaks of cellulose were observed in FTIR spectra of both pristine CNC and mCNC: at 1109 cm^{-1} , 1162 cm^{-1} , between 1300 and 1440 cm^{-1} and between 3100 and 3600 cm^{-1} , related to O-H association, C-O-C stretching vibration, C-O stretching vibration, O-H bending vibration and O-H stretching vibration, respectively[138]. All these peaks showed the typical bonds of cellulose molecules and indicated that the surface modification did not affect the nature of CNC [139]. Moreover, two peaks at 2985 cm^{-1} and 1480 cm^{-1} (pointed by arrows on Fig. 3.3) appeared in the spectra of mCNC, which correspond to R_xNH and NH_3^+ groups, respectively. The successful surface modification of CNC was hence confirmed by the appearance of these two peaks in FTIR spectra of mCNC. The same peaks were observed for chemical grafting of PEI onto cellulose nanofiber [134].

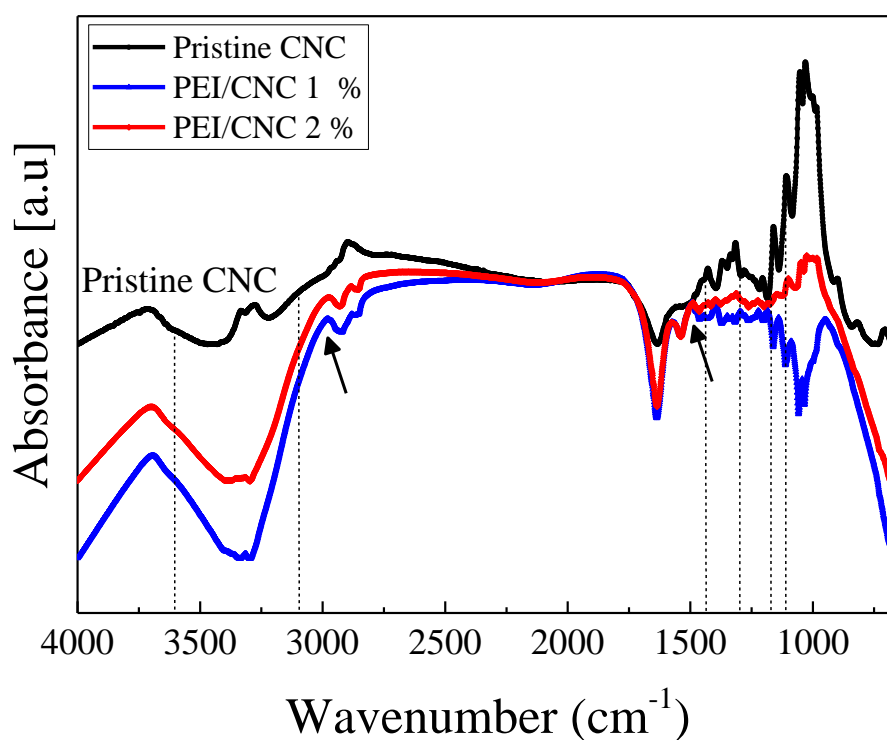


Figure 3.3. FT-IR spectra of pristine CNC and mCNC with PEI/CNC ratio 1 and 2 %

3.3.3. Particle size measurements through dynamic light scattering

Dynamic light scattering (DLS) was used to determine the equivalent hydrodynamic diameter of mCNC. Pristine CNC and mCNC were dispersed in DI water (pH 6.8) at a very low CNC concentration (0.05 wt.%) [140, 141]. Ultrasonication energy (2000 J/g_{CNC}) was applied to the suspensions. Particle size distribution of pristine CNC after applying 2000 J/g_{CNC} ultrasonication energy) is presented in Fig 3.4. DLS measurements were performed using Malvern Zetasizer Nano-S (ZS) instrument with a detection angle of 173°. The non-invasive backscatter detection of light at an angle of 173° improved the sensitivity, reduced multiple scattering issues, and minimized the effects of large particle contaminants. All the measurements were performed at 25 °C and repeated three times to obtain the average values.

The equivalent hydrodynamic size (*Z*-average) and polydispersity index (PDI)⁵ of pristine CNC and mCNC are presented in Table 3.2. In this method, the diffusion of particles moving under Brownian motion are measured and converts to size using the *Stokes-Einstein* relationship:

$$D = K_B T / 6\pi\eta R \quad \text{Eq.3.1}$$

D : Diffusion constant

K_B: Boltzmann's constant

T: Temperature

η: Solvent viscosity

R: The radius of equivalent spherical particle

Knowing that CNC particles are rod-like and *Stokes Einstein* equation is for the diffusion of spherical particles, the size of CNC particles measured by DLS is not the exact size of particle.

⁵ PDI is 0.0 for a perfectly uniform sample and PDI ≥ 0.7 (very broad distribution) indicates that sample is not suitable for DLS measurements.

However, the results can be used for comparison between different samples (before and after surface modification).

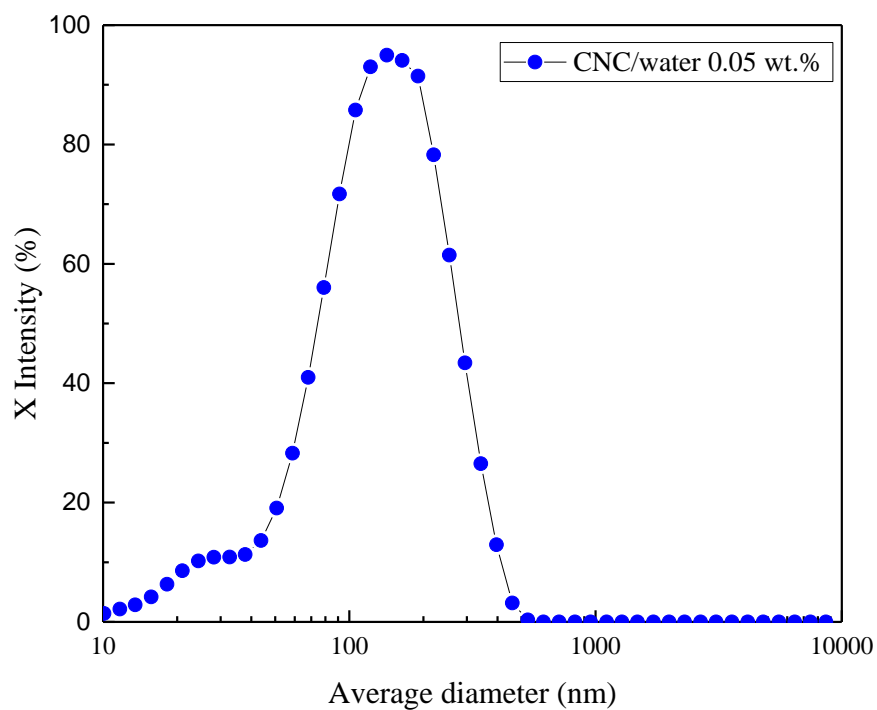


Figure 3.4. The CNC particle size distribution in CNC water suspension at concentration of 0.05 wt.%

Table 3-2. Z-average hydrodynamic size and PDI of pristine CNC and mCNC at (T= 25 °C)

Sample		Average diameter (nm)	PDI
Pristine CNC		121 ±1	0.29
mCNC	PEI/CNC 1%	189 ±5	0.38
	PEI/CNC 2 %	319 ±6	0.51

The hydrodynamic diameter of CNC increased after surface modification (Table 3.2). This is attributed to PEI adsorption onto CNC surface via strong electrostatic interactions and possible hydrogen bonding. Similar results were also reported by *Huang et al.* [81] for CNC modification with quaternary ammonium.

3.3.4. Zeta potential measurements

Zeta potential measurements were performed using Malvern Instruments Zetasizer (Nano ZSP). The samples were prepared as for DLS measurements at CNC concentration of 0.05 wt.%. The electrophoretic mobility of particles was measured and using the *Smoluchowski* equation, electrophoretic mobility values were converted to zeta potential values (ζ -potential). ζ -potential was measured at different pHs, adding solutions of HCl 0.1 M and NaOH 12 M. All measurements were done at 25 °C and the reported values were an average of 15 measurements.

The ζ - potential as a function of pHs for pristine CNC and mCNC are presented in Table 3.3.

Table 3-3. ζ - potential of pristine CNC and mCNC at different pH (T=25 °C)

Sample		ζ - potential (mV) without pH adjustment	ζ - potential (mV) pH 3.0	ζ - potential (mV) pH 7.0
Pristine CNC		-52.0±2.1 (pH 6.7)	-33.0±0.1	-54.0±5.2
mCNC	PEI/CNC 1 %	-23.0±0.6 (pH 7.1)	-2.0±1.5	-24.0±0.2
	PEI/CNC 2 %	-20.0±2.7(pH 7.3)	18.0±0.7	-20.0 ±4.2

The ζ - potential can be affected by pH due to the presence of sulfate and amine groups (Table 3.3). At pH 7.0, pristine CNC showed a negative ζ - potential (-54.0 ± 5.2 mV) due to the presence of OSO_3^- on its surface. This value increased to -33.0 ± 0.1 mV when pH decreased to 3.0, due to the partial protonation of the sulfate half-ester groups [142].

After modification, mCNC (PEI/CNC 1 %) showed a decrease in absolute value of ζ - potential to -24.0 ± 0.2 mV at pH 7.0 and close to the isoelectric point (-2.0 ± 1.5 mV) when decreasing pH to 3.0. Furthermore, at pH 3.0 the ζ -potential became positive with increasing PEI concentration, indicative of surface coverage by the modifier [142].

PEI contains a high density of amine groups having various pKa, which explains its protonation degree at different pH. The pKa of each amine group is affected by the amine type (primary, secondary and tertiary, with pKa of 4.5, 6.7 and 11.3, respectively), steric factor and position within the polyamine structure[143]. The protonation degree of branched PEI with $M_w = 25,000$ g mol⁻¹ was reported as 55% and 75% at pH 7.0 and 3.0, respectively [144]. This extent of protonation explains the ζ - potential trend observed for mCNC. Such a significant increase in ζ - potential was also reported for PEI on silica surfaces [34]. It should be noted that, at pH 3.0 (for highest protonation degree), a significant ζ -potential difference was observed (+ 20 mV) between mCNC with 2 and 1 % of PEI/CNC ratio.

Coupled with the chemical characterization, these ζ -potential values strongly indicate the presence of PEI on the mCNC surface and the likelihood that dispersion into non-polar media will be possible.

3.3.5. Rheological measurements

Rheometry can be an efficient technique to characterize the dispersion state of nanoparticles in different media, because the rheological properties are sensitive to changes in particle size, shape and surface characteristics of the dispersed particles [145].

The process of CNC preparation from cellulosic materials can affect the rheological properties of CNC suspensions[67, 146, 147]. The charges on the CNC surface also affect the viscoelastic behavior of CNC colloidal suspensions [148, 149]. *Shafiei sabet et al.*[149], studied two CNC

suspensions with different charges levels. They demonstrated that changing the charges of the CNC greatly affect the viscoelastic, steady-shear properties and gel state of CNC suspensions. Because particle repulsive interactions among charged particles lead to larger viscosity values, due to the secondary electroviscous effect [150]. In another publication *Lenfant et al.* [151] demonstrated that the primary electroviscous effect, had a major contribution to the intrinsic viscosity of ECNC aqueous suspensions, being a function of both pH and ionic strength. The intrinsic viscosity was correlated with the charges on the particles obtained from zeta potential (ζ) measurements.

All rheological measurements were performed using a rotational rheometer (MCR 502, Anton Paar) using a double-Couette flow geometry at 25 °C. In small-amplitude oscillatory shear (SAOS) experiments, the linear viscoelastic region was first determined using strain sweep tests ($\gamma = 1$ to 100%) at two angular frequencies ($\omega = 1$ and 10 rad s⁻¹). Then, SAOS tests were carried out in the angular frequency range of 0.1 – 100 rad s⁻¹. The complex viscosity (η^*), storage modulus (G') and loss modulus (G''), for pristine and PEI/CNC aqueous suspensions, were measured. Before starting the SAOS test, a pre-shearing at a shear rate $\dot{\gamma}$ of 10 s⁻¹ for 1 min was applied and followed by 2 min rest time. Steady-shear experiments were also performed in a range of $\dot{\gamma} = 0.1$ to 100 s⁻¹. A thin layer of mineral oil was placed on the surface of samples to prevent water evaporation during the rheological measurements, and was shown not to affect the tests. It should be mentioned that the rheological measurements were performed in aqueous suspensions for CNC concentrations of 1 wt. % before drying the modified particles. Indeed, after freeze-drying, mCNC quickly precipitated in DI water and did not form a homogenous suspension during rheological measurements. The measurements were performed immediately after surface modification due to the increase of the viscoelastic properties of PEI/CNC aqueous suspension and gel stiffness gain over time. All the experiments were performed at least three times to verify repeatability. The complex viscosity (η^*) and steady shear viscosity (η) were measured for aqueous suspensions of pristine and PEI/CNC, and the Cox–Merz relation $\eta^*(\omega) = \eta(\dot{\gamma})$ [152] was used to compare steady shear and complex viscosity in the same graph (Fig. 3.5a). The viscoelastic properties of pristine and PEI/CNC aqueous suspensions (G' and G'') are also presented in Fig. 3.5b.

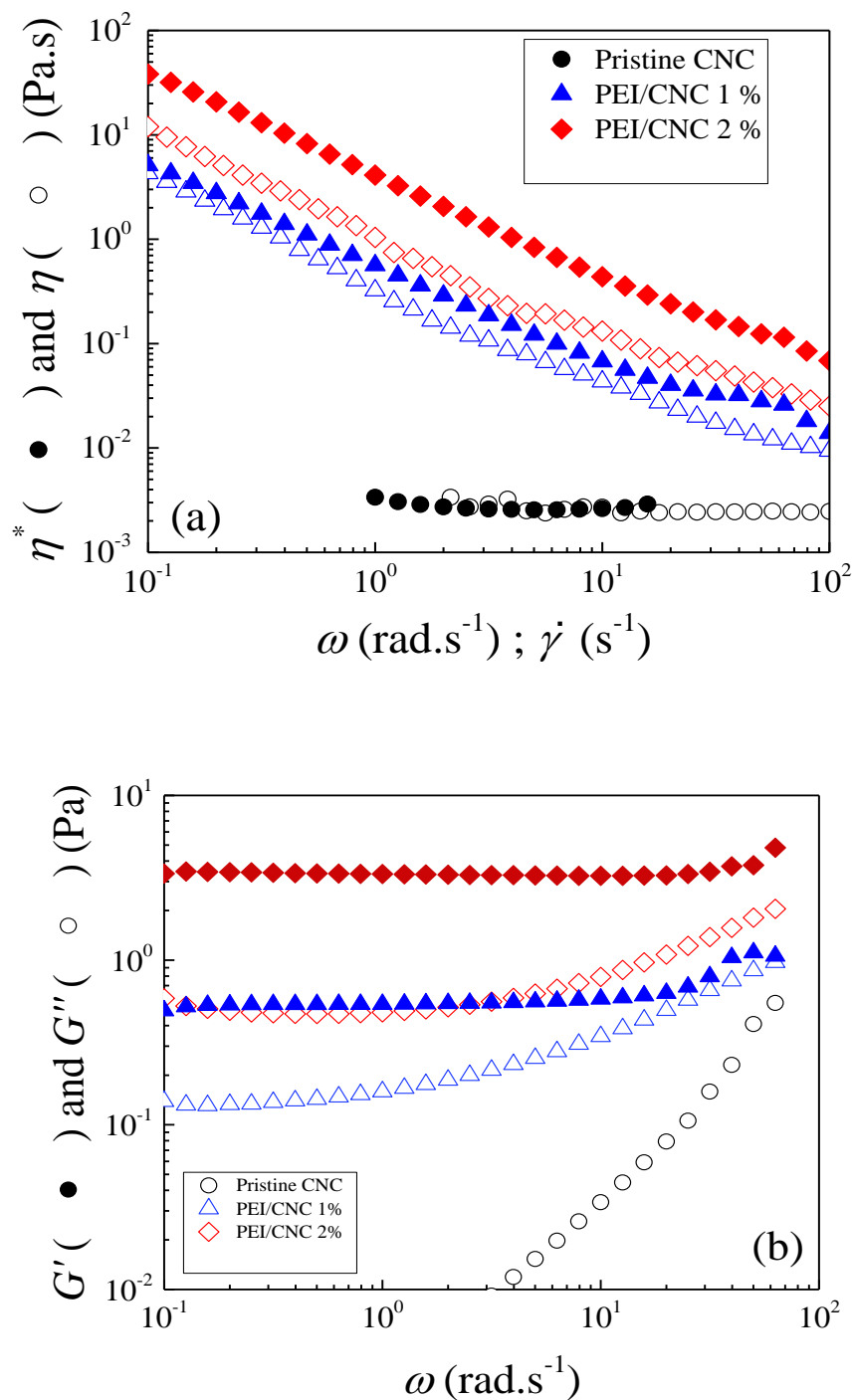


Figure 3.5. a) Steady shear viscosity η (open symbols), complex viscosity η^* (solid symbols) as a function of shear rate $\dot{\gamma}$ and angular frequency ω , respectively b) Storage modulus G' (solid symbols) and loss modulus G'' (open symbols) as a function of angular frequency ω .

As shown in Fig 3.5a, Newtonian behavior was observed for the pristine CNC aqueous suspension at 1 wt.%. Regarding the pristine CNC, only G'' values were measurable, confirming the Newtonian liquid-like behavior of this system (Fig. 3.5b).

On the other hand, the addition of a very low amount of PEI in the system generated a notable shear-thinning, and complex and steady shear viscosity increased with increasing PEI concentration (Fig. 3.5a). Indeed, at low frequencies/shear rates, yield behavior was observed for all PEI/CNC suspensions (Fig. 3.5a). Both storage and loss moduli exhibited a plateau over the whole frequency range and G' was higher than G'' (Fig. 3.5b), characterizing a gel-like structure. Moreover, both G' and G'' increased with increasing PEI ratio up to 2%.

While pristine CNC solutions obeyed the Cox-Merz rule (Fig. 3.5a), PEI/CNC did not follow this rule and higher η^* values were observed compared to η . The gap between these two types of viscosity increased with PEI ratio up to 2 %. This indicates that a structure of agglomerates formed in aqueous suspensions. Shear flow breaks down this network structure and the oscillatory data are higher than steady shear data. In fact, the Cox-Merz rule is only valid for isotropic CNC systems with negligible structure [92, 153]. It should be mentioned that the viscoelastic behavior of PEI/CNC aqueous suspensions was time-dependent; G'' was approximately constant while a 24% increase in G' was observed over 1800 s for the samples (Appendix B).

3.3.6. Contact angle measurements

The contact angle measurements of CNC surface and DI water were done using the sessile drop method (2 μL per drop at a rate of 2 $\mu\text{L/s}$) at room temperature. To prepare a smooth surface and to minimize the porosity of the surface a disk was made from the fine powder of pristine CNC and mCNC (Fig.3.6) using a mini cold press. To avoid the effect of humidity the measurement was done directly after the disk preparation.

The sessile drop contact angle being stable on the minute time frame, one measurement per location was taken immediately using a FDS tensiometer (OCA DataPhysicsTBU90E). Measurements were taken at several spots on the surface of pristine CNC and mCNC. The images were taken 2s after deposition of the DI water drops on the CNC surface.



Figure 3.6. Prepared samples for contact angle measurements.

Fig 3.7 shows the contact angles of the: (a) Pristine CNC and (b) mCNC (PEI ratio of 2 %) with water. The water contact angle of pristine CNC obtained ($43\pm 3^\circ$) which was very close to obtained value ($45\pm 1^\circ$) by *Khoshkava et al.* [62] for unmodified spray-dried CNC. *Salajková et al.* [31] reported a water contact angle of 48° for unmodified cellulose nanocrystals.

The contact angle between water and mCNC with (PEI/CNC 2%) increased to $57\pm 16^\circ$, which indicates that a slight increase in hydrophobicity. However, a broad range of contact angle was observed due to the porosity and non-homogenous surface of modified CNC [154-157]. These values are comparable with the solvent-based silylation performed by *Goussé et al.* [110]. Similar results were also reported for CNC surface modification using gas-phase PICVD [26].

It should be mentioned that based on the macroscopic observation, the water droplets on the surface of the CNC tablets quickly adsorbed. However, the water droplets on the surface of mCNC disappeared at a much slower rate.



Figure 3.7 . Contact angles of: (a) pristine CNC and (b) mCNC (PEI/CNC 2%).

3.3.7. The dispersion of mCNC in fresh DI water and organic solvents

To evaluate the hydrophobicity level of CNC after modification, pristine and mCNC (PEI/CNC 2 %) were dispersed in DI water (RPI 1) at pH 6.8 and organic solvents with different Relative Polarity Index (RPI) [158]; ethanol (RPI 0.654), isopropanol (RPI 0.546), toluene (RPI 0.099) and cyclohexane (RPI 0.006) as shown in Fig 3.8.

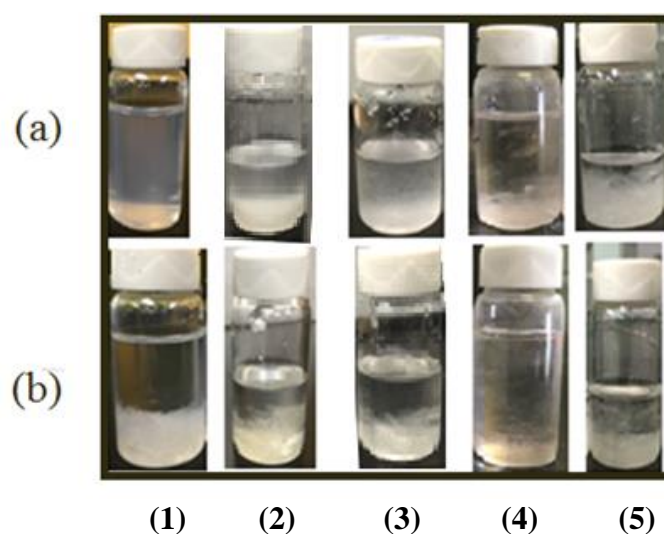


Figure 3.8.Dispersion state of (a) pristine CNC (b) mCNC (PEI/CNC 2%) in (1) DI water (2) ethanol (3) isopropanol (4) toluene (5) cyclohexane.

As expected, pristine CNC showed a stable dispersion in DI water (Fig. 3.8a.1). However, the mCNC precipitated in DI water, even after applying 5000J/g_{CNC} ultrasonication energy (Fig. 3.9). This observation correlates to the surface change of CNC after surface modification.

Pristine CNC could partially be dispersed in semi-polar solvents such as ethanol (Fig. 3.8a.2) and isopropanol (Fig. 3.8a.3). However, it did not disperse in toluene (Fig. 3.8a.4) and cyclohexane (Fig. 3.8a.5), with immediate sedimentation observed. This is expected for pristine CNC and is in agreement with previous reports[159]. Modified CNC with a PEI/CNC ratio of 2 % precipitated in ethanol (Fig. 3.8b.2) and isopropanol (Fig. 3.8b.3). However, they remained dispersed in lower polarity toluene (Fig. 3.8b.4). The mCNC precipitated in cyclohexane after 30 min (Fig. 3.8b.5), due to the very low polarity of this solvent compare to other non-polar solvents such as toluene[160] as well the polymer–solvent interaction (*Flory–Huggins* interaction parameter

χ) [161]. Similar behavior in toluene and cyclohexane had been reported for CNC modified with alkenyl succinic anhydride (ASA) [159]. Moreover, the compatibility of ASA-CNC with polypropylene as a non-polar matrix was also reported [159]. Therefore, our observations further demonstrate the hydrophobic nature of mCNC and suggest the efficiency of PEI to improve CNC dispersion in non-polar media such as polyolefins.

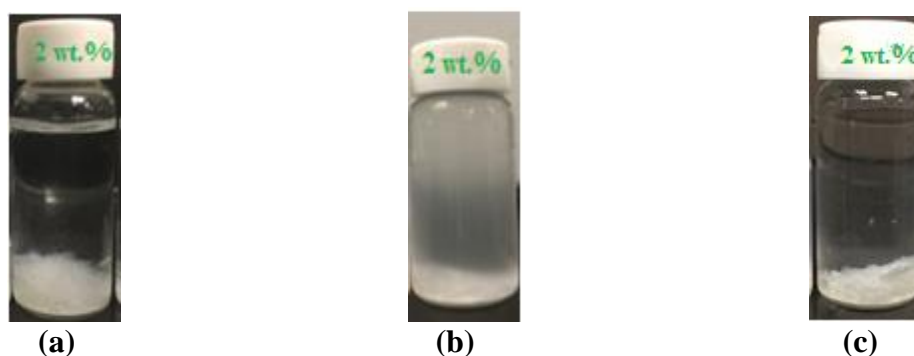


Figure 3.9. The dispersion of mCNC in DI water a) before ultrasonication b) 5 min c) 15 min after applying ultra sonication energy.

3.3.8. Precipitation rate and the stability of modifier using UV-Vis spectroscopy

UV-Vis spectroscopy was used to evaluate the stability of CNC in DI water before and after surface modification. UV transmission was measured as a function of time using UV-Vis spectrometer (Ocean optics DH-2000). Integration time and interval time were 10 ms and 1 min, respectively. Ultrasonication was applied at an amplitude of 20% for 15 s before starting the measurement. A specific volume (1 mL) of each sample at neutral pH was transferred to a plastic disposable cuvette with 1 cm path length for transmittance measurements at a wavelength of 657 nm, every 1 min for a total duration of 60 min. The transmission measurements were repeated three times for each sample. The concentration of CNC suspensions was kept at 1 wt.% and all the measurements were performed at room temperature.

Dispersion stability was also assessed in different media and as a function of temperature. Indeed, since the PEI surface modification is a non-covalent approach (*i.e.* physically grafted on the surface through electrostatic interactions), its stability after being in contact with a non-polar

medium could be challenging[162]. Hence, the efficiency and stability of surface modifier after being in contact with neutral medium (mineral oil) at two different temperatures (room temperature $\sim 22^{\circ}\text{C}$ and 70°C) was investigated. For this evaluation, mCNC (PEI/CNC ratio 2 wt. %) were dispersed in mineral oil and mechanically stirred at a speed of 200 rpm for 1 h at room temperature. The particles were then extracted using a Büchner funnel, washed three times with DI water and subsequently re-dispersed in fresh DI water at a CNC concentration of 1 wt. % (Cycle 1). The particles were then separated, dried at room temperature, and again re-dispersed in mineral oil. Afterwards the above-mentioned steps were repeated for a second cycle (Cycle 2). To investigate the effect of suspending media temperature on the efficiency of surface modifier, the same steps were repeated for the mixture of mCNC in mineral oil at 70°C for 1 h at a mixing speed of 200 rpm (Cycle 3). The precipitation rate of mCNC after each cycle was measured.

As shown in Fig .3.10, the water suspension of pristine CNC was stable over 60 min while, the mCNC precipitated in DI water in the 10 first minutes. This behavior was confirmed by macroscopic observations (Fig.3.9) and can be explained by the ζ - potential (Table.3.3).

The precipitation rate of mCNC (PEI/CNC 2%), did not change comparing to the initial modified sample after re-dispersion in mineral oil at room temperature and 70°C . This demonstrates that the PEI chains remain attached to the CNC surface despite coming into contact with an ionically neutral medium, due to strong electrostatic interaction and possible hydrogen bonding.

The stability of PEI on the CNC surface was also investigated through the study of relative viscosity of PEI/CNC suspensions at 22, 50 and 70°C (appendix B).

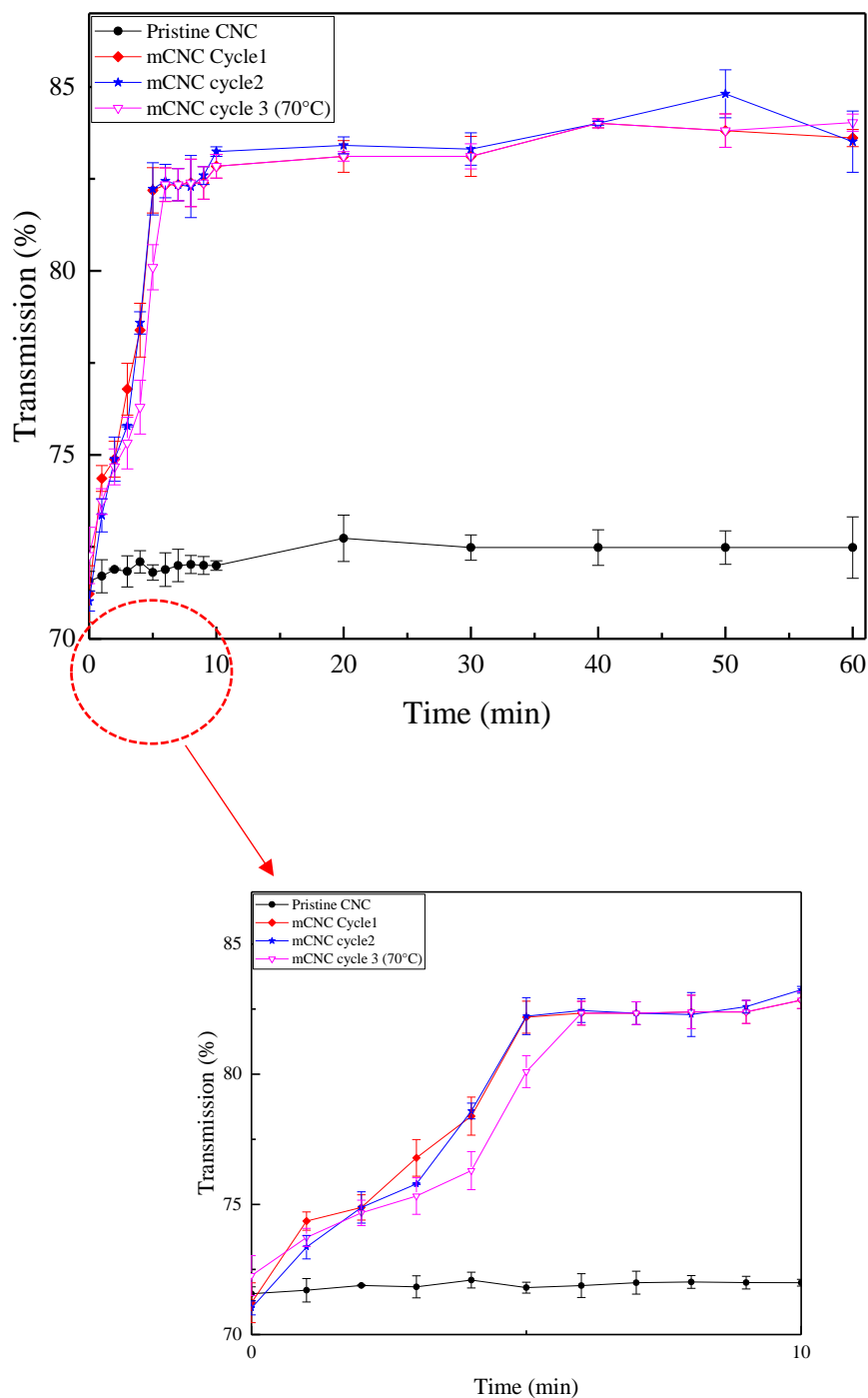


Figure 3.10. UV-Vis transmittance (at 656.732 nm) for pristine CNC and mCNC (PEI/CNC 2wt.%) water suspensions as a function of time and mineral oil cycling.

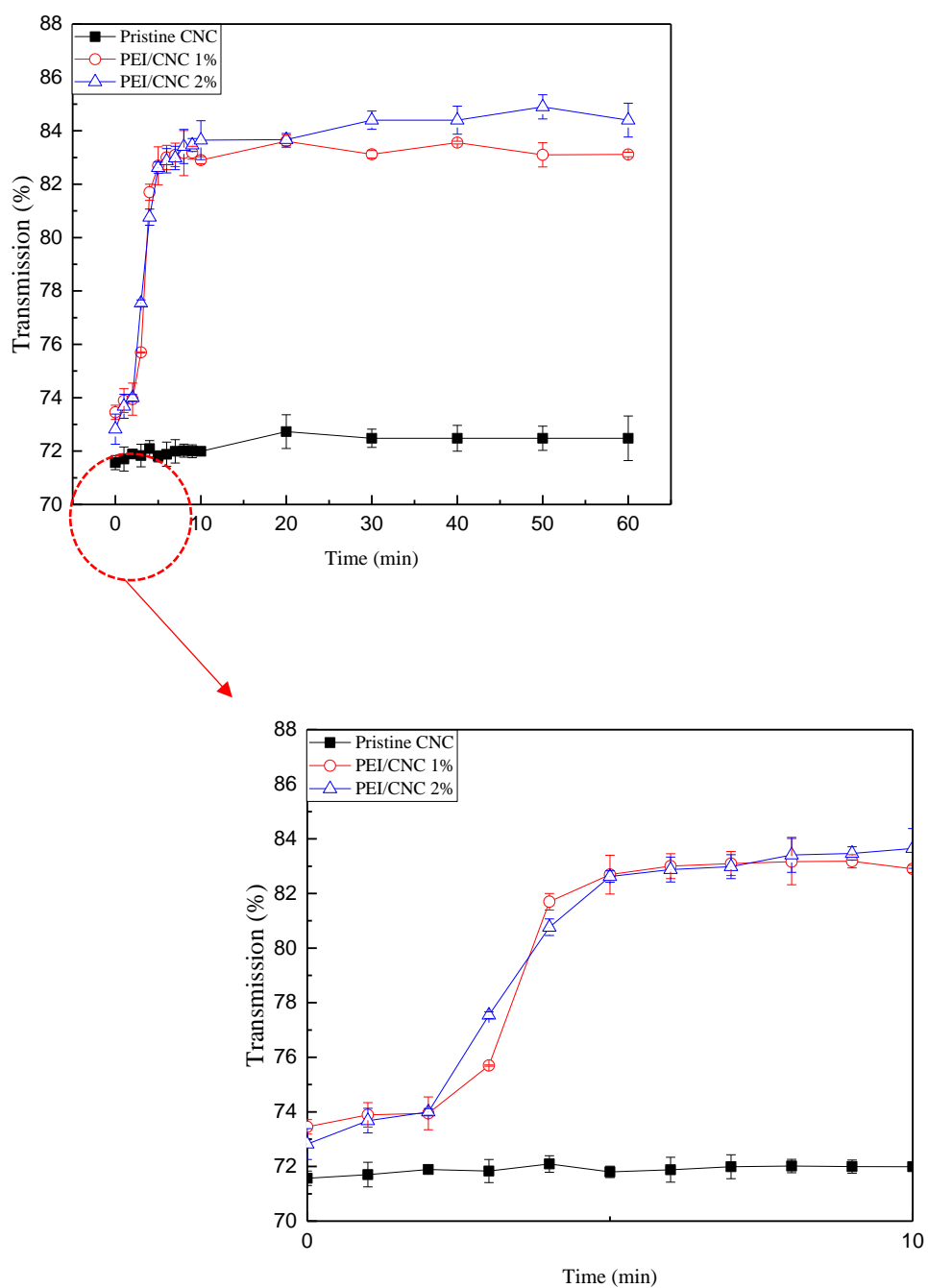


Figure 3.11. Percentage of the intensities of UV transmittance measured at maximum wavelength (656.732 nm) for water suspension of pristine and modified CNC (at concentration 1 wt.%) as a function of time at different PEI ratio.

No significant change was observed between the precipitation rate of mCNC with PEI ratio of 1 and 2 wt.%. It should be mentioned that, based macroscopic observation using very low amount of PEI (PEI/CNC ratio of 0.1 and 0.5 %) did not provide efficient CNC surface modification and the mCNC with PEI/ratio of 0.1 and 0.5 % made the stable aqueous suspensions (with a few visible agglomerate) over times.

3.3.9. Thermogravimetric Analysis (TGA)

The most common organic surface modifiers are not thermally stable at typical polymer nanocomposite processing temperatures [163]. The decomposition of surface modifiers can also affect the filler-matrix interfacial properties as well as physical and mechanical properties of the final product. Moreover, the degradation of polymer matrix can occur during preparation of nanocomposites due to modifier decomposition[164]. In addition, previous studies were reported the desorption and low efficiency of surface modifiers with increasing temperature (above 70 °C) [37, 38]

The thermal stability of modified CNC is a key issue and to assess this performance criterion for PEI modification, thermogravimetric analysis (TGA) of pristine CNC and mCNC was conducted. TGA analyses were carried out using a *TGA Q500* from TA Instruments. The measurements were done at a heating rate of 20 °C/min in air and nitrogen atmospheres⁶ with a flow rate of 60 and 40 mL/min respectively. Temperature range were between 50 to 800 °C and isothermal test was carried out at 220 °C over one hour in air atmosphere. The values of T_{onset} , $T_{10\%}$ and $T_{50\%}$ (corresponding to the beginning of the main degradation, 10% and 50% material weight loss, respectively) as well as the isothermal stability of mCNC close to the melt processing temperature (220 °C) of conventional polymer (polypropylene and polyethylene) are presented in Fig. 3.12 and Table 3.4.

⁶ -The TGA results in nitrogen are presented in Appendix C

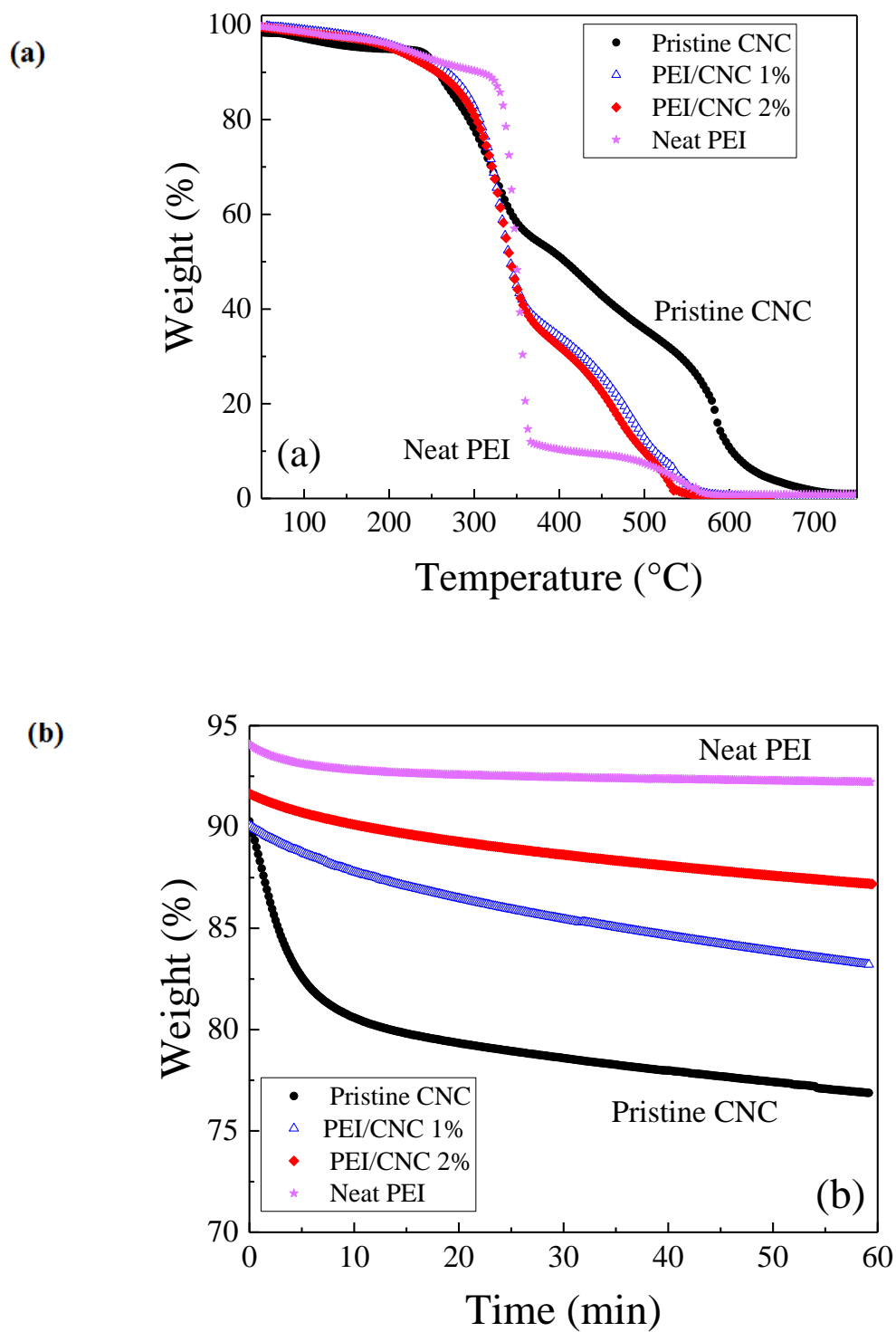


Figure 3.12 Weight as a function of **a)** temperature **b)** time at 220°C for pristine CNC, mCNC and neat PEI.

The thermal decomposition of pristine CNC and mCNC consisted of three main steps: [36] i) the evaporation of moisture at low temperature range ($T < 150^{\circ}\text{C}$), ii) the primary pyrolysis catalyzed with sulfate groups ($250^{\circ}\text{C} < T < 350^{\circ}\text{C}$), and iii) the slow charring process of the solid residue ($T > 350^{\circ}\text{C}$). As shown in Fig .3.13, PEI exhibited a main thermal degradation between 320°C and 350°C and then, a progressive carbonization from 500°C . T_{onset} increased to $\sim 264^{\circ}\text{C}$ for mCNC (PEI/CNC 2%), in agreement with a delay of the primary pyrolysis (Fig. 3.12, Table. 3.4).

Table 3-4.Characteristic thermal degradation temperatures

Samples		$T_{10\%}$ ($^{\circ}\text{C}$)	T_{onset} ($^{\circ}\text{C}$)	$T_{50\%}$ ($^{\circ}\text{C}$)	Isothermal weight loss (220°C for 60 min) (%)
Pristine CNC		265	248	406	14.0 ± 1.7
mCNC	PEI/CNC 1 %	276	263	345	6.0 ± 2.6
	PEI/CNC 2 %	273	264	343	4.0 ± 0.3
Neat PEI		312	320	347	0.8 ± 1.2

Furthermore, mCNC showed 4-6% weight loss in isothermal conditions, while pristine CNC showed $14.0 \pm 1.7\%$ weight loss (Fig. 3.12b, Table 3.4). These results suggest the covering of the sulfate half-ester groups with PEI, which can accelerated CNC degradation [36], leading to increase thermal stability and capacity of preparing CNC/polymer nanocomposite through melt processing.

3.4. Discussion

Two possible mechanisms are considered to explain the viscosity increase and gel-like behavior of PEI/CNC aqueous suspension;

1) Bridging

Commercial CNC is a negatively charged particle and it is expected to interact with the PEI through electrostatic attractions, leading to formation of a layer. A few studied proposed that bridging could be important in case of adsorbed polymer on particle surfaces [165, 166].

In the other words, if the polymer chains are long enough, some parts can adsorb onto one particle surface, while other parts are accessible to adsorb onto other particles (bridging effect). Bridging can increase the viscosity and lead to a gel-like behavior. [165, 166].

As mentioned before, bridging will occur when the adsorption density is not too high [167].

In addition, with increasing the concentration of polymer the inter particle interaction (through polymer bridging) tend to weaken [168].

Regarding the current study, the rigid structure of branched PEI and its short-length chains, restrict the chains extension and formation of bridge between particles. Moreover, the viscoelastic properties of PEI/CNC aqueous suspension increased with increasing PEI ratio from 1 to 2 % (Fig.3.5). Hence, the possibility of bridging in this case is low [165, 169]. However, occurring the bridging due the polydispersity of commercial PEI is possible. *Raj et al.* [46] reported a bridging mechanism for micro-fibrillated cellulose and branched PEI with high molecular weight (750 kg mol^{-1} , compared to our PEI's 25 kg mol^{-1}), because the long chains of PEI were able to overcome the electrostatic double layer to interact with other micro-fibrillated cellulose.

2) Electroviscous effect

Viscosity can also increase due to electroviscous effects in the case of charged rigid particles [63, 170]. With applying shear during rheological measurements of PEI/CNC aqueous suspension, the distortion of electrical double layer (EDL) around CNC leads to increased energy dissipation and, as a result, the viscosity increases.

On the other hand, similar charged particles repel each other and pushing each other across the streamline leading to increase viscosity. This effect is more important and determinant when charged polymers are grafted (chemically) or adsorbed (physically) onto the particle surface, because in this case the inter particle repulsion is a combination of electrostatic and steric effects [170].

This mechanism can explain the observed viscosity increase in the PEI/CNC suspensions.

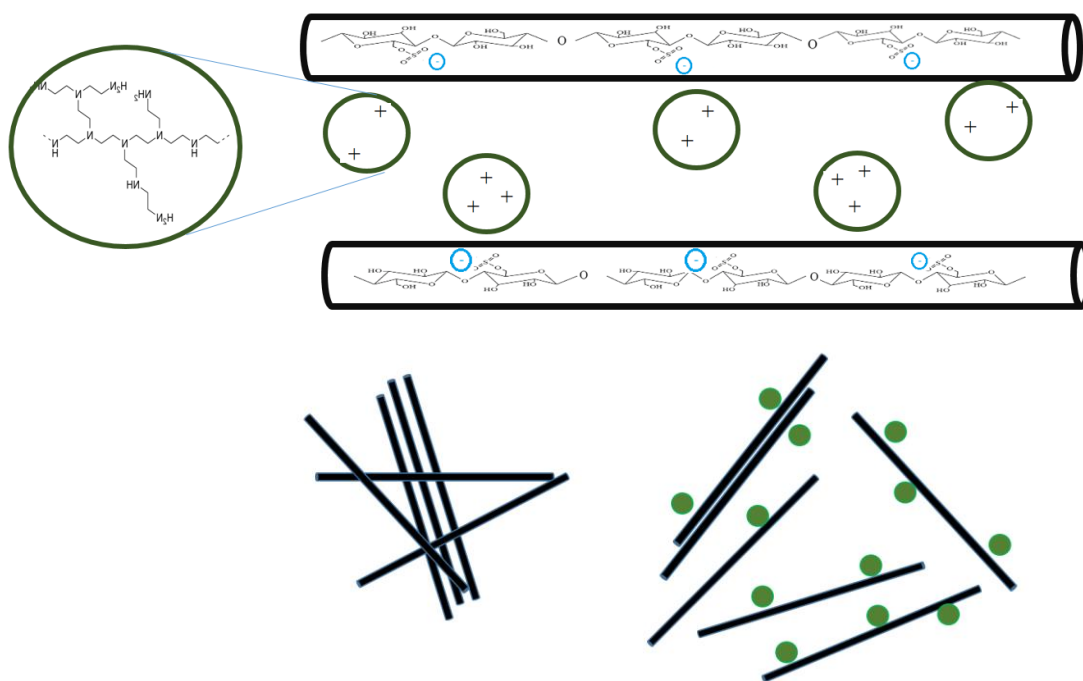


Figure 3.13. Schematic drawing of CNC surface modification with polyethyleneimine.

Branched PEI (M_w 25,000 g mol⁻¹) adsorbs as rigid spheres (Fig. 3.13) with a hydrodynamic radius of 4.6 ± 0.2 nm [171]. Its high degree of branching and specific structure allows it to approximately maintain its shape upon adsorption [105, 135]. In addition to the above, the formation of agglomerates is also expected due to the surface charges of modified CNC, which can lead to increased viscosity and gel-like behavior.

As mentioned before, gel-like behavior was observed for all PEI/CNC ratios in aqueous suspension (Fig 3.5). In PEI/CNC aqueous suspensions at high PEI ratio a very stiff gel is formed over time (appendix B). This strong gel behavior could be related to the solid structure of agglomerates and double layer overlap, which strongly reduce particles diffusion and lead to the formation of a stiff gel [68].

Based on the ζ - potential, rheological measurements and XPS results, we suggest that the ratio of PEI as a threshold for maximum CNC surface coverage and efficient surface modification would be close to 2 %. Regarding the mCNC with PEI ratio of 1 %, the ζ - potential obtained was close to zero (-2.0 ± 1.5 mV) (Table 3.3), however it was still in the negative region. The negative ζ - potential indicated that the majority of PEI molecules have been adsorbed on CNC surface and it can be assumed that the PEI concentration was not sufficient to interact with the all negative groups on the surface [46].

The maximum polymer surface coverage of cellulose fibers by branched PEI with molecular weight of 2,000 and 750,000 g mol⁻¹ were reported as 0.17 and 0.2 mg m⁻², respectively [46]. Considering the specific surface area (Fig 2.5) of the CNC used in this study (90 m²g⁻¹), the maximum surface coverage of CNC by our PEI is 17 mg PEI/g_{CNC}, which corresponds to a PEI/CNC ratio of 1.7 %. This value is in good agreement with the zeta potential measurements, showing a change between 1 and 2% PEI/CNC. However, the maximum adsorption of PEI on spray dried CNC and the optimum ratio of PEI/CNC to achieve efficient CNC surface modification using various methods remains to be studied.

CHAPTER 4 CNC SURFACE MODIFICATION WITH CHITOSAN

4.1. Chitosan

Chitosan (CHI) is an amino polysaccharide with several interesting properties such as biodegradability, antimicrobial properties. This polymer is produced from the second most abundant polymer in nature after cellulose (chitin) [172] (Fig 4.1). Shrimp and crab shells are the main sources of chitin.

Chitosan has positive charges on its structure in acidic media due to the protonation of its amino groups [172, 173]. This positive charge allows the interaction and electrostatic bonding of CHI with different anionic surfaces such as CNC. Hence, CHI has a great potential to interact with negatively charged commercial CNC surfaces. Therefore, considering the similar expected adsorption mechanism (electrostatic interaction) as with PEI, on top of the structural similarity of CNC and CHI and the other beneficial properties of chitosan [172, 173], its use for cationic surface modification of CNC is proposed.

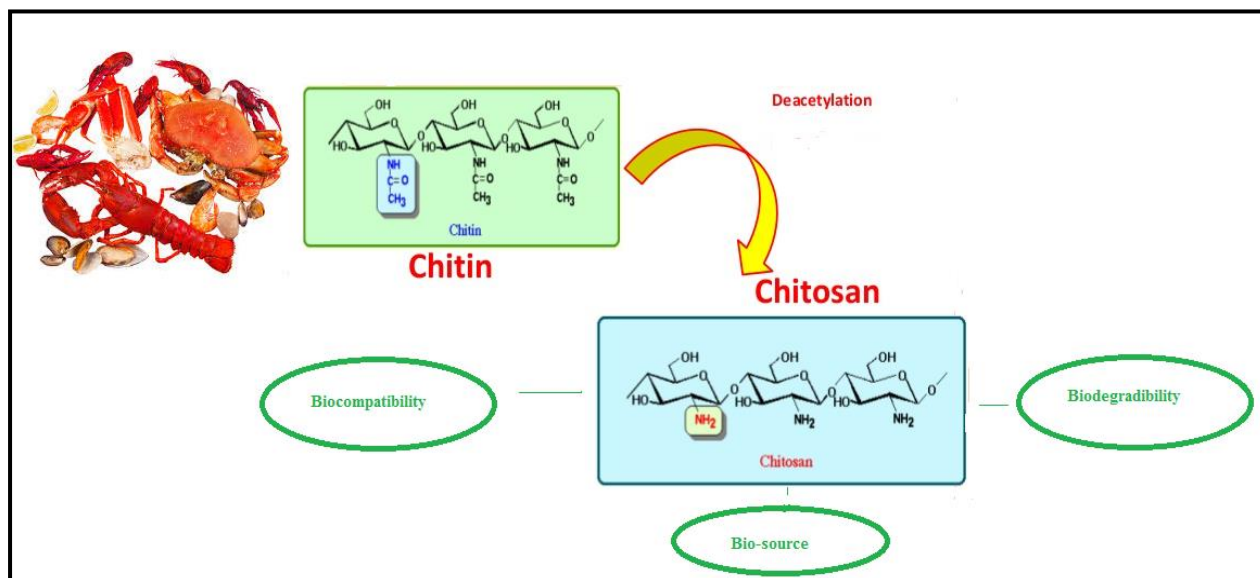


Figure 4.1. The structure of chitosan and its characteristic properties (adapted from [173]).

Akhlaghi et al. [22] suggested the use of a complex of chitosan/CNC for drug delivery. They reported a chemical modification process to produce a chemically grafted chitosan on TEMPO-CNC. In the first step, primary hydroxyl groups on the CNC surfaces were oxidized to carboxylic acid groups using TEMPO-mediated oxidation then, the amino groups of chitosan were reacted with carboxylic acid groups of CNC via carbodiimide.

To the best of our knowledge, no attempts have been made to modify the surface of commercial CNC (containing OSO_3^- groups) with chitosan and improve the dispersion level in non-polar media. Since chitosan possesses interesting biological properties, such as antibacterial, haemostatic, and wound healing properties, in combination with unique properties of CNC, their applications will be developed. In this preliminary study, two different grades of chitosan with different properties were employed (Table 4.1).

Table 4-1. The properties of the two grades of chitosan used in this study

Chitosan	DDA %	Viscosity (mPa.s)	Mw (KDa)	Supplier
Chitosan-87	95	87	144	Primex
Chitosan-1000	85	1000	344	Biolog

- **Samples preparation**

As described in Section 3.3 (surface modification with PEI), in a typical batch of CNC modification, spray-dried CNC was added in deionized (DI) water at pH 6.8 at CNC concentration of 1 wt.%. An ultrasonic homogenizer was used to disperse the CNC in DI water. To achieve perfect dispersion of CNC in DI water, 2000 J/g_{CNC} ultrasonication energy was applied to the suspension. Two grades of chitosan were separately added in DI water and pH was adjusted at 2.5 using HCl 0.1 M to promote the protonation of chitosan in water. These were then heated at 50 °C and agitated using a magnetic stirrer for 30 min at a speed of 300 rpm. Afterwards, the two solutions of chitosan were separately added to the CNC suspension and mechanically stirred at 50 °C at a speed of 500 rpm for 4 h. The ratio of chitosan/CNC was kept at 1 %. The chitosan/CNC aqueous suspensions were quickly frozen for 48h and then were put into the freeze-dryer for 72 h (as

described in section 3.3). Dried modified CNC with chitosan-1000 (CHI1000-CNC) and chitosan-87 (CHI87-CNC) were obtained for further characterization.

4.2. Structure characterization of CHI-CNC

FTIR spectra of CNC was collected to show the chemical structure changes of CNC after surface modification with chitosan(CHI-CNC) (Fig.4.2). A fine powder of dried pristine and CHI-CNC was used in FTIR characterization.

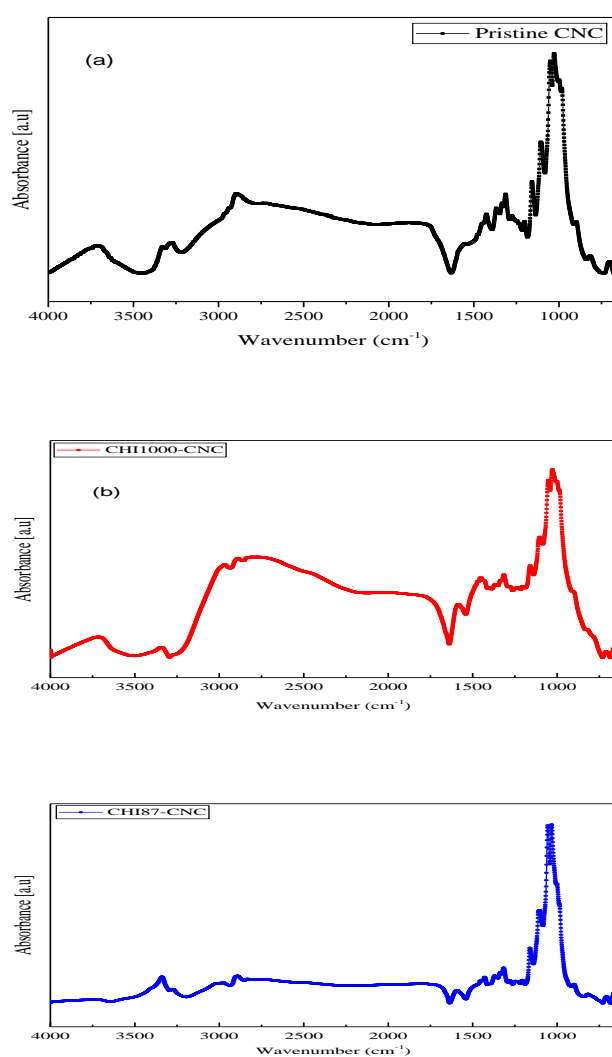


Figure 4.2. FTIR spectra of a) pristine CNC and b) CHI1000-CNC c) CHI87-CNC.

Due to the similarities in the chemical structures of cellulose and chitosan, The FTIR spectra of CNC and CHI-CNC were very similar, as previously reported in the literature[174]. However, some changes were apparent in the spectra of CHI-CNC. The FTIR spectra of CHI-CNC (Fig. 4.1b, c) showed a broader peak between 3,500 and 3,000 cm^{-1} , which corresponded to O–H and N–H stretching vibrations [175]. In addition, the spectra of CHI-CNC showed some additional peaks at 1,620 and 1,510 cm^{-1} , attributed to amide-I and II respectively, and at 1,616 cm^{-1} , corresponding to NH_3^+ [134, 176]. The appearance of these peaks in the spectra of CHI-CNC confirmed successful modification. However, for further study of the surface of CHI-CNC, XPS analysis is proposed.

4.3. Zeta potential measurements

Pristine and CHI-CNC were dispersed in DI water at CNC concentration of 0.05wt.% As described in Section 3.3.4, 2000 J/g CNC was applied to the suspensions.

As presented in Table 4.2, after surface modification with chitosan, the zeta potential values increased to positive values for modified CNC with both chitosan grades. The positive zeta potential of CHI-CNC in acidic medium (pH 3.0) are attributed to the protonation of amine and amide groups. Similar results were also reported by *Akhlaghi et al.* [138]. The increase of zeta potential value for CHI-CNC can act as an indirect proof of successful CNC surface modification.

Table 4-2. The zeta potential value of CHI-CNC and neat chitosan

Samples	Zeta potential (mV) at pH 3.0
CHI-1000	52.0±2.0
CHI-87	44.0±0.5
Pristine CNC	-33.0±0.1
CHI1000-CNC	27.0±2.2
CHI87-CNC	19.0±4.3

The zeta potential value of CHI1000-CNC is higher (10 mV) than that of CHI87-CNC, which can be related to the higher molecular weight of CHI-1000 compared to CHI-87. Furthermore, both

CHI-CNC exhibited higher zeta potential values at pH 3.0 compared to mCNC at the same ratio of modifier (1 % with respect to CNC). It can be attributed to the higher protonation degree of chitosan, to structural similarity of CNC and chitosan as well as chain conformation of chitosan compared to PEI.

4.4. Thermogravimetric analysis of CHI-CNC

Pristine CNC, CHI-CNC and neat chitosan powders were used in thermogravimetric analysis. The thermal stability of pristine CNC and CHI-CNC was investigated by TGA in air with the rate of 20 °C/min ranging from 50 to 800 °C. The onset decomposition temperature (T_{onset}) and the temperature at 50 % weight loss ($T_{50\%}$) are presented in Table 4.3 and Fig .4.3.

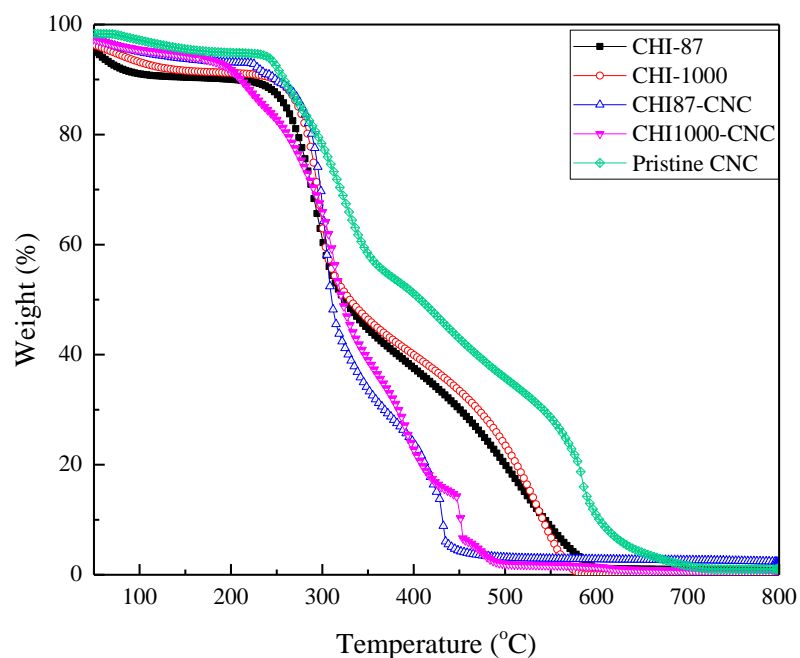


Figure 4.3. Weight as a function of temperature for pristine CNC, CHI-CNC, and neat CHI

Pristine CNC and CHI-CNC showed a three-stage weight loss [36]; the small weight loss in the low temperature range is due to the evaporation of absorbed water as discussed in section 3.3.9, whereas the two other weight losses are due to pyrolysis of carbon chains.

Table 4-3. Characteristic thermal degradation temperatures of CHI-CNC and neat chitosan

Samples	T _{Onset} (°C)	T _{50%} (°C)
Pristine CNC	248	405.9
CHI87-CNC	241	313.9
CHI1000-CNC	238	317.3
CHI-87	236	324.2
CHI-1000	251	328.5

After modification, the onset temperature of both CHI-CNC decreased compared to pristine CNC (7 and 10 °C for CHI87-CNC and CHI1000-CNC, respectively), as shown in Fig 4.3 and Table 4.3. It can be related to the lower thermal stability of neat chitosan than pristine CNC (Fig 4.3). In addition, it was reported that the complex of CNC/CHI weakens the intra-and intermolecular bonds lead them to decompose more easily [177].

4.5. Dispersion of CHI-CNC in fresh DI water

To evaluate the hydrophobicity level of CHI-CNC, they were dispersed in DI water at CNC concentrations of 1wt.% with the application of 2000 J/g_{CNC} ultrasonication energy. The dispersion state of CNC before and after surface modification with chitosan is presented in Fig.4.4.

The pristine CNC made a stable suspension in DI water, however both CHI-CNC precipitated (Fig 4.4). Based on macroscopic observations, no significant difference between the precipitation rate of CHI-CNC with both chitosan grades in DI water was observed. However, to confirm this finding, the precipitation rate should be measured as described for mCNC (section 3.3.8) using UV-Vis spectroscopy.



Figure 4.4. The dispersion state of **1)** pristine CNC⁷ and **2)** modified CNC with Chitosan in DI water (a) CHI1000-CNC (b) CHI87-CNC.

4.6. Conclusion

Whereas CHI has a great potential to interact with negatively charged CNC surfaces due to the presence of amine groups on its chain, and considering a similar adsorption mechanism (electrostatic interactions), the structural similarity as well as the other beneficial properties of chitosan, the use of chitosan for cationic surface modification of CNC was proposed. In this preliminary study, two different grades of chitosan with different properties were used for CNC surface modification.

The obtained results from FTIR and zeta potential measurements confirm successful surface modification. The macroscopic observations showed the precipitation of CHI-CNC in DI water, confirming the surface change of modified CNC with chitosan .

The thermal stability of CNC decreased after the modification with chitosan. However, the onset temperature of both CHI-CNC obtained is more than 220 °C. Based on these results, the CHI-CNC could be compatible with melt processing of commercial polymers, but the study of isothermal stability at temperatures around 200 °C is proposed to confirm this further.

⁷ - The white color in the bottom of vial is due to the light reflection.

The rheological behavior of aqueous suspension of CHI/CNC was measured immediately after the modification process (Appendix E). The complex viscosity increased with adding a low amount of CHI (1 % respect to CNC) and a notable shear-thinning was observed. This rheological behavior could be related to the interaction of chitosan with CNC surfaces. In addition, CHI-CNC demonstrated higher viscoelastic properties compared to mCNC (PEI-modified) with the same ratio of modifier (1 %), which could be related to the similar structure of chitosan and CNC as well as the chains conformation of CHI compared to rigid and spherical structure of branched PEI (higher affinity for adsorption).

It should be noted that different parameters can affect the protonation degree of chitosan and efficiency of surface modification, such as molecular weight, degree of deacetylation (DDA), pH, etc. *Wang et al* reported that the pKa of chitosan slightly decreased from 6.51 to 6.39 when the molecular weight changed from 1370 to 60 kDa. In addition they showed that the DDA also influenced the balance of hydrophobic interactions and hydrogen bonding on chitosan, and affected pKa [178]. Therefore, to achieve an efficient surface modification, depending on the application, these issues should be considered in further studies.

CHAPTER 5 CONCLUSION AND RECOMMENDATIONS

Cellulose nanocrystals (CNC) are unique and interesting nanomaterials that find applications in many fields. However, to develop industrial and commercially viable applications, some properties of this nanomaterial should be adapted, such as their surface properties to be compatible with non-polar media.

In the present work, surface modifications were performed on CNC through different approaches.

a) CNC surface modification with PEI

The hydrophilic surface of CNC was modified using a cationic polymer (PEI) through a low cost and simple process, without using any organic solvents, to improve the compatibility with non-polar media. The successful surface modification, as well as the increase hydrophobicity level of mCNC and the stability of surface modifier, were confirmed through different techniques. The main obtained results are:

- ✓ A low amount of PEI (2 % with respect to CNC) has a high capability of changing the hydrophilic surface of CNC due the high number of amine and amide groups, without altering the CNC molecular structure.
- ✓ Modification improved the dispersibility of CNC in organic solvents with low polarity such as toluene.
- ✓ The efficiency of mCNC in terms of hydrophobic properties did not change after several contact cycles with neutral media, thereby illustrating processing stability.
- ✓ PEI slightly enhances the thermal stability of CNC around melt processing temperature of commercial thermoplastics.
- ✓ **The results of this study indicated that, PEI has a great potential to be used commercially for CNC surface modification to improve the compatibility between this nanofiller and nonpolar thermoplastics.**

Recommendations

They are some issues recommended to complete this study, such as examining:

- The effect of branched PEI molecular weight and structure (linear and branched) on adsorption mechanism and the efficiency of surface modification.
- The effect of PEI/CNC ratio and confirming the proposed ratio of PEI/CNC (2 %) to achieve efficient CNC surface modification through different analytical methods.
- The extraction of un-reacted PEI without causing any negative effect on PEI structure and molecular weight
- Substitution of some amine groups of PEI by another chemical group to increase the compatibility between CNC and host matrix.
- The effect of pH on rheological and surface properties of PEI/CNC aqueous suspensions
- The methodology of surface modification; the use of ultra sonication during surface modification, they way (how and when) of adding PEI to the CNC suspension as well as the effect of modification conditions such as pH and temperature
- Finally, the use of mCNC in non-polar polymer matrix such as polyethylene (PE), polypropylene (PP) and a blend of PE and thermoplastic starch (TPE) through melt processing (using a twin-screw extruder or internal mixer) and the study of morphology, mechanical properties, optical properties as well as rheological behavior of prepared nanocomposites (or composites).

b) CNC surface modification with chitosan

Furthermore, the change of the hydrophilic nature of CNC using two grades of a bio cationic polymer, chitosan (CHI), was also preliminary investigated.

- ✓ The results showed the chitosan has a great potential to adsorb onto negatively charged CNC and change the surface properties of CNC. However, there remain several issues to be studied:

Recommendations

- The effect of chitosan molecular weight and DDA on efficiency of surface modification;
- The effect of CHI/CNC ratio on the efficiency of CHI-CNC and adsorption mechanism;
- The stability of CHI on CNC surface after being contact with neutral media;
- The study of optimum ratio of CHI/CNC to achieve efficient surface modification;
- The study of the dispersion state of CHI-CNC in non-polar solvents;
- The dispersion of CHI-CNC in a biopolymer (or a polyolefin) through melt processing (<200°C) and study the morphology, mechanical properties as well as the rheological behavior of prepared nanocomposites (composites);
- The dispersion of CHI-CNC in low density polyethylene (LDPE) and study the antimicrobial, barrier and mechanical properties of obtained nanocomposites (composites) to use in packaging industries.

BIBLIOGRAPHY

- [1] M. M. De Souza Lima, Borsali, Redouane, "Rodlike Cellulose Microcrystals: Structure, Properties, and Applications," *Macromolecular Rapid Communications*, vol. 25, pp. 771-787, 2004.
- [2] R. J. Moon, Martini, A.;Nairn, J.,Simonsen, J.,Youngblood, J., "Cellulose nanomaterials review: structure, properties and nanocomposites," *Chem Soc Rev*, vol. 40, pp. 3941-94, Jul 2011.
- [3] D. Klemm, F. Kramer, S. Moritz, T. Lindstrom, M. Ankerfors, D. Gray, *et al.*, "Nanocelluloses: a new family of nature-based materials," *Angew Chem Int Ed Engl*, vol. 50, pp. 5438-66, Jun 6 2011.
- [4] J. S. Juntao Tang, Nathan Grishkewich, Kam Chiu Tam, "Functionalization of cellulose nanocrystals for advanced applications," *Journal of Colloid and Interface Science*, vol. 494, pp. 397-409, 2017.
- [5] S. K. Camarero Espinosa, T.;Foster, E. J.;Weder, C., "Isolation of thermally stable cellulose nanocrystals by phosphoric acid hydrolysis," *Biomacromolecules*, vol. 14, pp. 1223-30, Apr 8 2013.
- [6] Han YangDezhi ChenTheo G. M. v. d. Ven, "Preparation and characterization of sterically stabilized nanocrystalline cellulose obtained by periodate oxidation of cellulose fibers," *cellulose*, vol. 22, p. 1743, 2015.
- [7] Han Y. M. Nur AlamTheo G. M. v. de Ven, "Highly charged nanocrystalline cellulose and dicarboxylated cellulose from periodate and chlorite oxidized cellulose fibers," *Cellulose*, vol. 20, pp. 1865–1875, 2013.
- [8] M. R. Stephanie Beck-Candanedo, Derek G. Gray, "Effect of Reaction Conditions on the Properties and Behavior of Wood Cellulose Nanocrystal Suspensions," *Biomacromolecules*, pp. 1048-1054, 2005.
- [9] L. Brinchi, Cotana, F.,Fortunati, E.,Kenny, J. M., "Production of nanocrystalline cellulose from lignocellulosic biomass: technology and applications," *Carbohydr Polym*, vol. 94, pp. 154-69, Apr 15 2013.
- [10] K. T. Dong XM, Revol JF, Gray DG, "Effects of ionic strength on the isotropic-chiral nematic phase transition of suspensions of cellulose crystallites," *Langmuir* vol. 12, pp. 2076–2082, 1996.
- [11] L. Lucian A., ,Orlando J. Rojas,John Simonsen,Youssef Habibi, "Cellulose Nanocrystals in Polymer Matrices," *Chapter 10*, 2009.
- [12] S. N. S. Johnsy George , Siddaramaiah, "Water Soluble Polymer-Based Nanocomposites Containing Cellulose Nanocrystals," *Eco-friendly Polymer Nanocomposites*, vol. 75, pp. 259-293, 2015.

- [13] W. T. N. L. Garcia de Rodriguez, and A. Dufresne, "Sisal cellulose whiskers reinforced polyvinyl acetate nanocomposites," *Cellulose*, vol. 13, pp. 261-270, 2006.
- [14] M. Roohani, ;Habibi, Youssef;Belgacem, Naceur M.Ebrahim, Ghanbar;Karimi, Ali Naghi;Dufresne, Alain, "Cellulose whiskers reinforced polyvinyl alcohol copolymers nanocomposites," *European Polymer Journal*, vol. 44, pp. 2489-2498, 2008.
- [15] C. Salas, Nypelö, Tiina,Rodriguez-Abreu, Carlos,Carrillo, Carlos,Rojas, Orlando J., "Nanocellulose properties and applications in colloids and interfaces," *Current Opinion in Colloid & Interface Science*, vol. 19, pp. 383-396, 2014.
- [16] L. A. L. Youssef Habibi, and a. O. J. Rojas, "Cellulose Nanocrystals: Chemistry, Self-Assembly, and Applications," *American Chemical Society*, vol. 110, pp. 3479–3500, 2010.
- [17] S. J. Eichhorn, "Cellulose nanowhiskers: promising materials for advanced applications," vol. 7, pp. 303-315 2011.
- [18] N. C. Ljungberg, J.Y.; Heux, L. , "nanocomposites of isotactic polypropylene reinforced with rod-like cellulose whiskers," *Polymer*, vol. 47, pp. 6285–6292, 2006.
- [19] Y. Habibi, "Key advances in the chemical modification of nanocelluloses," *Chem Soc Rev*, vol. 43, pp. 1519-42, Mar 7 2014.
- [20] J. M. Ashori Alireza, "Solvent-free acetylation of cellulose nanofibers for improving compatibility and dispersion," *Carbohydrate Polymers*, vol. 102, 2014.
- [21] N. Lin, Dufresne, A., "Surface chemistry, morphological analysis and properties of cellulose nanocrystals with gradiented sulfation degrees," *Nanoscale*, vol. 6, pp. 5384-93, May 21 2014.
- [22] M. Z. Seyedeh Parinaz Akhlaghia, Nishil Mohammeda, César Brinattib, Rasim Batmaza, Richard Berryc, Watson Lohb, Kam Chiu Tam, "Synthesis of amine functionalized cellulose nanocrystals: optimization and characterization," *Carbohydrate Research*, vol. 409, pp. 48-55, 2015.
- [23] Y. Habibi ., Henri Chanzy,Michel R. Vignon, "TEMPO-mediated surface oxidation of cellulose whiskers," *Cellulose*, vol. 13, p. 679, 2006.
- [24] H. S. Kargarzadeh, Rasha M.; Ahmad, Ishak; Abdullah, Ibrahim; Dufresne, Alain, "Cellulose nanocrystal reinforced liquid natural rubber toughened unsaturated polyester: Effects of filler content and surface treatment on its morphological, thermal, mechanical, and viscoelastic properties," *Polymer* vol. 71, pp. 51-59, 2015.
- [25] W. Z. Juntao Tang Micky Fu Xiang Lee, † Boxin Zhao, Richard M. Berry,§ and Kam C. Tam, "Dual Responsive Pickering Emulsion Stabilized by Poly[2(dimethylamino)ethyl methacrylate] Grafted Cellulose Nanocrystals " *Biomacromolecules*, vol. 15, pp. 3052-3060, 2014.
- [26] T. R. Javanbakht, W.1; Tavares, J.R, "3Physicochemical properties of cellulose nanocrystals treated by photo-initiated chemical vapour deposition (PICVD)," *94*, vol. 6, pp. 1135-9, 2016.

- [27] J. R. T. C.A. Dorval Dion, "Photo-initiated chemical vapor deposition as a scalable particle functionalization technology (a practical review)," *Powder Technology*, vol. 239, pp. 484–491, 2013.
- [28] K. B. Missoum, Mohamed Naceur; Bras, Julien, "Nanofibrillated cellulose surface modification: A review," *Materials*, vol. 6, pp. 1745-1766, 2013.
- [29] L. C. Heux, G.; Bonini, C. , "Nonflocculating and chiral-nematic self-ordering of cellulose microcrystals suspensions in nonpolar solvents. ," *Langmuir*, vol. 16, pp. 8210–8212, 2000.
- [30] M. C. Hasani, Emily D.;Westman, Gunnar;Gray, Derek G., "Cationic surface functionalization of cellulose nanocrystals," *Soft Matter*, vol. 4, pp. 2238-2244, 2008.
- [31] M. Salajková, Berglund, Lars A,Zhou, Qi, "Hydrophobic cellulose nanocrystals modified with quaternary ammonium salts," *Journal of Materials Chemistry*, vol. 22, p. 19798, 2012.
- [32] M. Zaman, Xiao, H.,Chibante, F.,Ni, Y., "Synthesis and characterization of cationically modified nanocrystalline cellulose," *Carbohydr Polym*, vol. 89, pp. 163-70, Jun 05 2012.
- [33] A. Kaboorani and B. Riedl, "Surface modification of cellulose nanocrystals (CNC) by a cationic surfactant," *Industrial Crops and Products*, vol. 65, pp. 45-55, 2015.
- [34] M. S. Ye C, Hu K, "Cellulose Nanocrystal Microcapsules as Tunable Cages for Nano- and Microparticles," *ACS Nano*, vol. 9, pp. 10887–10895, 2015.
- [35] M.-C. M. Li, Changtong;Xu, Xinwu, Lee, Sunyoung, "Cationic surface modification of cellulose nanocrystals: Toward tailoring dispersion and interface in carboxymethyl cellulose films," *Polymer*, vol. 107, pp. 200-210, 2016.
- [36] E. D. Neng Wang, Rongshi Cheng, "Thermal degradation behaviors of spherical cellulose nanocrystals with sulfate groups," *Polymer*, vol. 48, pp. 3486-3493, 2007.
- [37] D. E. Wang N, Cheng R, "Thermal degradation behaviors of spherical cellulose nanocrystals with sulfate groups," *polymer* vol. 48, pp. 3486–3493, 2004.
- [38] Y. M. Mirjalili V, Hubert P, "Dispersion stability in carbon nanotube modified polymers and its effect on the fracture toughness," *Nanotechnology*, vol. 23, 2012.
- [39] Bruce Lyne, "market prospects for nanocellulosebru," *Alberta Biomaterials Development Centre* vol. 12th, 2013.
- [40] Y. H. Bin Liu, "Polyethyleneimine modified eggshell membrane as a novel biosorbent for adsorption and detoxification of Cr(VI) from water," *J. Mater. Chem*, vol. 21, pp. 17413-17418, 2011.
- [41] M. V. D. Claudiu N. Lungu , Mihai V. Putz, and Ireneusz P. Grudzi ´ nski, "Linear and Branched PEIs (Polyethylenimines) and Their Property Space," *International journal of molecular science*, vol. 17, p. 555, 2016.
- [42] G. E. I. G. Ham, E. J., Ed, "Polymeric Amines and Ammonium Salts," *Pergamon Press*, vol. Oxford, 1980.

- [43] R. Y. Yanjun Zhao, 1 Dong Liu, Mingjing Sun, Lijun Zhou, Zheng Wang, Ying Wan, "Starburst low-molecular weight polyethylenimine for efficient gene delivery," *Journal of Biomedical Materials Research Part A*, vol. 100, pp. 134-140, 2011.
- [44] D. R. H. a. M. Chai, "Comprehensive NMR Studies of the Structures and Properties of PEI Polymers," *Macromolecules*, vol. 46, pp. 6891-6897, 2013.
- [45] T. G. M. v. d. V. J. Petlicki, "Adsorption of polyethylenimine onto cellulose fibers," *Colloids and Surfaces A: Physicochemical and Engineering Aspects*, vol. 83, pp. 9-23, 1994.
- [46] P. Raj, ;Batchelor, Warren;Blanco, Angeles;de la Fuente, Elena;Negro, Carlos;Garnier, Gil, "Effect of polyelectrolyte morphology and adsorption on the mechanism of nanocellulose flocculation," *Journal of Colloid and Interface Science*, vol. 481, pp. 158-167, 2016.
- [47] B. Y. X.-Z. Tang, R.V. Hansen, X. Chen, X. Hu, J. Yang, "Grafting low contents of branched polyethylenimine onto carbon fibers to effectively improve their interfacial shear strength with an epoxy matrix," *Advanced Materials Interfaces*, vol. 2, pp. 1500122–1500129, 2015.
- [48] L. M. Ma, G. Wu, Y. Wang, M. Zhao, C. Zhang, , "Improving the interfacial properties of carbon fiber-reinforced epoxy composites by grafting of branched polyethyleneimine on carbon fiber surface in supercritical methanol," *Composites Science and Technology*, vol. 114, pp. 64-71, 2015.
- [49] D. H. Klemm, B ; Fink, HP; Bohn, A (Bohn, A), "Cellulose: Fascinating biopolymer and sustainable raw material " *ANGEWANDTE CHEMIE-INTERNATIONAL EDITION* vol. 44, pp. 3358-3393 2005.
- [50] a. F. Madhu Kaushik¹, Grégory Chauve, Jean-Luc Putaux, and Audrey Moores, "Transmission Electron Microscopy for the Characterization of Cellulose Nanocrystals," p. Chapter 6, 2015.
- [51] J. Moon R , Martini A, Nairn, J., Simonsen, J., Youngblood, J., *Chem Soc Rev*, vol. 40, pp. 3941-94, Jul 2011.
- [52] Q. Yujie Meng, Timothy M. Young, Biao Huang, and a. Y. L. Siqun Wang, "investigation the general shape of nanocrystal," *Plastic research*, 2016.
- [53] P. Lu and Y.-L. Hsieh, "Preparation and properties of cellulose nanocrystals: Rods, spheres, and network," *Carbohydrate Polymers*, vol. 82, pp. 329-336, 2010.
- [54] L. P. Novo, J. Bras, A. García, N. Belgacem, and A. A. d. S. Curvelo, "A study of the production of cellulose nanocrystals through subcritical water hydrolysis," *Industrial Crops and Products*, vol. 93, pp. 88-95, 2016.
- [55] D. J. Gardner, G. S. Oporto, R. Mills, and M. A. S. A. Samir, "Adhesion and Surface Issues in Cellulose and Nanocellulose," *Journal of Adhesion Science and Technology*, vol. 22, pp. 545-567, 2008.

- [56] Y. L. Nishiyama, P ; Chanzy, H, "Crystal structure and hydrogen-bonding system in cellulose 1 beta from synchrotron X-ray and neutron fiber diffraction " *JOURNAL OF THE AMERICAN CHEMICAL SOCIETY* vol. 124, pp. 9074-9082 2002.
- [57] N. Lin, Huang, Jin, Chang, Peter R., Anderson, Debbie P., "Preparation, Modification, and Application of Starch Nanocrystals in Nanomaterials: A Review," *Journal of Nanomaterials*, vol. 2011, pp. 1-13, 2011.
- [58] N. Lin, Dufresne, Alain, "Nanocellulose in biomedicine: Current status and future prospect," *European Polymer Journal*, vol. 59, pp. 302-325, 2014.
- [59] J. Lin Ning Huang, Chang, Peter R. Anderson, Debbie P., "Preparation, Modification, and Application of Starch Nanocrystals in Nanomaterials: A Review," *Journal of Nanomaterials*, vol. 2011, pp. 1-13, 2011.
- [60] T. K. Sandra Camarero Espinosa, E. Johan Foster*, and Christoph Weder, "Isolation of Thermally Stable Cellulose Nanocrystals by Phosphoric Acid Hydrolysis," *Biomacromolecules*, vol. 14, pp. 1223–1230, 2013.
- [61] S. Spinella, A. Maiorana, Q. Qian, N. J. Dawson, V. Hepworth, S. A. McCallum, *et al.*, "Concurrent Cellulose Hydrolysis and Esterification to Prepare a Surface-Modified Cellulose Nanocrystal Decorated with Carboxylic Acid Moieties," *ACS Sustainable Chemistry & Engineering*, vol. 4, pp. 1538-1550, 2016.
- [62] K. V. K. M. R, "Effect of surface energy on dispersion and mechanical properties of polymer/nanocrystalline cellulose nanocomposites," *Biomacromolecules*, vol. 14, pp. 3155-63, Sep 9 2013.
- [63] Y. Boluk, ;Lahiji, Roya;Zhao, Liyan;McDermott, Mark T., "Suspension viscosities and shape parameter of cellulose nanocrystals (CNC)," *Colloids and Surfaces A: Physicochemical and Engineering Aspects*, vol. 377, pp. 297-303, 2011.
- [64] Youssef Habibi, Lucian A. Lucia, and a. O. J. Rojas, "Cellulose Nanocrystals: Chemistry, Self-Assembly, and Applications," *American Chemical Society*, vol. 110, pp. 3479–3500, 2010.
- [65] A. Brinkmann, M. Chen, M. Couillard, Z. J. Jakubek, T. Leng, and L. J. Johnston, "Correlating Cellulose Nanocrystal Particle Size and Surface Area," *Langmuir*, vol. 32, pp. 6105-14, Jun 21 2016.
- [66] T. Phan-Xuan, A. Thuresson, M. Skepö, A. Labrador, R. Bordes, and A. Matic, "Aggregation behavior of aqueous cellulose nanocrystals: the effect of inorganic salts," *Cellulose*, vol. 23, pp. 3653-3663, 2016.
- [67] S. H. Shafiei Sabet, W. Y.;Hatzikiriakos, S. G., "Rheology of nanocrystalline cellulose aqueous suspensions," *Langmuir*, vol. 28, pp. 17124-33, Dec 11 2012.
- [68] J. B. Stephanie beck "Ions strenght control of sulfated cellulose nanocrystal suspension," *Tappi*, vol. 15, pp. 363-372, 2016.

- [69] M.-C. Li, Wu, Qinglin, Song, Kunlin, Lee, Sunyoung, Qing, Yan, Wu, Yiqiang, "Cellulose Nanoparticles: Structure–Morphology–Rheology Relationships," *ACS Sustainable Chemistry & Engineering*, vol. 3, pp. 821-832, 2015.
- [70] Y. S. N. Anuj Kumar¹, Veena Choudhary², Nishi Kant Bhardwaj³, "Characterization of Cellulose Nanocrystals Produced by Acid-Hydrolysis from Sugarcane Bagasse as Agro-Waste," *Journal of Materials Physics and Chemistry*, vol. 2, pp. 1-4, 2014.
- [71] M. Mariano, N. El Kissi, and A. Dufresne, "Cellulose nanocrystals and related nanocomposites: Review of some properties and challenges," *Journal of Polymer Science Part B: Polymer Physics*, vol. 52, pp. 791-806, 2014.
- [72] F. A. Corsello, P. A. Bolla, P. S. Anbinder, M. A. Serradell, J. I. Amalvy, and P. J. Peruzzo, "Morphology and properties of neutralized chitosan-cellulose nanocrystals biocomposite films," *Carbohydr Polym*, vol. 156, pp. 452-459, Jan 20 2017.
- [73] I. A. S. C. N. J. B. J. S. J. W. J. F. T. O. J. W. Gilman, "Comparison of the Properties of Cellulose Nanocrystals and Cellulose Nanofibrils Isolated from Bacteria, Tunicate, and Wood Processed Using Acid, Enzymatic, Mechanical, and Oxidative Methods," *ACS Appl. Mater*, vol. 6, pp. 6127–6138, 2014.
- [74] R. R. a. S. J. Eichhorna, "Determination of the stiffness of cellulose nanowhiskers and the fiber-matrix interface in a nanocomposite using Raman spectroscopy " *Applied Physics Letters* vol. 93, 2008.
- [75] N. Lin, J. Huang, and A. Dufresne, "Preparation, properties and applications of polysaccharide nanocrystals in advanced functional nanomaterials: a review," *Nanoscale*, vol. 4, pp. 3274-94, Jun 7 2012.
- [76] Fernando L. Dri, Louis G. Hector Jr., Robert J. Moon, Pablo D. Zavattieri, "Anisotropy of the elastic properties of crystalline cellulose I β from first principles density functional theory with Van der Waals interactions," *Cellulose*, vol. 20, pp. 2703–2718, 2013.
- [77] F. L. Xue, Zhu Xu, Long Jiang, J. Y. Zhu, Darrin Haagensohn, and Dennis P. Wiesenborn, "Cellulose Nanocrystals vs. Cellulose Nanofibrils: A Comparative Study on Their Microstructures and Effects as Polymer Reinforcing Agents," *ACS Appl. Mater. Interfaces*, vol. 5, pp. 2999–3009, 2013.
- [78] A. L. A. Yit Thai Ong, Sharif Hussein Sharif Zein and Soon Huat Tan, "A review on carbon nanotubes in an environmental protection and green engineering perspective," *Brazilian Journal of Chemical Engineering*, vol. 27, pp. 227-242, 2010.
- [79] M. H. Farzana Hussain, "Review article: Polymer-matrix Nanocomposites, Processing, Manufacturing, and Application: An Overview," *Journal of Composite Materials*, vol. 40, pp. 1151-1575, 2006.
- [80] E. Abraham, Y. Nevo, R. Slattegard, N. Attias, S. Sharon, S. Lapidot, *et al.*, "Highly Hydrophobic Thermally Stable Liquid Crystalline Cellulosic Nanomaterials," *ACS Sustainable Chemistry & Engineering*, vol. 4, pp. 1338-1346, 2016.

- [81] L. Huang, Ye, Zhibin, Berry, Richard, "Modification of Cellulose Nanocrystals with Quaternary Ammonium-Containing Hyperbranched Polyethylene Ionomers by Ionic Assembly," *ACS Sustainable Chemistry & Engineering*, vol. 4, pp. 4937-4950, 2016.
- [82] M. Pereda, N. El Kissi, and A. Dufresne, "Extrusion of polysaccharide nanocrystal reinforced polymer nanocomposites through compatibilization with poly(ethylene oxide)," *ACS Appl Mater Interfaces*, vol. 6, pp. 9365-75, Jun 25 2014.
- [83] H. Du, C. Liu, X. Mu, W. Gong, D. Lv, Y. Hong, *et al.*, "Preparation and characterization of thermally stable cellulose nanocrystals via a sustainable approach of FeCl₃-catalyzed formic acid hydrolysis," *Cellulose*, vol. 23, pp. 2389-2407, 2016.
- [84] W. T. W. Maren Roman "Effect of Sulfate Groups from Sulfuric Acid Hydrolysis on the Thermal Degradation Behavior of Bacterial Cellulose," *Biomacromolecules*, vol. 5, pp. 1671–1677, 2004.
- [85] M. W. J. Araki, S. Kuga, T. Okano, "Flow properties of microcrystalline cellulose suspension prepared by acid treatment of native cellulose," *Colloids and Surfaces A: Physicochemical and Engineering Aspects* vol. 142, pp. 75-82, 1998.
- [86] "TAPPI Nanotechnology," December 2015.
- [87] Z. r. market, 2016.
- [88] "La nanocellulose, le nouvel or vert," *Technique de l'ingenieur*, pp. 45-47, 2017.
- [89] H. H. Sojoudiasli, Marie-Claude; Carreau, Pierre J., "Mechanical and morphological properties of cellulose nanocrystal-polypropylene composites," *Polymer Composite*, 2017.
- [90] D. Dehnad, Z. Emam-Djomeh, H. Mirzaei, S. M. Jafari, and S. Dadashi, "Optimization of physical and mechanical properties for chitosan-nanocellulose biocomposites," *Carbohydr Polym*, vol. 105, pp. 222-8, May 25 2014.
- [91] D. Ray and S. Sain, "In situ processing of cellulose nanocomposites," *Composites Part A: Applied Science and Manufacturing*, vol. 83, pp. 19-37, 2016.
- [92] D. C. Bagheriasl, Pierre J.; Riedl, Bernard; Dubois, Charles;, "Shear rheology of polylactide (PLA)-cellulose nanocrystal (CNC) nanocomposites," *Cellulose*, vol. 23, pp. 1885-1897, 2016.
- [93] A. Khan, R. A. Khan, S. Salmieri, C. Le Tien, B. Riedl, J. Bouchard, *et al.*, "Mechanical and barrier properties of nanocrystalline cellulose reinforced chitosan based nanocomposite films," *Carbohydr Polym*, vol. 90, pp. 1601-8, Nov 06 2012.
- [94] E. P. Fortunati, M.; Armentano, I.; *et al.*, "Effects of modified cellulose nanocrystals on the barrier and migration properties of PLA nano-biocomposites " *CARBOHYDRATE POLYMERS* vol. 90, pp. 948-956 2012.
- [95] K. B. M. Khaled A. Mahmoud, Sabahudin Hrapovic and John H. T. Luong*, "Cellulose Nanocrystal/Gold Nanoparticle Composite as a Matrix for Enzyme Immobilization," *ACS Appl. Mater. Interfaces*, vol. 1, pp. 1383–1386, 2009.

- [96] M. R. D. H. Y. W. Lee, "Cellulose Nanocrystals for Drug Delivery," *CS Symposium Series*, vol. 1017, pp. 81-91, 2010.
- [97] S. D. a. M. R. *, "Fluorescently Labeled Cellulose Nanocrystals for Bioimaging Applications," *J. Am. Chem. Soc.*, 2, vol. 129, 2007.
- [98] W. A. H. L. F. von Helmholtz, 1880.
- [99] V. ZHULINA EB; BORISOV PRIAMITSYN, "THEORY OF STERIC STABILIZATION OF COLLOID DISPERSIONS BY GRAFTED POLYMERS " *JOURNAL OF COLLOID AND INTERFACE SCIENCE* vol. 137, pp. 495-511 1990.
- [100] P. P. Claesson, E Blomberg, E.; Dedinaite, A, "Polyelectrolyte-mediated surface interactions " *ADVANCES IN COLLOID AND INTERFACE SCIENCE* vol. 114, pp. 173-187 2005.
- [101] Z. W. b. a. T. N. Xiangjun Gong a, "Direct measurements of particle–surface interactions in aqueous solutions with total internal reflection microscopy," *Chem commun.*, vol. 50, 2014.
- [102] J. Gregory and S. Barany, "Adsorption and flocculation by polymers and polymer mixtures," *Adv Colloid Interface Sci*, vol. 169, pp. 1-12, Nov 14 2011.
- [103] S. P. Julio Benegas, ;Marc A.G.T van den Hoop, "Affinity interactions in counterion-polyelectrolyte systems: Competition between different counterions," *Macromolecular Theory and Simulations*, vol. 8, pp. 61-64, 1999.
- [104] L.-E. Enarsson, L. Wågberg, J. Carlén, and N. Ottosson, "Tailoring the chemistry of polyelectrolytes to control their adsorption on cellulosic surfaces," *Colloids and Surfaces A: Physicochemical and Engineering Aspects*, vol. 340, pp. 135-142, 2009.
- [105] T. G. M. v. d. V. L. C. N. Tufenkji, "Fractionating polydisperse polyelectrolytes in packed beds of cellulose fibers," *Colloids and Surfaces A: Physicochemical and Engineering Aspects*, vol. 385, pp. 134-138, 2011.
- [106] B. A. U. K. Z. Mitina NS, vol. 56, p. 578, 1990.
- [107] S. M. F. G. Pelssers EGM, "Colloids surface," vol. 38, p. 15, 1989.
- [108] J. M. Raquez, Y. Murena, A. L. Goffin, Y. Habibi, B. Ruelle, F. DeBuyl, *et al.*, "Surface-modification of cellulose nanowhiskers and their use as nanoreinforcers into polylactide: A sustainably-integrated approach," *Composites Science and Technology*, vol. 72, pp. 544-549, 2012.
- [109] S. E. a. W. Thielemans, "Surface modification of cellulose nanocrystals," *nanoscale*, vol. 6, pp. 7764-7779, 2014.
- [110] C. Goussé, "Stable suspensions of partially silylated cellulose whiskers dispersed in organic solvents " *Polymer*, vol. 43, pp. 2645-2651, 2002.
- [111] N. Lin, Huang, Jin, Chang, Peter R. Feng, Jiwen, "Surface acetylation of cellulose nanocrystal and its reinforcing function in poly(lactic acid)," *Carbohydrate Polymers*, vol. 83, pp. 1834-1842, 2011.

- [112] J. A. Avila Ramirez, Fortunati, E., Kenny, J. M., Torre, L., Foresti, M. , "Simple citric acid-catalyzed surface esterification of cellulose nanocrystals," *Carbohydr Polym*, vol. 157, pp. 1358-1364, Feb 10 2017.
- [113] J. H. S. Lin, P. R. Chang, S. Wei, Y. Xu and Q. Zhang, *Carbohydr. Polym*, vol. 95, pp. 91-99, 2013.
- [114] T. Z. Philippe Tingaut, and Francisco Lopez-Suevos, "Synthesis and Characterization of Bionanocomposites with Tunable Properties from Poly(lactic acid) and Acetylated Microfibrillated Cellulose," *Biomacromolecules*, vol. 11, pp. 454-464, 2010.
- [115] W. Y. H. C. Miao, "Cellulose reinforced polymer composites and nanocomposites: A critical review," *Cellulose*, vol. 20, pp. 2221–2262, 2013.
- [116] T. S. a. H. F. Akira Isogai *, "TEMPO-oxidized cellulose nanofibers," *Nanoscale*, vol. 3, pp. 71-85, 2011.
- [117] R. V. Natacha Bitinis a, Julien Brasb, Elena Fortunatic, "Poly(lactic acid)/natural rubber/cellulose nanocrystal bionanocomposites Part I. Processing and morphology," *Carbohydrate Polymers*, vol. 96, pp. 611–620, 2013.
- [118] D. Roy, M. Semsarilar, J. T. Guthrie, and S. Perrier, "Cellulose modification by polymer grafting: a review," *Chem Soc Rev*, vol. 38, pp. 2046-64, Jul 2009.
- [119] F. Azzam, E. Siqueira, S. Fort, R. Hassaini, F. Pignon, C. Travelet, *et al.*, "Tunable Aggregation and Gelation of Thermoresponsive Suspensions of Polymer-Grafted Cellulose Nanocrystals," *Biomacromolecules*, vol. 17, pp. 2112-2119, Jun 13 2016.
- [120] A. Carlmark, E. Larsson, and E. Malmström, "Grafting of cellulose by ring-opening polymerisation – A review," *European Polymer Journal*, vol. 48, pp. 1646-1659, 2012.
- [121] Y. Habibi, A.-L. Goffin, N. Schiltz, E. Duquesne, P. Dubois, and A. Dufresne, "Bionanocomposites based on poly(ϵ -caprolactone)-grafted cellulose nanocrystals by ring-opening polymerization," *Journal of Materials Chemistry*, vol. 18, p. 5002, 2008.
- [122] A. L. Goffin, J. M. Raquez, E. Duquesne, G. Siqueira, Y. Habibi, A. Dufresne, *et al.*, "From interfacial ring-opening polymerization to melt processing of cellulose nanowhisker-filled polylactide-based nanocomposites," *Biomacromolecules*, vol. 12, pp. 2456-2465, Jul 11 2011.
- [123] A. Dufresne, "Processing of Polymer Nanocomposites Reinforced with Polysaccharide Nanocrystals," *Molecules*, vol. 15, pp. 4111-4128, 2010.
- [124] B. Couturaud B, Mas , Robin JJ, "Improvement of the interfacial compatibility between cellulose and poly(L-lactide) films by plasma-induced grafting of L-lactide: the evaluation of the adhesive properties using a peel test.," *J Colloid Interface Sci*, vol. 448, pp. 427-36, 2015.
- [125] Iari Filpponen† and Dimitris S. Argyropoulos*, ‡, "Regular Linking of Cellulose Nanocrystals via Click Chemistry: Synthesis and Formation of Cellulose Nanoplatelet Gel," *Biomacromolecules*, vol. 11, pp. 1060-1066, 2010.

- [126] S. H. Feese E1, Gracz HS, Argyropoulos DS, Ghiladi RA., "Photobactericidal porphyrin-cellulose nanocrystals: synthesis, characterization, and antimicrobial properties," *Biomacromolecules*, vol. 10, pp. 3528-39, 2011.
- [127] I. F. a. D. S. Argyropoulos, "Regular Linking of Cellulose Nanocrystals via Click Chemistry: Synthesis and Formation of Cellulose Nanoplatelet Gels," *Biomacromolecules*, vol. 11, pp. 1060–1066, 2010.
- [128] Y. A. P. M. Visakh, "Thermal Degradation of Polymer Blends, Composites and Nanocomposites," *Springer*, 2015.
- [129] D. O. Bondeson, K. , "Dispersion and characteristics of surfactant modified cellulose whiskers nanocomposites.," *Compos. Interfaces*, vol. 14, pp. 617–630., 2007.
- [130] G. M. Jooyoun Kim, Youssef Habibi, Juan P. Hinestroza, Jan Genzer, and 2054–2061 Dimitris S. Argyropoulos, "Dispersion of cellulose crystallites by nonionic surfactants in a hydrophobic polymer matrix," *polymer engineering and science*, vol. 49, pp. 2054–2061 2009.
- [131] Q. Zhou, H. Brumer, and T. T. Teeri, "Self-Organization of Cellulose Nanocrystals Adsorbed with Xyloglucan Oligosaccharide–Poly(ethylene glycol)–Polystyrene Triblock Copolymer," *Macromolecules*, vol. 42, pp. 5430-5432, 2009.
- [132] J. M. Kim, G.; Habibi, Y.; Hinestroza, J. P.; Genzer, J.; Argyropoulos, D. S.; Rojas, O., "Dispersion of cellulose crystallites by nonionic surfactants in a hydrophobic polymer matrix," *Polymer Engineering and science*, vol. 49, pp. 2054–2061 2009.
- [133] M. S. Farhan Ansari, Qi Zhou, and Lars A. Berglund "Strong Surface Treatment Effects on Reinforcement Efficiency in Biocomposites Based on Cellulose Nanocrystals in Poly(vinyl acetate) Matrix," *Biomacromolecules*, vol. 16, pp. 3916–3924, 2015.
- [134] J. Zhao, Q. Li, X. Zhang, M. Xiao, W. Zhang, and C. Lu, "Grafting of polyethylenimine onto cellulose nanofibers for interfacial enhancement in their epoxy nanocomposites," *Carbohydrate Polymers*, vol. 157, pp. 1419-1425, 2017.
- [135] S. H. Kobayashi, K.; Tokunoh, M.; Saegusa, T., *Macromolecules*, vol. 20, p. 1496, 1987.
- [136] shirly, "High-Resolution X-Ray Photoemission Spectrum of the Valence Bands of Gold.," *Phys Rev B* vol. 5, pp. 4709–4714., 1972.
- [137] Y. H. X. Cao, L.A. Lucia, "One-pot polymerization, surface grafting, and processing of waterborne polyurethane-cellulose nanocrystal nanocomposites," *J. Mater. Chem.*, vol. 19, pp. 7137–7145, 2009.
- [138] S. P. Akhlaghi, Berry, Richard C., Tam, Kam C., "Surface modification of cellulose nanocrystal with chitosan oligosaccharide for drug delivery applications," *Cellulose*, vol. 20, pp. 1747-1764, 2013.
- [139] W. Zhu, Liu, Lin, Liao, Qian, Chen, Xuan, Qian, Zhouqi, Shen, Junyan, "Functionalization of cellulose with hyperbranched polyethylenimine for selective dye adsorption and separation," *Cellulose*, vol. 23, pp. 3785-3797, 2016.

- [140] L. Z. Jie Cai, *Shilin Liu, Yating Liu, "Dynamic Self-Assembly Induced Rapid Dissolution of Cellulose at Low Temperatures"
" *Macromolecules*, vol. 41, pp. 9345-9351, 2008.
- [141] A. D. A. Yuan Xua, Jason R. Stokesa, "Rheology and Microstructure of Aqueous Suspensions of Nanocrystalline Cellulose Rods," *Journal of Colloid and Interface Science*, vol. 496, pp. 130-140, 2017.
- [142] A. S. Dhar N, Tam KC, "Biodegradable and biocompatible polyampholyte microgels derived from chitosan, carboxymethyl cellulose and modified methyl cellulose," *Carbohydr Polym* vol. 87, pp. 101-109, 2012.
- [143] K. D. P. Demadis, Maria;Theodorou, Joanna, "Controlled Release of Bis(phosphonate) Pharmaceuticals from Cationic Biodegradable Polymeric Matrices," *Industrial & Engineering Chemistry Research*, vol. 50, pp. 5873-5876, 2011.
- [144] A. P. P. C. Griffiths;, P. Stilbs; E. Petterson, "Charge on Poly(ethylene imine): Comparing Electrophoretic NMR Measurements and pH Titrations," *Macromolecules* vol. 38, pp. 3539-3542, 2005.
- [145] T. K. Mukherjee, Nhol;Gupta, Rahul K.;Quazi, Nurul;Bhattacharya, Sati, "Evaluating the state of dispersion on cellulosic biopolymer by rheology," *Journal of Applied Polymer Science*, vol. 133, pp. n/a-n/a, 2016.
- [146] L. Boluk Yaman, Roya,Zhao, Liyan,McDermott, Mark T., "Suspension viscosities and shape parameter of cellulose nanocrystals (CNC)," *Colloids and Surfaces A: Physicochemical and Engineering Aspects*, vol. 377, pp. 297-303, 2011.
- [147] G. A. V. A. D. Esteban E. Ureña-Benavides;, and Christopher L. Kitchens, "Rheology and Phase Behavior of Lyotropic Cellulose Nanocrystal Suspensions," *Macromolecules*, vol. 44, pp. 8990-8998, 2011
- [148] S. H. Shafiei-Sabet, W.Y.;Hatzikiriakos, S. G. , "Ionic strength effects on the microstructure and shear rheology of cellulose nanocrystal suspensions," *Cellulose*, vol. 21, pp. 3347-3359, 2014.
- [149] Wadood Y. HamadSavvas G. H. Sadaf Shafeiei-Sabet, "Influence of degree of sulfation on the rheology of cellulose nanocrystal suspensions," *Rheologica Acta*, vol. 52, pp. 741–751, 2013.
- [150] T. G. M. v. d. V. Koichi Takamura, "Comparisons of modified effective medium theory with experimental data on shear thinning of concentrated latex dispersions," *Journal of Rheology* vol. 54, 2010.
- [151] G. Lenfant, Heuzey, M. C.,van de Ven, T. G. M.,Carreau, P. J., "Intrinsic viscosity of suspensions of electrosterically stabilized nanocrystals of cellulose," *Cellulose*, vol. 22, pp. 1109-1122, 2015.
- [152] C. a. Merz, "Correlation of dynamic and steady flow viscosities," *Polymer chemistry*, vol. 28, pp. 619–622 1985.

- [153] W. Y. H. Sadaf Shafiei-Sabet†, and Savvas G. Hatzikiriakos*†, "Rheology of Nanocrystalline Cellulose Aqueous Suspensions," *Langmuir*, vol. 28, pp. 17124–17133, 2012.
- [154] A. N. Nakagaito and H. Yano, "Novel high-strength biocomposites based on microfibrillated cellulose having nano-order-unit web-like network structure," *Applied Physics A*, vol. 80, pp. 155-159, 2005.
- [155] T. Javanbakht, A. Bérard, and J. R. Tavares, "Polyethylene glycol and poly(vinyl alcohol) hydrogels treated with photo-initiated chemical vapor deposition," *Canadian Journal of Chemistry*, vol. 94, pp. 744-750, 2016.
- [156] Audrey Z.-S. Richard K. Johnson, "Preparation and characterization of hydrophobic derivatives of TEMPO-oxidized nanocelluloses " *CELLULOSE* vol. 18, pp. 1599-1609 2011.
- [157] H. M. a. Tiffany Abitbol, Emily D. Cranston "Surface modification of cellulose nanocrystals with cetyltrimethylammonium bromide " *Nordic Pulp & Paper Research*, vol. Vol 29 no (1) 2014.
- [158] D. C. Harris, *third edition*, 2015.
- [159] V. K. M. R. Khoshkava, "Effect of surface energy on dispersion and mechanical properties of polymer/nanocrystalline cellulose nanocomposites," *Biomacromolecules*, vol. 14, pp. 3155-3163, Sep 9 2013.
- [160] R. C, "Solvents and Solvent Effects in Organic Chemistry,," *Wiley-VCH Verlag GmbH & Co.*, vol. Third Edit., 2003.
- [161] P. A. A. Robert A. Orwoll, "Polymer–Solvent Interaction Parameter χ ," *Physical Properties of Polymers Handbook*, pp. 233-257, 2007.
- [162] H. P. Agostoni V, Noiray M, "A “green” strategy to construct non-covalent, stable and bioactive coatings on porous MOF nanoparticles. ," *Sci Rep*, vol. 5, p. 7225, 2015.
- [163] S. Su, Wilkie, Charles A., "The thermal degradation of nanocomposites that contain an oligomeric ammonium cation on the clay," *Polymer Degradation and Stability*, vol. 83, pp. 347-362, 2004.
- [164] N. O. Visakh PM, "Thermal Degradation of Polymer Blends, Composites and Nanocomposites," pp. 1-16, 2015.
- [165] M. Borkovec, Szilagy, I., Popa, I.; Finessi, M.; Sinha, P., "Investigating forces between charged particles in the presence of oppositely charged polyelectrolytes with the multi-particle colloidal probe technique," *Adv Colloid Interface Sci*, vol. 179-182, pp. 85-98, Nov 1 2012.
- [166] B. G. Bolto, J., "Organic polyelectrolytes in water treatment," *Water Res*, vol. 41, pp. 2301-24, Jun 2007.
- [167] G. Pelssers, *Colloids surface*, vol. 38, 1989.

- [168] V. P. Megha Surve , and Venkat Ganesan "Nanoparticles in Solutions of Adsorbing Polymers: Pair Interactions, Percolation, and Phase Behavior," *Langmuir*, vol. 22, pp. 969–981, 2006.
- [169] H. Oguzlu, Danumah, Christophe, Boluk, Yaman, "The role of dilute and semi-dilute cellulose nanocrystal (CNC) suspensions on the rheology of carboxymethyl cellulose (CMC) solutions," *The Canadian Journal of Chemical Engineering*, vol. 94, pp. 1841-1847, 2016.
- [170] A. S. S. Khair, Andrew G., "The bulk electroviscous effect," *Rheologica Acta*, vol. 52, pp. 255-269, 2012.
- [171] N. H.-T. Homas Hellweg, Marc Chambon, Didier Rouxa, Nelly Henry-Toulme, Marc Chambon, "Interaction of short DNA fragments with the cationic polyelectrolyte poly(ethylene imine): a dynamic light scattering study," *Colloids and Surfaces A: Physicochemical and Engineering Aspects*, vol. 163, pp. 71-80, 2000.
- [172] M. Rinaudo, "Chitin and chitosan: Properties and applications," *Progress in Polymer Science*, vol. 31, pp. 603–632, 2006.
- [173] P. G. a. T. K. M. Chinmayee Saikia, "Chitosan: A Promising Biopolymer in Drug Delivery Applications," *Molecular and Genetic Medicine*, 2015.
- [174] C. K. S. Abdul Khalil H.P.S, Adnan A.S.c, M.R. Nurul Fazitaa, M.I. Syakira, Y. Davoudpoura, M. Rafatullaha, C.K. Abdullaha, M.K. M. Haafiza, R. Dunganid, "A review on chitosan-cellulose blends and nanocellulose reinforced chitosan biocomposites: Properties and their applications," *Carbohydrate Polymers*, vol. 150, pp. 216–226, 2016.
- [175] S. P. B. Akhlaghi, Richard C.; Tam, Kam C., "Surface modification of cellulose nanocrystal with chitosan oligosaccharide for drug delivery applications," *Cellulose*, vol. 20, pp. 1747-1764, 2013.
- [176] M. R. Chen Y, Gray B, "Synthesis of albumin-dextran sulfate microspheres possessing favourable loading and release characteristics for the anticancer drug doxorubicin," *Controlled Release* vol. 31, pp. 49-54, 1994.
- [177] K. J. Cai Z, "Characterization and electromechanical performance of cellulose–chitosan blend electro-active paper," *Smart Materials and Structures*, vol. 17, pp. 1-8, 2008.
- [178] Q. Z. Wang, X. G. Chen, N. Liu, S. X. Wang, C. S. Liu, X. H. Meng, *et al.*, "Protonation constants of chitosan with different molecular weight and degree of deacetylation," *Carbohydrate Polymers*, vol. 65, pp. 194-201, 2006.
- [179] L. Huang, Z. Ye, and R. Berry, "Modification of Cellulose Nanocrystals with Quaternary Ammonium-Containing Hyperbranched Polyethylene Ionomers by Ionic Assembly," *ACS Sustainable Chemistry & Engineering*, vol. 4, pp. 4937-4950, 2016.

**APPENDIX A : SURVEY N1s AND O1s FOR PRISTINE AND mCNC
WITH RATIO (1,2 AND 5%)**

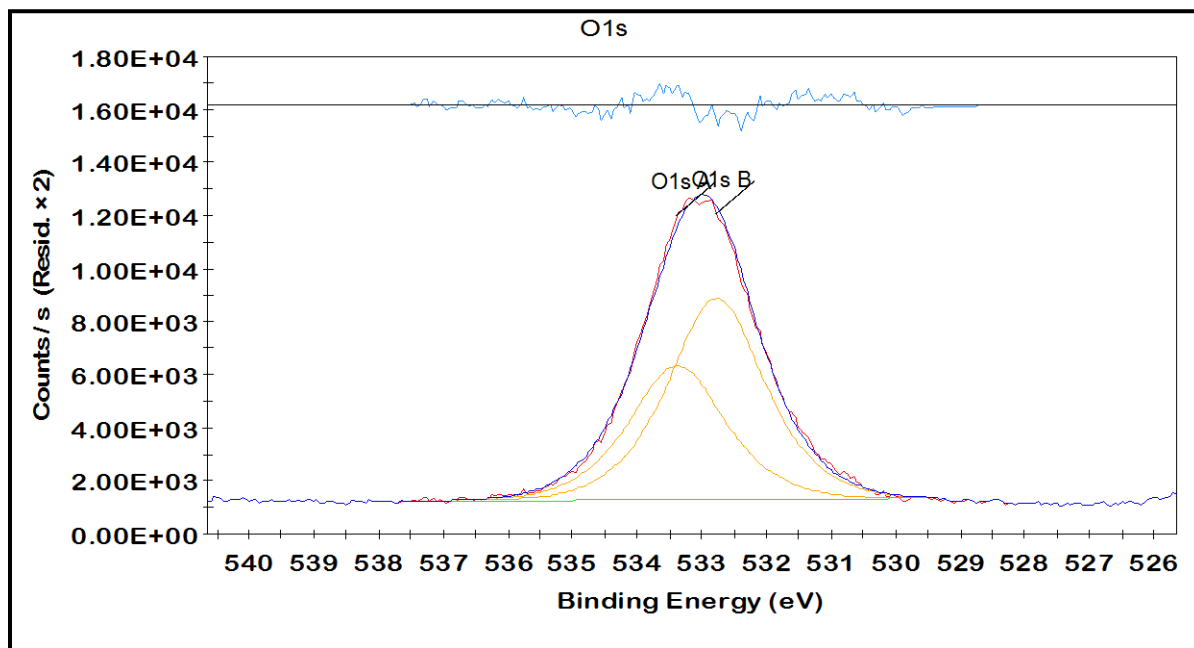


Figure A1. Survey O1s for pristine CNC.

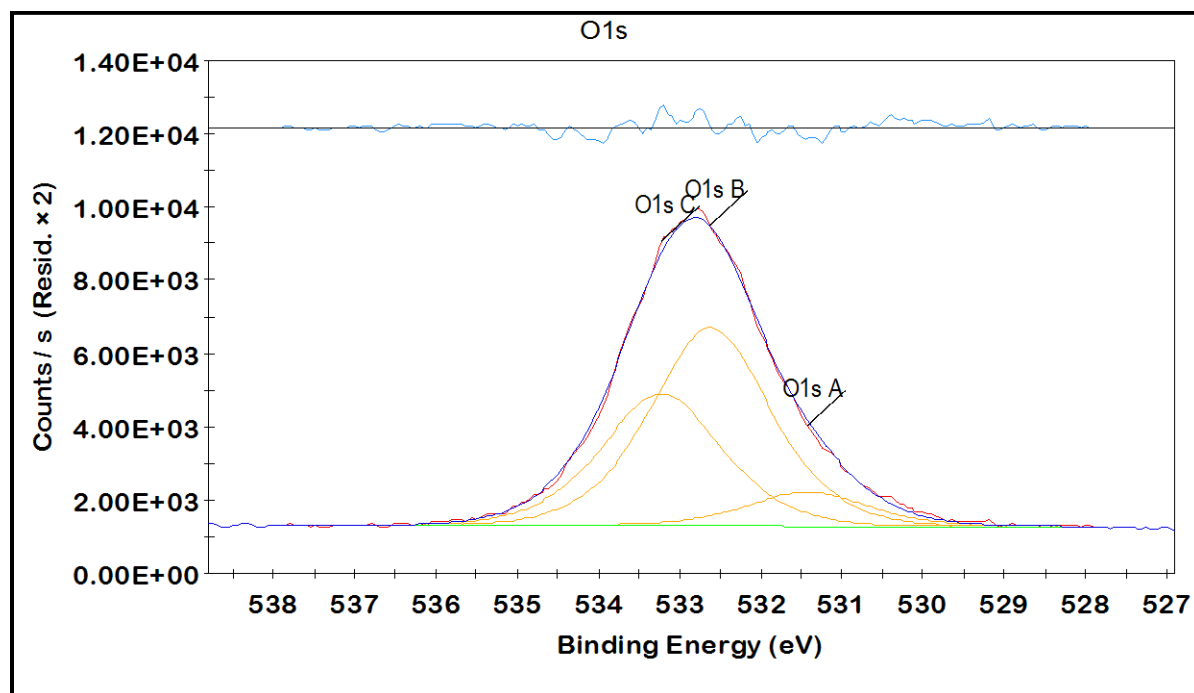


Figure A2. Survey O1s for mCNC (PEI/CNC 1%).

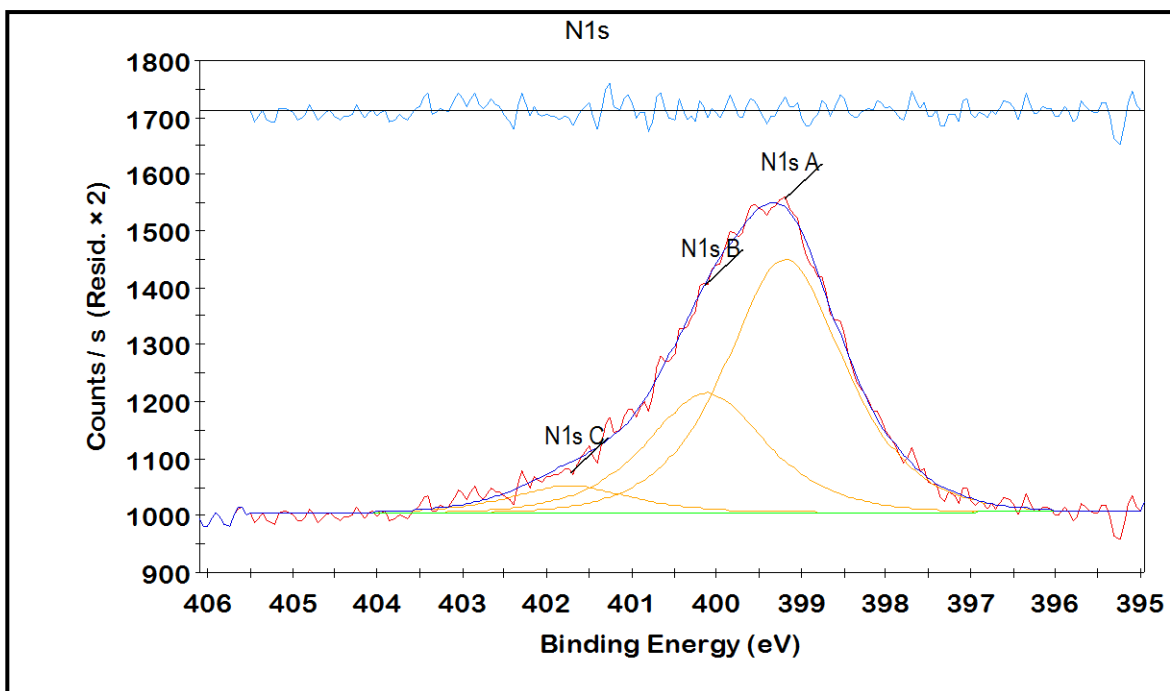


Figure A3. Survey N1s for mCNC (PEI /CNC 1%).

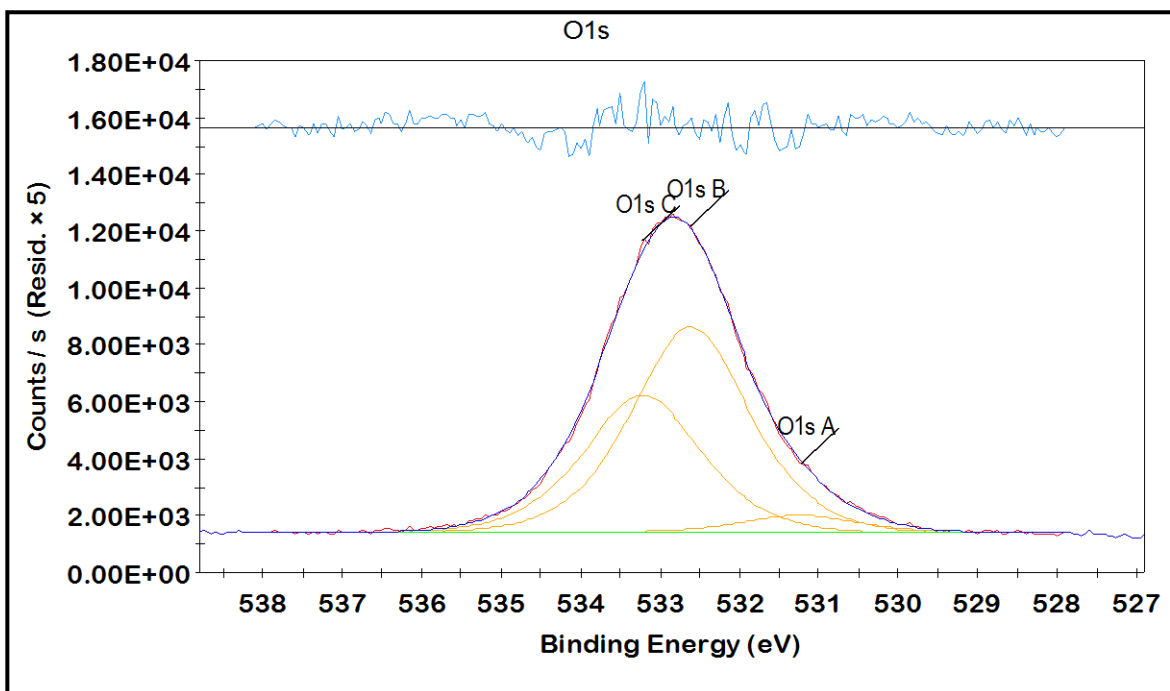


Figure A4. Survey O 1s for mCNC (PEI/CNC 2%).

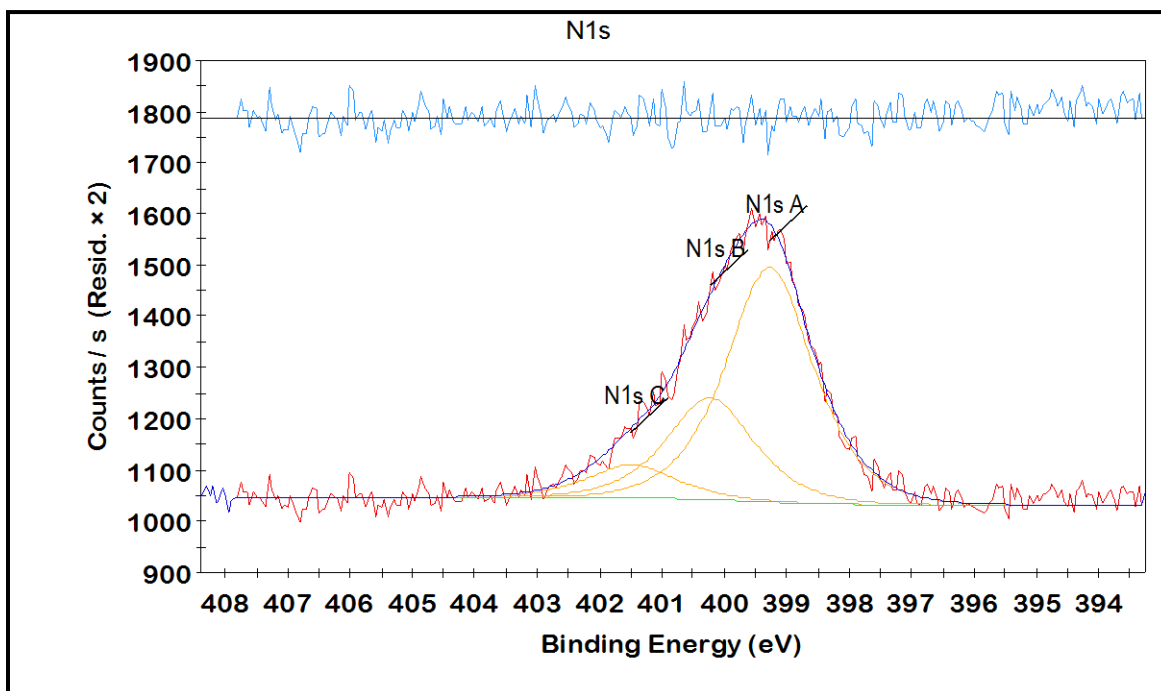


Figure A5. Survey N 1s for mCNC (PEI/CNC 2%).

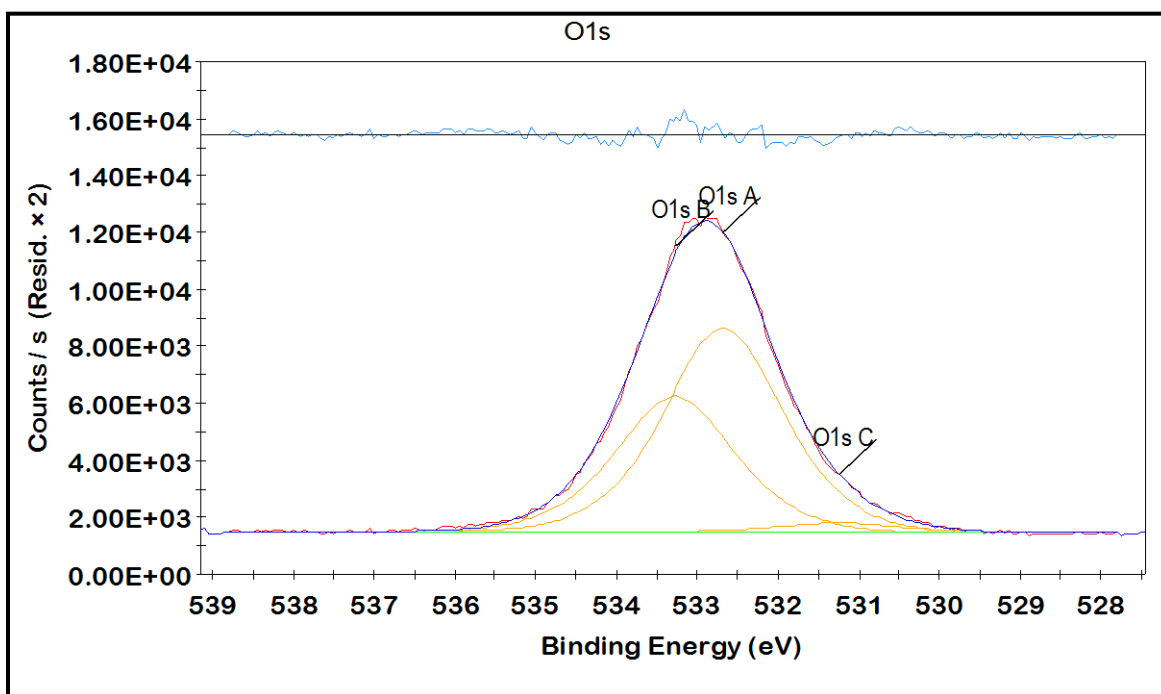


Figure A6. Survey O 1s for mCNC (PEI/CNC 2%).

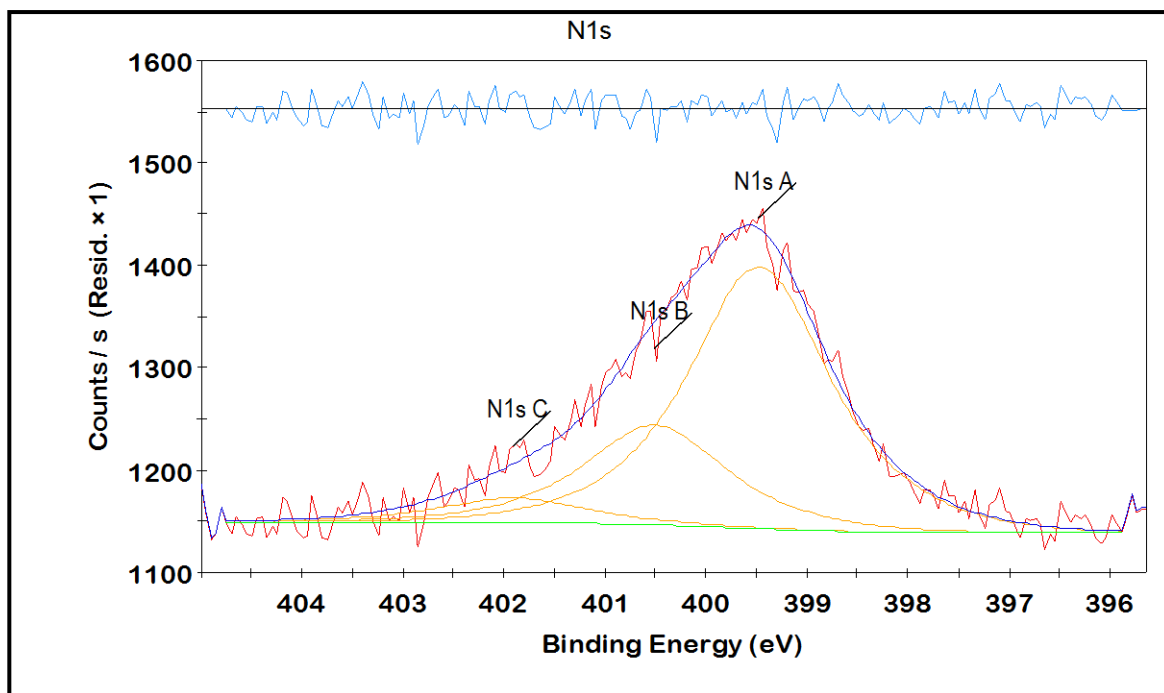


Figure A7. Survey N 1s for mCNC (PEI/CNC 5%).

APPENDIX B: RHEOLOGICAL BEHAVIOR OF PEI/CNC AQUEOUS SUSPENSIONS

B.1 The effect of PEI ratio on rheological properties

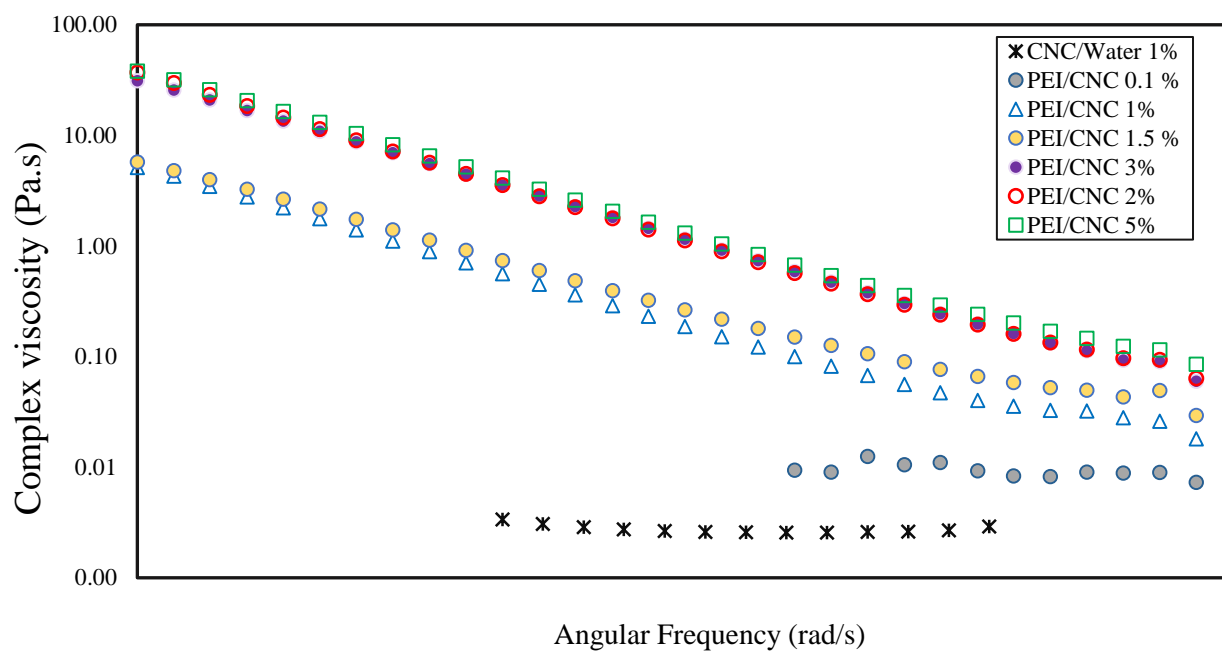


Figure B1 Complex viscosity as function of angular frequency for PEI/CNC aqueous suspension of PEI/ CNC (CNC concentration of 1wt.%, T=25 °C).

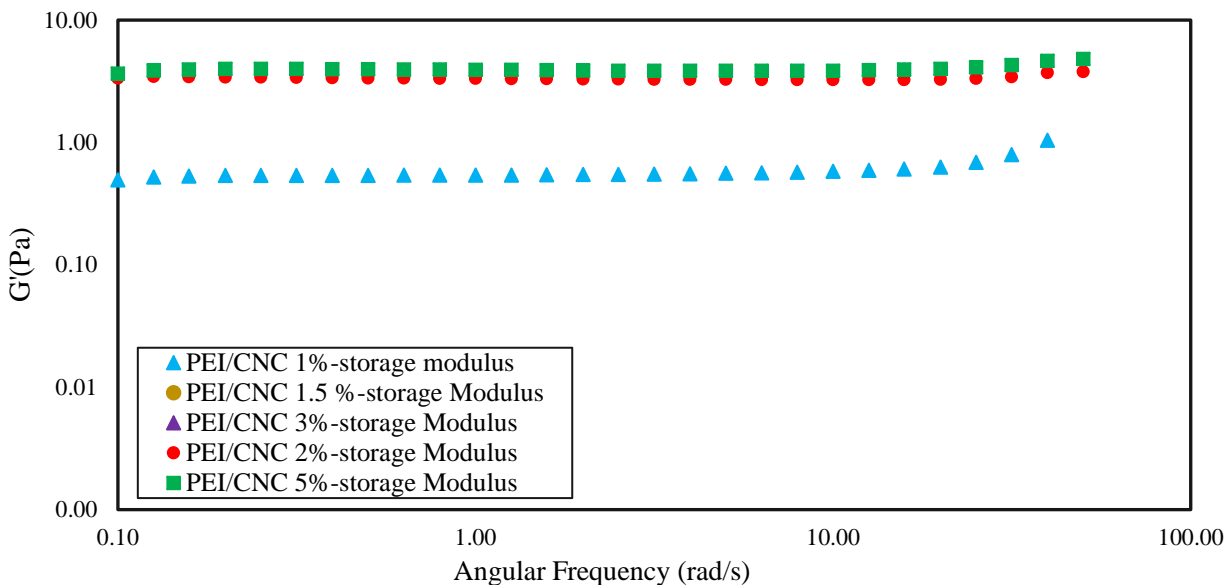


Figure B2. Storage modulus as a function of angular frequency for PEI/CNC aqueous suspensions (CNC concentration of 1wt.%, $T=25\text{ }^{\circ}\text{C}$).

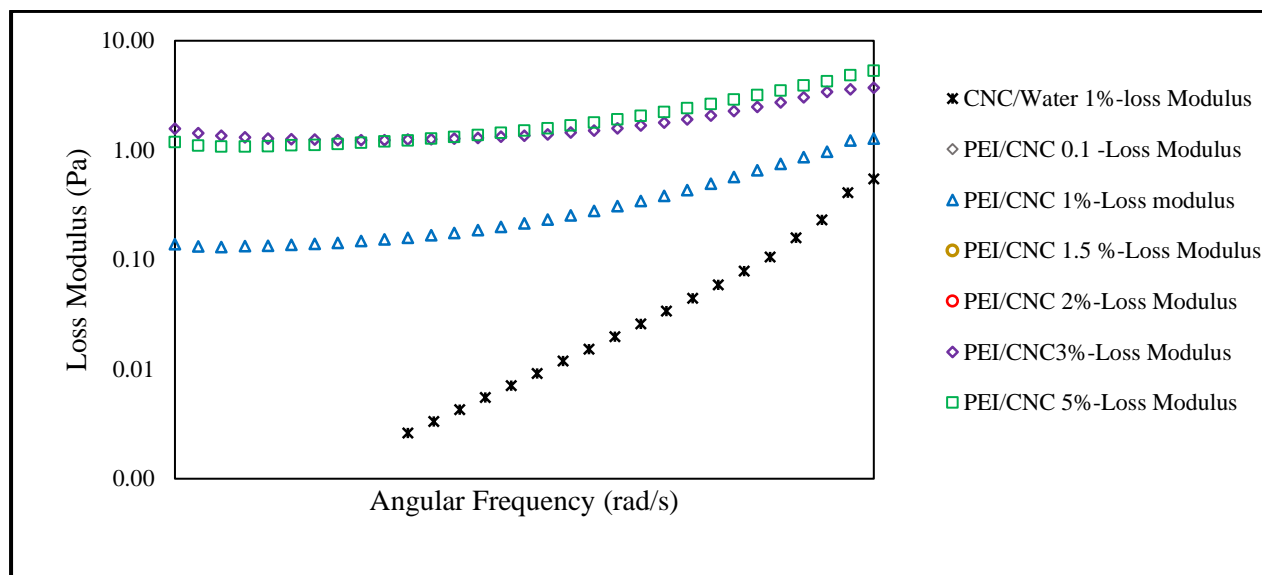


Figure B3. Loss modulus (G'') as a function of angular frequency for PEI/CNC aqueous suspensions (CNC concentration of 1wt.%, $T=25\text{ }^{\circ}\text{C}$).

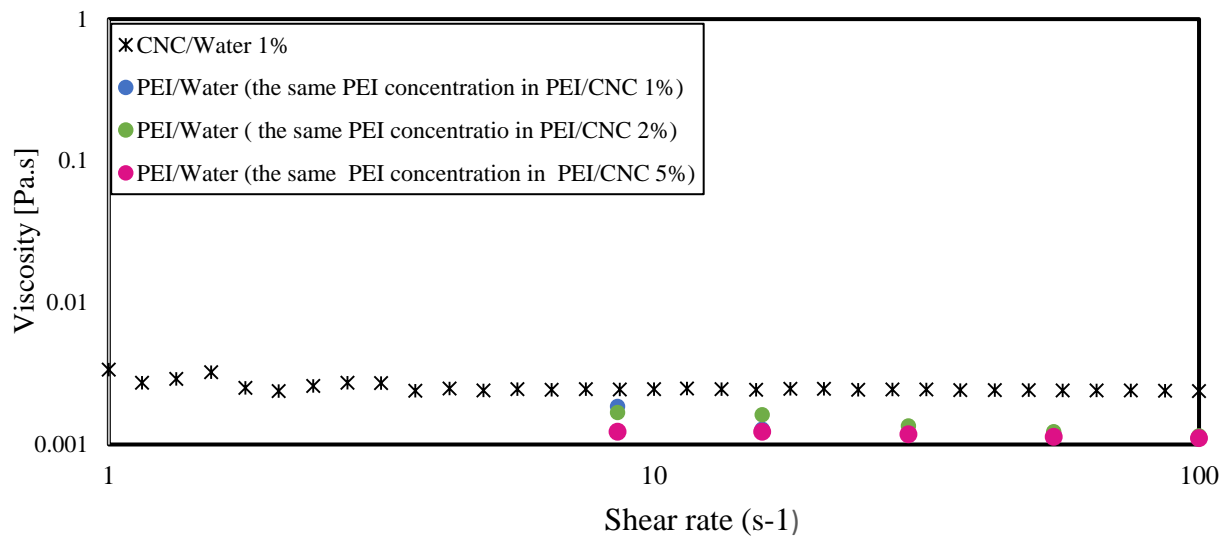


Figure B4. Viscosity as a function of shear rate for PEI solutions at different concentrations ($T=25^{\circ}\text{C}$)

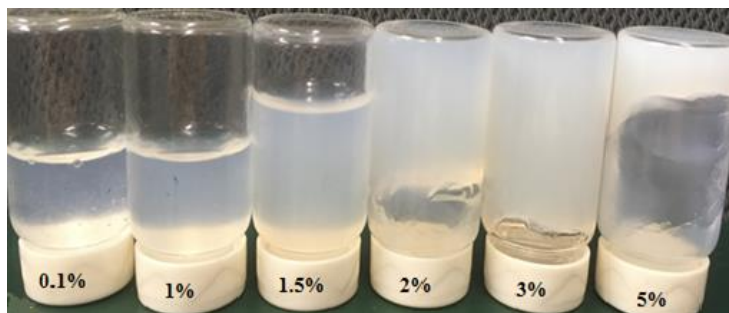


Figure B5. The suspension state of PEI/CNC aqueous suspensions at different PEI concentrations over time (4 h in room temperature).

B.2. The time effect on viscoelastic behavior of PEI/CNC aqueous suspensions

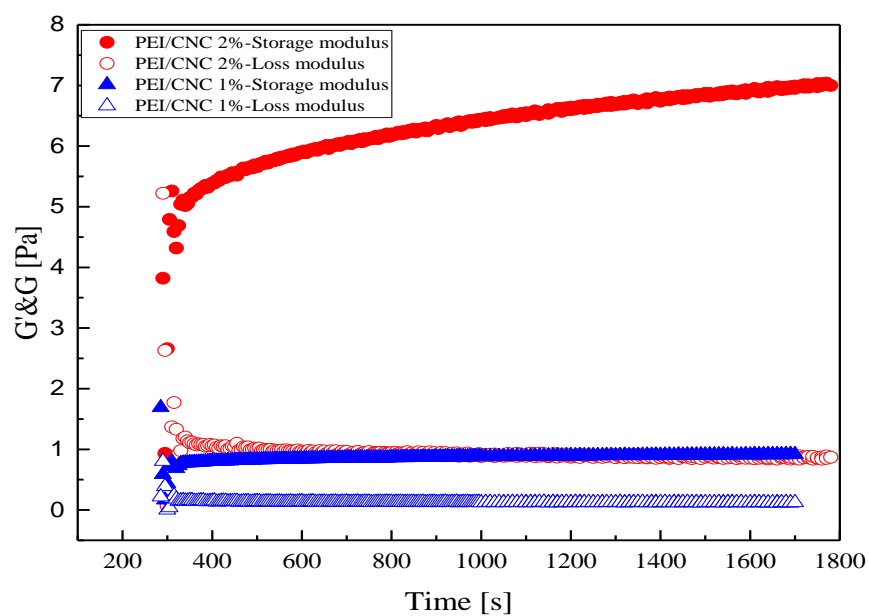


Figure B6. Variations of viscoelastic properties as a function of time for aqueous suspensions of PEI/CNC at frequency of 1 rad s^{-1} (CNC concentration of 1wt.%, $T=25 \text{ }^{\circ}\text{C}$).

B.3. Temperature effect on viscosity of PEI/CNC aqueous suspensions

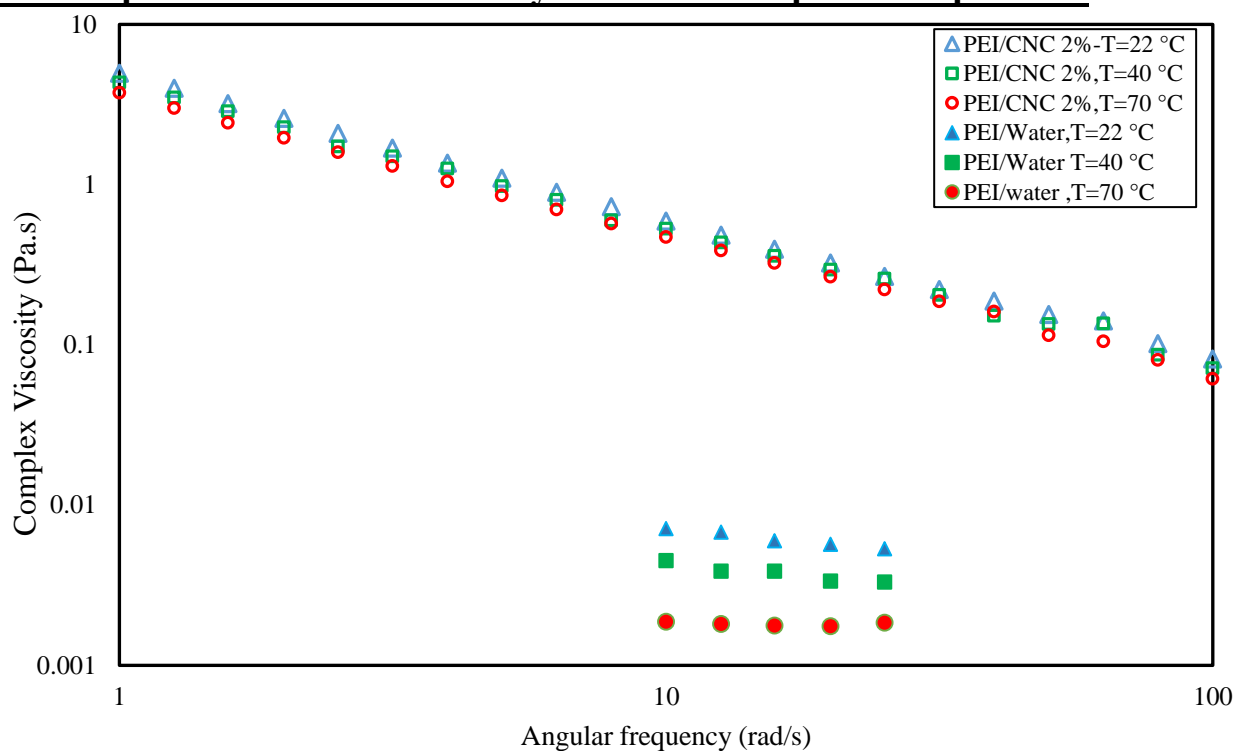


Figure B7. Complex viscosity as a function of angular frequency for PEI/CNC aqueous suspensions and PEI water solutions at different temperatures: 22, 40 and 70 °C .

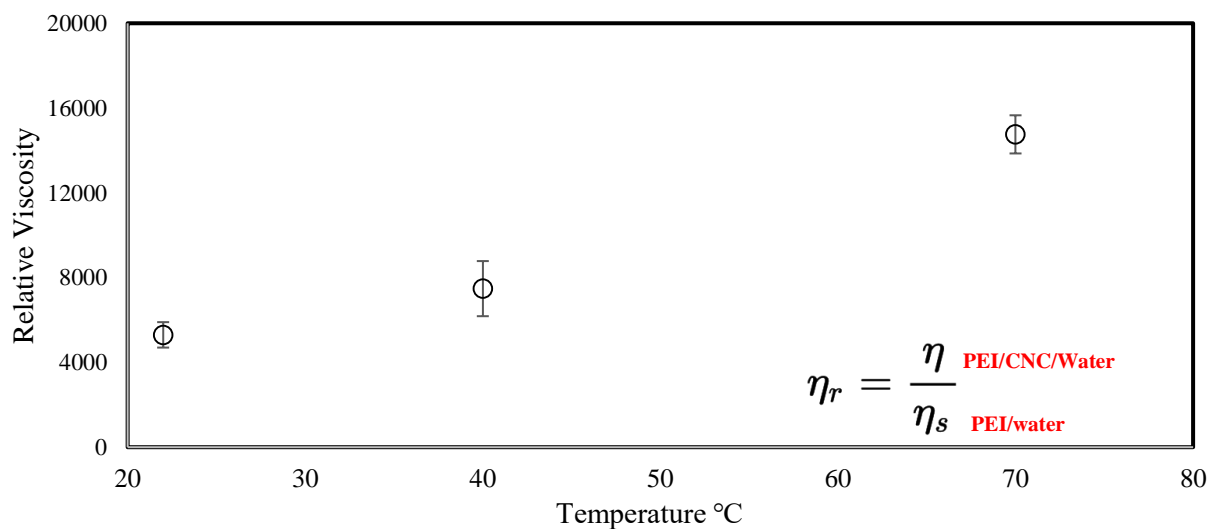


Figure B8. Relative viscosity as a function of temperature for aqueous suspensions of PEI/CNC 2% at CNC concentration of 1 wt.%.

APPENDIX C: TGA ANALYSIS OF mCNC IN NITROGEN

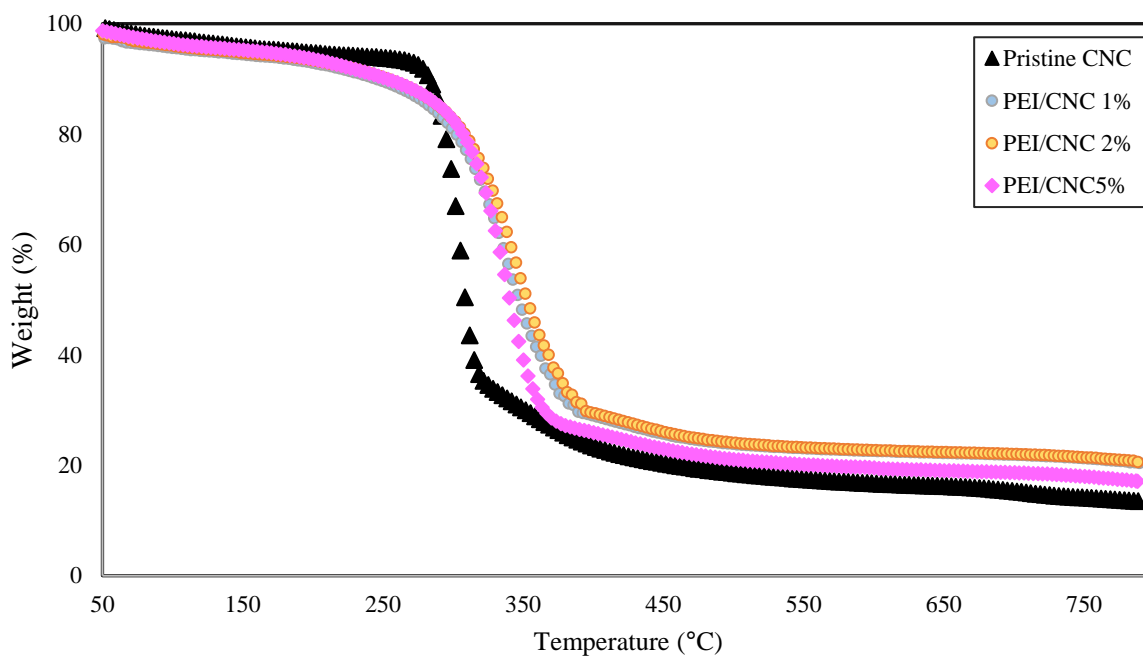


Figure C1. Weight as a function of temperature for pristine and mCNC with different PEI ratio in nitrogen.

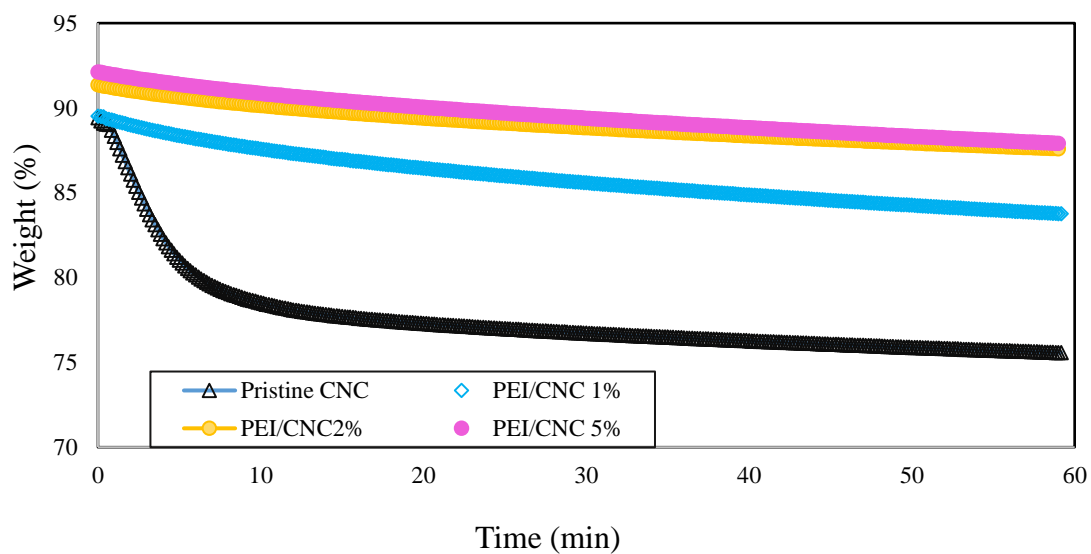


Figure C2. Weight as a function of time at 220 °C for pristine CNC and mCNC with different PEI concentrations in nitrogen.

APPENDIX D: THE DISPERSION STATE OF mCNC IN MINERAL OIL

Modified CNC with PEI ratio of 2 wt.% were dispersed in mineral oil at CNC concentration of ~ 1 wt.%. The stability of suspension was evaluated by UV-Vis spectroscopy over one hour. As shown in Fig. D1. The mCNC made a stable suspension in mineral oil over one hour. Macroscopic observation also confirmed it.

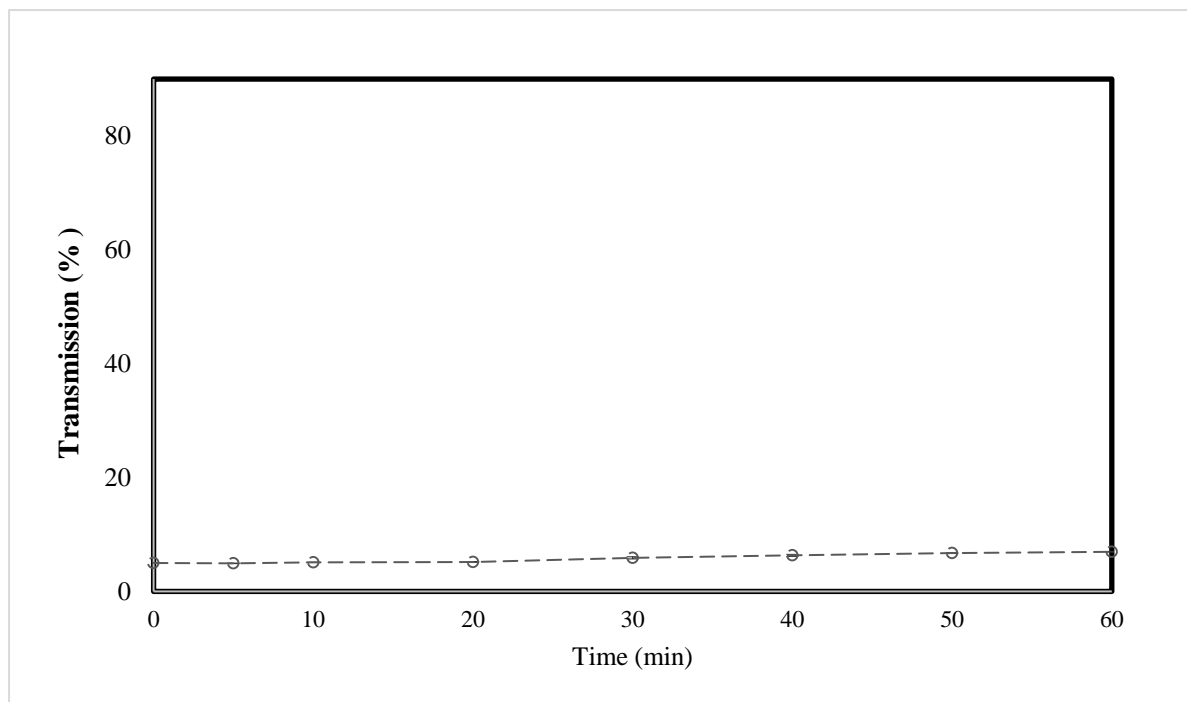


Figure. D1 Percentage of the intensities of UV transmittance measured at wavelength 582.185 nm –mCNC (2 wt.%) in mineral oil.

APPENDIX E: RHEOLOGICAL BEHAVIOR OF CHITOSAN/CNC WATER SUSPENSIONS

Rheological measurements were performed using a rotational rheometer (MCR 502) using a double-Couette flow geometry at 25 °C. In small-amplitude oscillatory shear (SAOS) experiments, the linear viscoelastic region was first determined using strain sweep test (1 to 100%) at two frequencies (1 and 10 rad s⁻¹). The results of rheological measurements for aqueous suspension of Chitosan/CNC at CNC concentration of 1 wt.% are presented in this section. The ratio of chitosan/CNC was kept at 1 wt.%

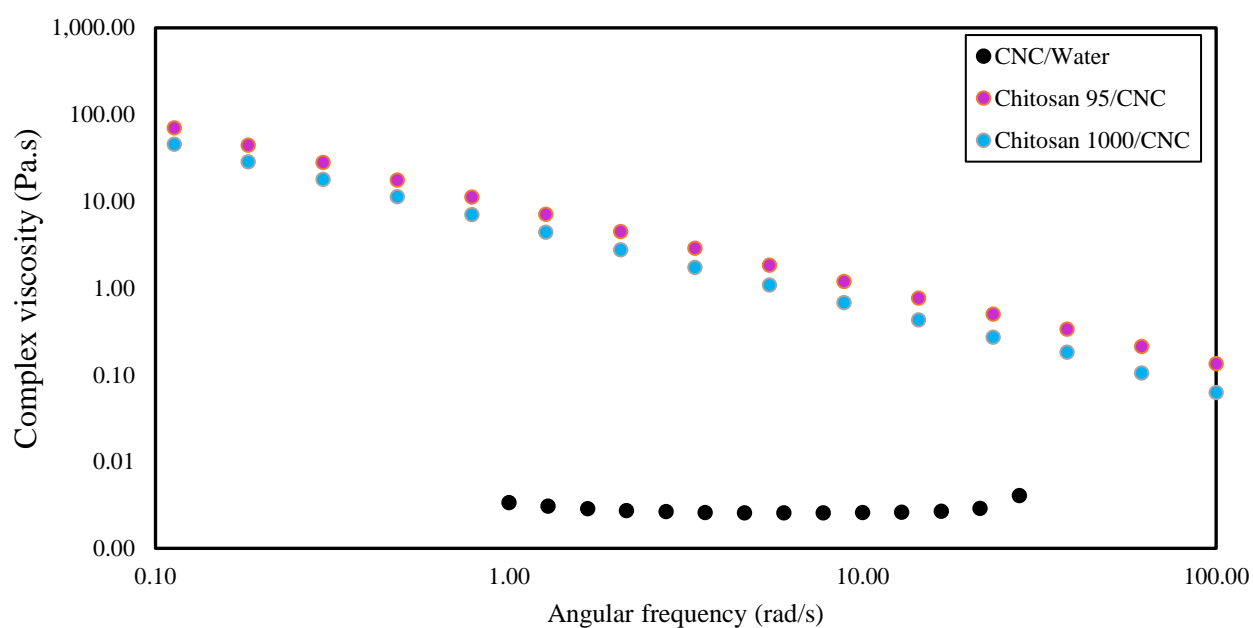


Figure. E1. Complex viscosity of pristine CNC and chitosan/CNC aqueous suspensions (CNC concentration of 1 wt.%, T=25 °C).

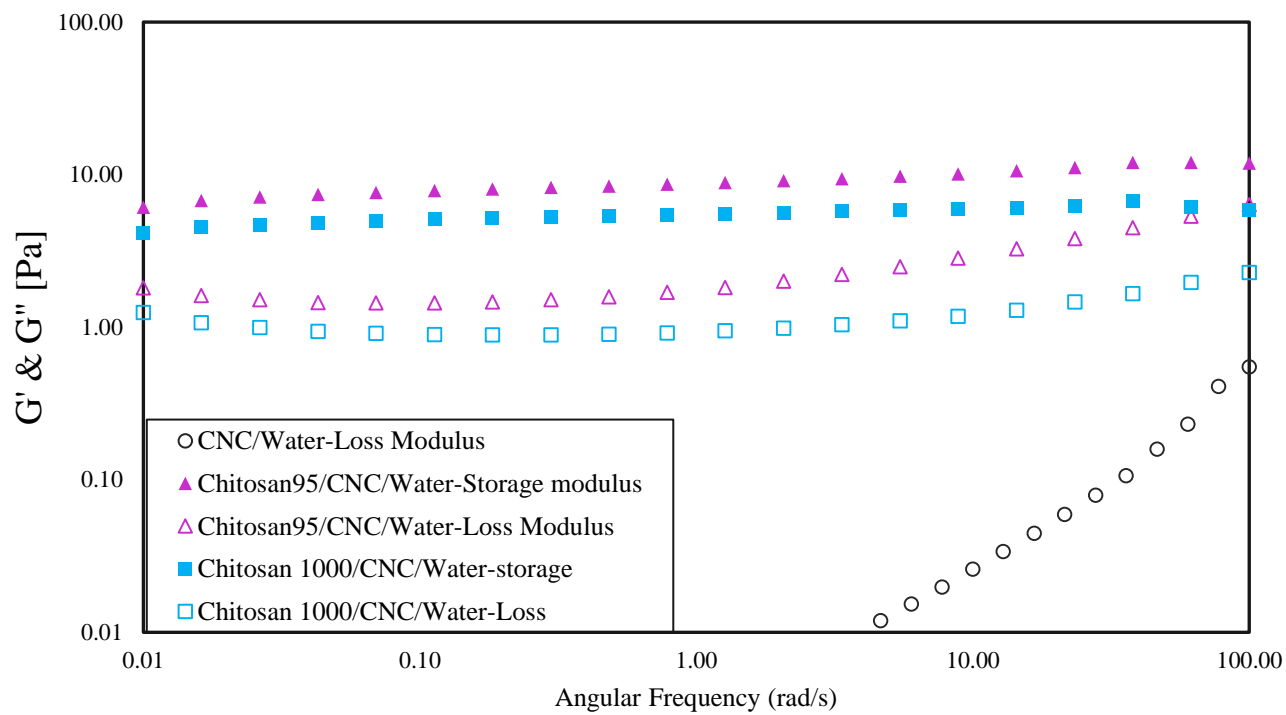


Figure E2. Viscoelastic properties of chitosan/CNC aqueous suspensions. (CNC concentration of 1wt.%, $T=25$ °C).

APPENDIX F: THE RESULTS OF PEI/CNC 5%

Table F.1. XPS analysis of modified CNC with PEI/CNC 5 %

Name	BE (eV)	Identification	PEI/CNC 5 %
C1s	285.0	C-C or C-H (C3)	17.5
	286.6	C-O in cellulose (C1)	34.8
	288.1	O-C-O in cellulose (C2)	7.6
	TOTAL		59.9
N1s	399.2	Amine	1.2
	400.1	Amide	0.5
	401.7	Protonated N	0.1
	TOTAL		1.8
O1s	531.4	O=C-N	1.1
	532.6	C-OH in cellulose	22.4
	533.2	C-O-C	14.9
	TOTAL		38.4

The amount of amine and amide groups decreased with increasing PEI ratio at 5 %. This decrease could be related to less accessibility of protonated groups to react with negative CNC sites at high PEI ratio (5% with respect to CNC). However, to explain these properties more experiments are required.

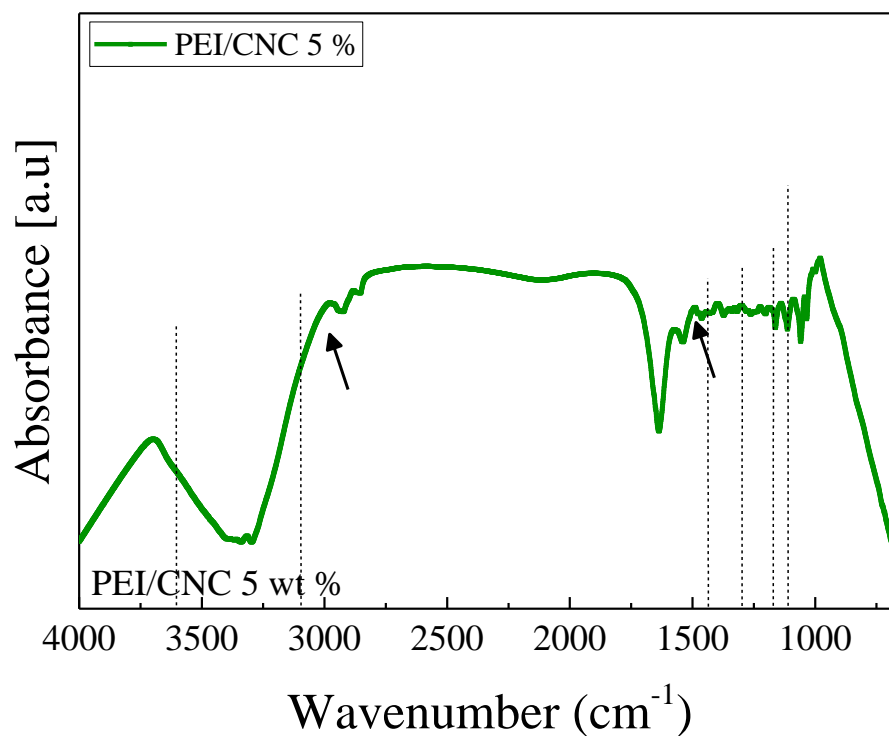


Figure F.1 FTIR spectra of mCNC with PEI/CNC 5 %).

Table F. 2 Z-average hydrodynamic diameter, PDI, and ζ - potential for mCNC (PEI/CNC 5%)

Sample	Average diameter (nm)	PDI	ζ - potential	ζ - potential	ζ - potential
			(mV) without pH adjustment	(mV) pH 3.0	(mV) pH 7.0
PEI/CNC 5 %	1171±10	0.80	-39.0±1.9 (pH 7.7)	24.0±0.4	-40.0±5.1

The difference of ζ - potential for mCNC with 5 % and 2 % of PEI/CNC ratio was not significant (+6 mV). At pH 7.0, the ζ - potential for 5 % of PEI/CNC ratio strangely decreases compared to 1 and 2 %. The significant increase in measured size and wide polydispersity index of mCNC with PEI/CNC 5 %, suggests the presence of large agglomerate due to the high concentration of PEI [179]. However, more accurate experiments are needed to explain these results.

Table F.3. Characteristic thermal degradation temperatures

Sample	T_{onset} (°C)	T_{50%} (°C)	Isothermal weight loss (220 °C for 60 min) (%)
PEI/CNC 5 %	270	334	4.0±1.1